BIOAFFINITY SEPARATION USING LIGAND-MODIFIED PLURONIC AND SYNTHETIC MEMBRANES

Selvakumaran Govender

Dissertation presented for the degree
Doctor of Philosophy (Biochemistry)
in the
Faculty of Science
at the
University of Stellenbosch

Promoter: Prof. P. Swart
Department of Biochemistry
University of Stellenbosch

Co-promoters: Prof. E.P. Jacobs and Dr. M.W. Bredenkamp
Department of Chemistry and Polymer Science
University of Stellenbosch

Stellenbosch, August 2005

Declaration:

I, the undersigned, hereby declare that the work contained in this dissertation is my own original work and that I have not previously in its entirety or in part submitted it at any university for a degree.

…….. ……

Selvakumaran Govender Date

SUMMARY

A new membrane based affinity separation system that is bio-specific, biocompatible, well characterised and capable of being regenerated or re-used is described. The amphiphilic non-ionic surfactant Pluronic® F108, was covalently derivatised to form two novel bioligands (Pluronic-Biotin and Pluronic-DMDDO) for the bio-specific immobilisation of avidin conjugated proteins and histidine tagged proteins respectively. Pluronic was also used to non-covalently functionalise nonporous membranes for ligand attachment and to simultaneously shield the surfaces from non-specific protein adsorption. Each component of this bioaffinity system (from the membrane matrix to the elution/desorption of the ligate/ligand system) was studied with the aim of producing a well characterised system and key quantitative data for the development of a robust, reliable, re-usable and scalable technology.

Specifically, this study describes:

1. The fabrication and partial characterisation of nonporous planar and capillary membranes as model affinity matrices.
2. The development and evaluation of a robust protocol for solvent desorption and accurate colorimetric quantification of Pluronic® F108 and its derivatives.
3. Interfacial analysis of Pluronic adsorption onto nonporous affinity membranes, including the direct solid-state analysis of model, halogenated Pluronic derivatives using nuclear microprobe analysis.
4. Development of a surfactant based protocol for affinity membrane regeneration and re-use.
5. Specific bioaffinity immobilisation of avidin conjugated peroxidase onto biotinylated membranes in the presence of model protein foulants.
6. Cloning and expression of C-terminal hex-histidine tagged human cytochrome b5 into the bacterial expression system *E. coli* BL-21 DE3.
7. Development and characterisation of an immobilised metal affinity membrane system for metal chelation (Ni^{2+}, Cu^{2+} and Zn^{2+}) using a new chelator Pluronic-*N,N*-dicarboxymethyl-3,6-diazaoctanedioate and the bio-specific immobilisation of N-terminal hex-histidine tagged pantothenate kinase.

OPSOMMING

'n Nuwe membraan-gebaseerde affiniteitskeidingsisteem word beskryf wat biospesifiek, bioversoenbaar en goed gekarakteriseer is, en geregenereer of hergebruik kan word. Die amfifiliese nie-ioniese surfaktant Pluronic is kovalent gederivatiseer om twee nuwe bioligande (Pluronic-Biotien en Pluronic-DMDDO) te vorm vir biospesifieke immobilisering van proteïnligate. Pluronic is ook gebruik om nie-poreuse membrane nie-kovalent te funksionaliseer vir ligandaanhegting en om hulle oppervlaktes teen nie-spesifieke proteïen-adsorbsie af te skerm. Elke komponent van hierdie bioaffiniteitsisteem (van die membraanmatriks tot die uitwas/desorpsie van die ligaat/ligand sisteem) is ondersoek met die doel om 'n goed-gekarakteriseerde sisteem te produseer en om kwantitatiewe data te genereer vir die ontwikkeling van 'n robuuste, betroubare, herbruikbare en opskaleerbare tegnologie.

Hierdie studie beskryf spesifiek:

1. Die fabrisering en gedeeltelike karakterisering van nie-poreuse planêre en kapillêre membrane as model affiniteitsmatrikse.
2. Die ontwikkeling en evaluering van 'n robuuste protokol vir oplosmiddel desorpsie en akkurate kolorimetriese kwantifikasie van Pluronic® F108 en afgeleides daarvan.
3. Intervlakanalises van Pluronic adsorpsie op nie-poreuse affiniteitsmembrane, insluitend die direkte vastetoestand analise van model ligand-gemodifiseerde Pluronic deur die gebruik van kern-mikrosonde analise.
4. Ontwikkeling van 'n surfaktant-gebaseerde protokol vir affiniteitsmembraan regenerering en hergebruik.
5. Spesifieke bioaffiniteitsimmobilisering van avidien-gekonjugeerde peroksidase op gebiotinileerde membrane in die teenwoordigheid van model bevuilende proteïne.
6. Klonering en uitdrukking van C-terminaal hex-histidien geëtiketeerde menslike sitochroom b5 in die bakteriële uitdrukkingsisteem *E. coli* BL-21 DE3.
7. Ontwikkeling en karakterisering van 'n geïmmobiliseerde metaalaffiniteitsmembraansisteem vir metaalchelering (Ni^{2+}, Cu^{2+} en Zn^{2+}) met behulp van die nuwe cheleerder Pluronic-N,N-dikarboksimetiel-3,6-diasaoktaandioaat en die bio-spesifieke immobilisering van N-terminaal hex-histidiengeëtiketerde pantotenaatkinase.

LIST OF ABBREVIATIONS AND ACRONYMS

A_L	Lumen surface area
A_S	External surface area
ABTS	2,2'-azino-di-(3-ethylbenzthiazoline sulfonic acid)
AFM	atomic force microscopy
Amp	ampicillin
Ab	antibody
ATP	adenosine tri-phosphate
Cytb5	cytochome b5
Cytb5$(His)_6$	hex-histidine tagged cytochrome b5
dH_2O	deionised water
DMAc	*N*,*N*-dimethylacetamide
DNA	deoxyribonucleic acid
dNTP	deoxnucleotidephosphate
DCA	dynamic contact angle
DMDDO	dicarboxymethyl-3,6-diazaoctanedioate
ELISA	enzyme linked immunosorbant assay
EPA	environmental protection agency
F108	Pluronic® F108
FDA	food and drug administration
FT-IR	Fourier transform infra red spectroscopy
HF	hollow fibre
HFF	hollow fine fibre
His	histidine
ICP	inductively coupled plasma
IDA	iminodiacetate
IMAC	immobilised metal affinity chromatography
IMAM	immobilised metal affinity membrane
IPTG	isopropyl-β-D-thiogalactopyranoside
LDH	lactate dehydrogenase
MF	microfiltration
MCMM	multi-capillary membrane module
NADH	nicotinamide adenine dinucleotide

NMR	nuclear magnetic resonance
NTA	nirtilotriacetate
PAGE	polyacrylamide gel electrophoresis
PB	phosphate buffer
PCR	polymerase chain reaction
PEG	poly(ethylene glycol)
PEI	poly(ether imide)
PEO	poly (ethylene oxide)
PEP	phosphoenolpyruvate
PIXE	proton induced x-ray emission
PK	pantothenate kinase
$PK(his)_6$	histidine tagged pantothenate kinase
PPO	poly(propylene oxide)
PSU	polysulphone
PVDF	poly(vinylidene fluoride)
RNA	ribonucleic acid
RBS	Rutherford backscattering spectroscopy
RO	reverse osmosis
RUMP	Rutherford universal modification program
SCA	static contact angle
SDS	sodium dodecyl sulphate
SEM	scanning electron microscopy
TED	*N*,*N*,*N*'-tris-carboxymethyl ethylene diamine
UF	ultrafiltration
XPS	X-ray photoelectron spectroscopy
XRD	X-ray diffraction

ACKNOWLEDGEMENTS

I would like to express my gratitude to the following individuals and organisations.

Prof. Pieter Swart for accepting me as a student and for an excellent learning experience.
Prof. Ed Jacobs for the opportunity to work in the field of membrane technology.
Dr. Martin Bredenkamp for assistance in the organic chemistry laboratory.

Dr. Wojtek Przybylowicz for diligent assistance with PIXE.
Dr. Chris Theron for RBS analysis and for allowing me to work at iThemba LABS.
Prof. Lingam Pillay for actually getting things started.
Mr. David Richfield for numerous instances of excellent and invaluable assistance.
Ms. Ralie Louw for efficient technical support.

The Affinity Separation Group: Gavin Blewitt, Leon van Kralingen, Wesley Williams, Zyno Allie, Leisl Liebenberg.
The P450 Lab: Hannes Slabbert, Norbert Kolar, Nic Lombard, Grant Killian.
Mev. Lynnette Eygelaar and colleagues for administrative assistance.

My friends David Richfield, Dale Wilcox, Hannes Slabbert, Venthan Naidoo, Mike Vismer, Grant Killian and Wes for a thoroughly unprofessional, but fun environment.
My little friend Nazli for her colossal spirit.

The University of Stellenbosch for a perfect study and living environment.

Der deutsche akademische Austauschdienst und die technische Universität von Dresden für eine schöne Lernengelegenheit während der beschäftigten und angespannten Tage meiner Doktorprüfung.

The Water Research Commission for funding the project.

The National Research Foundation and the Andrew Mellon Foundation for personal financial support.

Bole So Nihal, Sat Sri Akal

Waheguru ji ka Khalsa

Waheguru ji ki Fateh

CHAPTER 1: INTRODUCTION

This introductory chapter highlights the concept of membrane affinity separation as an application of process biotechnology and outlines the objectives of this study within the confines of the broader aim of developing reliable affinity membranes for protein or bio molecule separation. A brief outline of the experimental objectives is also listed, together with a concise layout of the thesis.

1.1. BACKGROUND TO PRESENT STUDY

Column chromatography is by far the most widely used technique for the high resolution separation and purification of biomolecules, among which affinity chromatography is the most promising technology due to the possibility of achieving rapid, high purity, one step isolation of specific, high-value biological products [1-3]. Additionally, a trend in downstream processing is to apply affinity interactions as early as possible in the bioseparation process [4].

Traditionally the differences in the various reported systems are due largely to the selection of an inert support that was conventionally made using agarose, polyacrylamide, cellulose or glass as the resin matrix. Each has its merits and shortcomings – agarose for example is very porous, has few ionic groups and can be easily derivatised. However, it is also chemically and mechanically fragile and the derivatisation process frequently creates unwanted ionic groups on surfaces [5]. These conventional resin based, packed bed columns have numerous, well-documented limitations [1,3,6-10] that contribute to the high cost of biomolecule recovery and hamper the scalability of affinity purification applications.

Affinity membranes offer the following advantages to solve these problems:

- higher flow rates with low pressure drops;
- faster binding kinetics with short diffusive distances;
- operation at lower residence times;
- comparatively low cost of materials;

- conducive to process scale-up.

However, there remain a few major obstacles preventing the routine or extensive use of membrane technology:

- strong fouling tendency of commercial hydrophobic membranes;
- the ligand coupling technology frequently involves time-consuming, multi-step covalent coupling chemistry;
- a lack of information describing the interfacial properties of the membrane and the ligand capacity;
- insufficient studies on possible membrane regeneration strategies for efficient re-use.

1.1.1. Synthetic polymeric membranes

Synthetic membranes (porous and nonporous) can be defined as a permselective barrier between two phases [6]. Depending on the choice of fabrication polymer, solvent and conditions, membranes with varying surface architecture and chemistry can be formed. The membrane matrix is the first important consideration when designing a membrane affinity separation system, thus it is important that the surface is characterised with respect to the intended process application.

1.1.2. Pluronic surfactants

Pluronic or poly(ethylene oxide)$_m$-poly(propylene oxide)$_n$-poly(ethylene oxide)$_m$ triblock copolymers are water soluble, non-ionic, amphiphilic surfactants [11]. These surfactants have high chemical and thermal stability and are approved for use in biopharmaceutical, biomedical and environmental applications by the United States Food and Drug Administration and the Environmental Protection Agency [12]. Pluronic has also been used to modify conventional filtration membranes to reduce fouling and improve permeate flux [9] and as dynamic surface modifying polymers [6]. The adsorption behaviour of Pluronic® F108 at the solid interface is also an important area of research [11-15].

1.1.3. Affinity ligands and supports

Popular commercial affinity technologies of importance to the related fields of biochemistry and biotechnology are immobilised metal affinity chromatography and biosensor development [7-9]. The development and implementation of biocompatible ligands for membrane coupling will significantly improve the acceptance of membrane based affinity separation technology within the biological research community.

1.1.4. Membrane regeneration strategies

An important practical consideration for the implementation of membranes in affinity separation technology is its process lifetime [16], which is dependent on its ability to resist non-specific protein adsorption and its regeneration capacity. There are very few studies devoted to the regeneration of affinity membranes and colloidal polymers; however this is partially offset by the huge research thrust into defouling strategies for filtration membranes. Notable regeneration studies include steam sparging of silica membranes [16], air sparging and carbonate extraction of surfactant modified zeolites [17], detergent (Tween-20) and high salt (KSCN) regeneration of worn out sepharose affinity columns [18]. Bioaffinity membrane regeneration strategies should ideally be biocompatible, with low material and energy costs and incorporated *in situ* with the membrane system, utilising existing equipment.

1.1.5. Research Hypothesis

The central idea at the outset of this study was to develop affinity membrane separation systems using Pluronic bioligands for bio-specific protein immobilisation that were also: 1) well characterised at the membrane-liquid interface, 2) able to resist non-specific protein adsorption, 3) able to specifically remove proteins from solution and 4) capable of being regenerated and re-used.

1.2. OBJECTIVES

The overall objective of this study was to investigate the use of Pluronic® F108 coupled ligands in membrane based affinity immobilisation of proteins and to develop protocols for both the quantification of a new metal chelating ligand and the regeneration and re-use of the attendant membrane affinity separation technology. Noting the current state of affinity membrane technology and the research niche areas generated by some of its limitations, the specific objectives of this study were to:

a) fabricate nonporous membranes and characterise the surface properties of each membrane;
b) develop and evaluate protocols for both efficient Pluronic extraction and accurate colorimetric quantification;
c) interfacial analysis and solid-state estimation of ligand modified Pluronic;
d) investigate the protein shielding ability of the affinity linker Pluronic F108 and to develop a procedure for biocompatible membrane regeneration;
e) cloning and immobilisation of histidine tagged proteins;
f) coupling of the ligands biotin and *N'*,*N*-dicarboxymethyl-3,6-diazaoctanedioate to Pluronic for bio-specific protein immobilisation and metal chelation.

1.3. EXPERIMENTAL TASKS

In order to meet the specific objectives, the experimental rationale and the attendant tasks are listed below. A simplified flow diagram illustrating these experimental aims within this dissertation is depicted in Figure 1-1.

1.3.1. Membrane fabrication

Three candidate membranes were fabricated from the commercially available polymers polysulphone, poly(vinylidenefluoride) and poly(ether imide) using the immersion precipitation technique. Membrane sections (1 cm^2) were used as model matrices for Pluronic modifications and ligand coupling. These membrane surfaces were characterised using atomic force microscopy, electron microscopy and infra-red spectroscopy.

1.3.2. Pluronic estimation

A simple, reliable and reproducible assay was critical to the study of the adsorption of the Pluronic affinity-linker onto planar and curved membrane surfaces. A $CHCl_3$-NH_4FeSCN colorimetric assay was developed for the accurate quantification of membrane desorbed Pluronic and derivatised Pluronic [19] in solution.

1.3.3. Ligand synthesis and surface analysis

Model halogenated ligands were initially synthesised to mimic the coupling of bioaffinity ligands to Pluronic. Covalent coupling of the halogens Br and I to Pluronic was also used to help develop protocols for direct solid-state nuclear microprobe analysis of ligand-modified membranes. Solid-state analysis was performed with X-ray photon electron spectroscopy, proton induced X-ray emission and Rutherford backscattering spectroscopy.

1.3.4. Protein shielding and regeneration

The protein shielding ability of Pluronic F108 was investigated using the model protein foulants lysozyme and bovine serum albumin. Sodium dodecyl sulphate was used to develop a membrane regeneration strategy.

1.3.5. Cloning of histidine tagged human cytochrome b5

The gene for human cytochrome b5 was cloned into the plasmid pET22b. This histidine tagged ferric protein is a potential ‘marker’ for solid-state ligate quantification.

1.3.6. Affinity ligands

Biotinylated Pluronic and Pluronic-*N*,*N*-dicarboxymethyl-3,6-diazaoctanedioate were synthesised for membrane based protein immobilisation. These bioligands are specific for avidin conjugated peroxidase and histidine tagged proteins respectively.

Membrane matrix fabrication (nonporous planar, hollow fiber and hollow fine fiber membranes) and characterisation using microscopy and spectroscopy.
(Chapter 3)

↓

Development of a robust, extraction and detection system for membrane adsorbed Pluronic and the interfacial analysis of Pluronic adsorption onto planar and curved membranes.
(Chapter 4)

↓

Direct solid-state analysis of model, halogenated-Pluronic ligands on planar, nonporous poly(vinylidene fluoride), poly(sulphone) and poly(ether imide) membranes.
(Chapter 5)

↓

Use of a new biotinylated Pluronic for testing both the bio-specificity of ligand modified Pluronic and its ability to simultaneously inhibit non-specific protein adsorption. A practical, anionic surfactant based regeneration protocol is also investigated for the possibility of improving the process lifespan of affinity membrane systems.
(Chapter 6)

↓

Cloning and expression of histidine tagged human cytochrome b5 for possible testing of an immobilised metal affinity membrane.
(Chapter 7)

↓

Synthesis and characterisation of a novel metal chelating Pluronic. The ligand capacity of this chelating membrane for divalent cations and bio-specific binding of histidine tagged proteins was also investigated.
(Chapter 8)

Figure 1-1: A flow diagram illustrating the experimental aims discussed in the attendant chapters of this dissertation.

1.4. LAYOUT OF DISSERTATION

A brief description of the aims and significance of each chapter is given below.

1. **Chapter 1**. *Introduction*

2. **Chapter 2**. *Literature overview*

A literature overview of the fields of affinity chromatography and affinity membrane separation is discussed, with emphasis on bioaffinity separation and immobilised metal affinity membranes.

3. **Chapter 3**. *Fabrication and characterisation of model membrane affinity matrices.*

Partial characterisation of the candidate nonporous membranes and construction of capillary modules is described. Membranes were characterised using surface tension analysis, infrared spectroscopy, scanning electron microscopy and atomic force microscopy to provide a better understanding of this affinity matrix.

4. **Chapter 4**. *A robust approach to studying the adsorption of Pluronic F108 on nonporous membranes*.

This chapter was published in Journal of Colloid and Interface Science (2005), and focuses on the interfacial analysis of Pluronic adsorption onto planar and capillary membranes. It also describes a bisolvent extraction protocol for adsorbed Pluronic and details a bi-phasic colorimetric assay for Pluronic and ligand modified Pluronic [19]. This robust assay was subsequently used to routinely quantify Pluronic in solution.

5. **Chapter 5**. *Solid-state analysis of membrane-coupled ligand modified Pluronic.*

Attempts were made to directly study the interfacial behaviour of membrane adsorbed Pluronic derivatives using direct solid-state analysis. Solid-state analysis was performed with atomic force microscopy (AFM), X-ray photoelectron spectroscopy (XPS), proton induced X-ray emission and Rutherford backscattering spectroscopy (RBS). This was

achieved with the synthesis of model ligands via covalent coupling of halogens (I and Br) to tosylated Pluronic derivatives.

6. **Chapter 6**. *Affinity immobilisation of proteins on re-usable ligand modified membranes*.

This chapter was submitted as a manuscript to Journal of Biotechnology and describes the competitive affinity binding of avidin-peroxidase using biotinylated Pluronic membranes. Using this new bioligand (Pluronic-biotin) we investigated the ability of ligand-modified Pluronic to inhibit non-specific protein adsorption, while binding specifically to avidin conjugated peroxidase. A proposed protocol for affinity membrane regeneration and re-use is also discussed.

7. **Chapter 7**. *Cloning and expression of histidine tagged human cytochrome b5*.

The gene for the histidine tagged human cytochrome b5 ferrous hemoprotein was cloned and transformed into a bacterial expression vector. An intact expressed form of this heme protein could potentially serve as a ferric marker for solid-state quantification of the metal affinity immobilisation process. This histidine tagged protein can also be used as a test protein for the metal chelating Pluronic described in chapter 8.

8. **Chapter 8**. *A Pluronic coupled metal chelating ligand for membrane affinity chromatography*.

This chapter has been accepted as a full length paper in Journal of Membrane Science, and discusses the synthesis and characterisation of a novel metal-chelating ligand coupled via Pluronic to poly(vinylidene fluoride) membranes, the chelation of metal ions and the bio-specific immobilisation of histidine tagged bacterial pantothenate kinase.

9. **Chapter 9**. *Conclusions and recommendations*

This chapter summarises the findings of this study and discusses recommendations for future work.

1.5. REFERENCES

1 G.S. Chaga, J. Biochem. Biophys. Methods. **49** (2001) 313.

2 R. Ghosh, J. Chromatogr. A. **952** (2002) 13.

3 E. Lightfoot, J.S. Moscariello, Biotechnol. Bioeng. **87**(3) (2004) 259.

4 V. Gaberc-Porekar, V. Menart, J. Biochem. Biophys. Methods. **49** (2001) 335.

5 W.H. Scouten, Affinity chromatography. John Wiley & Sons, New York, **49** 1981, p.11.

6 J.A. Howell, V. Sanchez, R.W. Field, Membranes in bioprocessing: Theory and applications. Chapman & Hall, Cambridge, 1993, p.25.

7 D.K. Roper, E.N. Lightfoot, J. Chromatograph. A. **702** (1995) 3.

8 E. Klein, J. Mem. Sci. **179** (2000) 1.

9 S-Y. Suen, Y-C. Liu, C-S. Chang, J. Chromatogr. B. **797** (2003) 305.

10 X.J. Yang, A.G. Fane, C. Pin, Chemical Eng. Journal **88** (2002) 45.

11 C.R.E. Mansur, M.P. Barbarose, G. Gonzalez, E.P. Lucas, J. Colloid Interface Sci. **27** (2004) 232.

12 S. Stolnik, B. Daudali, B. Arien, J. Whetsone, C.R. Heald, M.C. Garnett, S.S. Davis, L. Illum, Biochimica Biophysica Acta **1514** (2001) 261.

13 J-T. Li, J. Carlsson, J-N. Lin, K.D. Caldwell, Bioconjugate Chem. **7** (1996) 592.

14 F. Ahmed, P. Alexandridis, S. Neelamegham, Langmuir **17** (2001) 537.

15 M. Bohner, T.A. Ring, K.D. Caldwell, Macromolecules **35** (2002) 6724.

16 M.C. Duke, J.C. Diniz da Costa, G.Q. Lu, M. Petch, P. Gray, J. Mem. Sci. **241** (2004) 325.

17 Z. Li, R.S. Bowman, Wat. Res. **35** (2001) 322.

18 F. Darlene Robinson, R.A. Moxley, H.W. Jarret, J. Chromatogr. A. **1024** (2004) 71.

19 S. Govender, E.P. Jacobs, M.W. Bredenkamp, P. Swart, J. Colloid Int. Sci. **282** (2005) 306.

CHAPTER 2: LITERATURE OVERVIEW

2.1. INTRODUCTION

The rapid and unprecedented developments in biotechnology and the progress and achievements in biopharmaceutical and medical applications have fuelled a demand for rapid, reliable and efficient downstream processing technologies. Recovery of sensitive biomolecules such as interferons, vaccines, polynuclueotides, antibodies, DNA, polypeptides, proteins, hormones, etc. from a biological host environment also requires attention to their unique characteristics [1,2].

In bio-separations, all products are labile and mild processing conditions are thus required [3]. Time consuming, multi-step processes can cause proteolysis, deamination and aggregation of proteins and degradation to many gene products. In addition to strict standards in purity inherent to the food and pharmaceutical industries, the American Food and Drug Administration (FDA) requires validating the removal of various contaminants such as: host cell-related biomolecules (DNA, endotoxin, protein, virus), product related factors (oxidation, deamination, acetylation, dimerisation) and process related chemicals (antibiotics, antifoam chemicals, inducing agents) [3,4].

Various column chromatographic techniques have been successfully used for biomolecule separation, among which affinity chromatography exhibited the best performance in terms of product purity due to its high specificity [5,6]. The high costs of conventional column chromatography have shifted research efforts towards modifying and developing traditional filtration membranes for use as affinity membranes. In large-scale processes the cost of biomolecule recovery dominates the total manufacturing costs [3] and as shown with bioreactors [7], membrane processes offer greater scope for scalability than conventional support matrices such as agarose gels and polymeric beads [8,9].

2.2. AFFINITY SEPARATION

2.2.1. Affinity chromatography

Affinity chromatography was a term first used in 1968 by Cuatrecasas *et al*., [10] to describe a new form of chromatography based on biological recognition. This paper signalled an immediate research effort resulting in the development of affinity separation techniques leading to the quest for 'short cuts' for the isolation and purification of biological compounds. This biological affinity chromatography initially involved covalently coupling bio-specific ligands to an inert solid matrix where they served as adsorption centres [6]. The interactions involved in this adsorption process are usually similar or identical to interactions that occur in nature. A comparison between different types of column chromatographic techniques is listed in Table 2-1.

Table 2-1: Comparison between different types of column chromatographic techniques [5]

Property	Affinity		Ion exchange	Reverse phase / Hydophobic interaction
	Group Specific	Bio-specific		
Adsorption capacity	Medium – high	Low	High	Medium – high
Selectivity	Medium – high	High	Low – medium	Low – medium
Recovery	High	Medium	High	Medium
Loading phase	Mild	Mild	Mild	Usually Harsh
Elution phase	Mild	Harsh	Mild	Mild
Regeneration	Complete	Incomplete	Complete	Incomplete
Cost	Low	High	Low	Low

Thus bio-specific affinity chromatography exploits some of natures' own information channels resulting in biologically functioning complexes. The molecular forces and bond interactions forming these complexes are systematised under the terms ionic bonds, hydrophobic interactions, hydrogen bonding, Van der Waals forces, London dispersive forces, dipole-dipole interactions and charge-transfer interactions [6]. The understanding and quantification of these interactions, which usually occur at the solid-liquid interface,

have recently become important areas of study after the advent of highly sensitive and non-destructive analytical techniques such as scanning probe microscopy, ellipsometry and surface plasmon resonance spectroscopy [11].

2.2.2. Biological affinity ligands

Bioaffinity chromatography usually involves the immobilisation of naturally occurring ligands onto a solid porous support [12,13]. The biotin-avidin complex was one of the systems chosen as a model for developing experimental work [12]. Proteins provide an almost unlimited array of molecular structures that might be used as ligands or ligates and the type of ligand employed provides an extensive applications listing. These include amino acids, dye ligands, metal-chelating ligands, ion-exchange ligands and immunoaffinity (antigen and antibody) ligands.

The production of recombinant proteins in a highly purified and well-characterised form has been another major catalyst in affinity separation techniques. Several epitope peptides and proteins have been developed recently to over-produce recombinant proteins [14]. These affinity-tag systems have the following common features:

- one step adsorption purification;
- minimal effect on tertiary structure and biological activity of the ligate;
- simple but specific removal to yield the native protein;
- a sensitive assay system for the recombinant protein;
- applicability to a number of different proteins.

However, a disadvantage of conventional bioaffinity tag systems is that in many cases a further step in the purification process is required to remove the affinity tag from the target protein, as in the maltose binding protein-amylose system [14].

2.2.3. Conventional affinity matrices

The affinity matrix is the first important consideration when designing an affinity system as it composes for the most part, the largest volume of the adsorbent. Certain characteristics of the matrix are essential [5,15,16]:

- it must be insoluble in the attendant solvents or buffers used;
- mechanical and chemical stability;
- possess good flow characteristics;
- contain sufficient surface area available for ligand accessibility.

Matrices currently employed can be divided into two groups, the first generation matrices that are predominantly single-composition matrices (e.g., agarose, controlled pore glass, cellulose, collagen) and the second-generation matrices (dual composition and or chemically modified matrices) [17]. The latter include agarose coated polyacrylamide, acrylic coated iron particles and crosslinked agarose [18]. Most commercial affinity supports use first generation matrices, but the best matrix for any given procedure will depend on the nature of the biomolecule to be purified and on any specific demands placed on the procedure such as separation time, high yields and high purity. There are many excellent texts and reviews [13,16-19], which describe the chemistry and applications of the various matrices that could be used in affinity chromatographic separations.

2.2.4. Affinity membrane separation

Synthetic, polymeric membranes are routinely used in many biotechnological and medical applications. Affinity membranes reflect technological advances in both membrane filtration and fixed-bed liquid chromatography. Membrane affinity separation systems function as short, wide chromatographic columns in which the adsorptive packing consists of one or more membranes in series, each derivatised with adsorptive moieties [1].

Adsorptive membranes for use in membrane based affinity separation have been the focus of intensive research in the last decade as an alternative to resin based chromatographic columns [1,5,8,16,20]. In addition to serving as affinity adsorbents these membranes can

also be modified or fabricated as ion-exchange, hydrophobic, reverse-phase or filtration membranes. In porous membranes, the interactions between the dissolved molecules and the active sites on the membrane occur in convective through-pores rather than in stagnant fluid inside the pores of an adsorbent polymer bed [20].

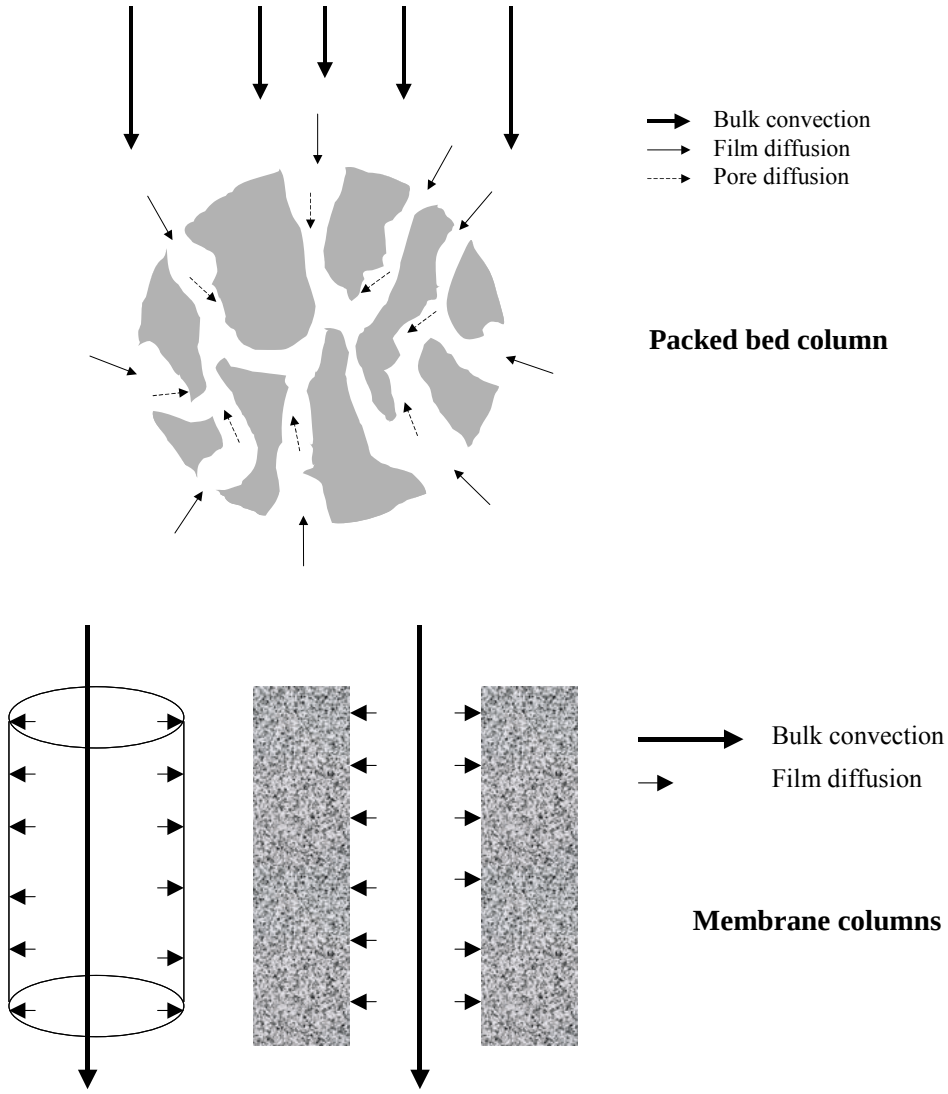

Figure 2-1: Solute transport in fixed packed bed chromatography and membrane chromatography.

Affinity separation using membrane matrices is superior to conventional fixed bed columns in the following aspects [1,5]. The macropores inside the membrane (filtration membranes) allow the convective flow of solute through the membrane and intra-bed diffusion does not feature in a permeable membrane system (Figure 2-1). The large cross-sectional area relative to the bed length allows high velocities and large volumetric capacity with a small or negligible pressure drop, enabling high flow rate operations for

flow processes. However a large diameter to length ratio introduces the challenge of achieving uniform flow distribution across the membrane [20].

A possible solution to the above problem, was introduced by Yuan *et al*., [21], where a rational approach to the design of flow distributors was shown to give uniform distribution in numerical simulations and laboratory prototypes. Adequate flow distribution is critical for maintaining column efficiency during scaling up of a membrane column. Nevertheless, compared to fixed bed columns, membrane processes are easier to scale-up, regenerate and are not limited by bed compaction [1,8].

2.2.5. Membrane configuration and module design

Module design is fundamental to the operation of a membrane separation process as this is the unit that must operate at a technical scale utilising large membrane surface areas. The module design is based on two general types of membranes, flat sheet or tubular. It is the method of packing the membrane and the relative membrane size that leads to a range of module configurations [22]. Affinity membranes can be organised into a variety of configurations (stacked membranes, hollow fibre membranes, spiral wound membranes). A schematic illustration of typical membrane module designs is shown in Figure 2-2.

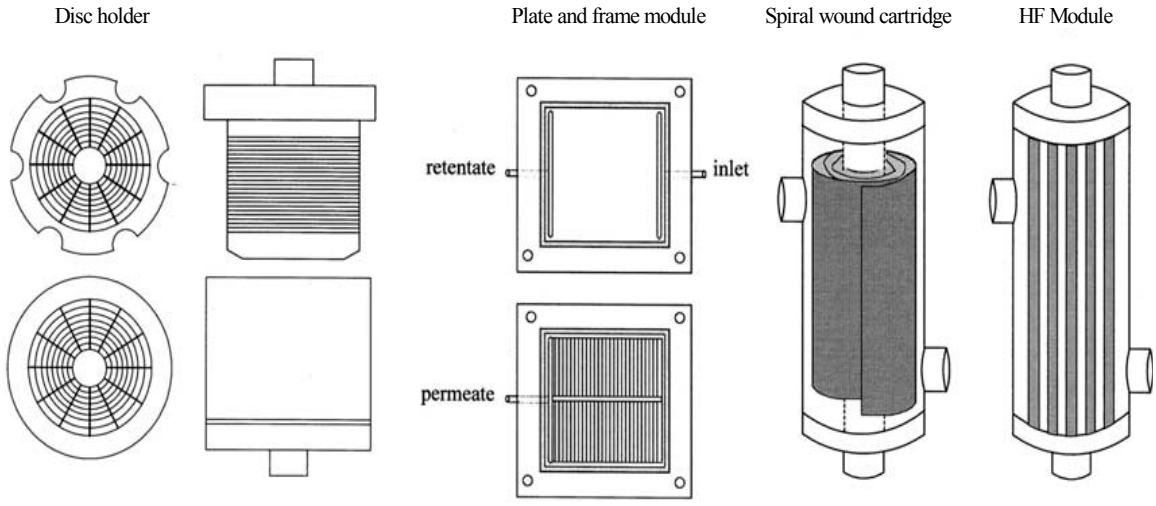

Figure 2-2: Schematic representations of some typical membrane modules [5].

Two important aspects of a membrane module are 1) the actual polymer used in its fabrication and 2) its final form and shape that influence the choice of the module. The design requirements of a particular separation and the mechanism of transport through the membrane will dictate and in many cases limit the material choice, thickness, pore size, etc. [22].

2.3. MEMBRANE BASED METAL AFFINITY SEPARATION

2.3.1. Immobilised metal affinity chromatography

The term immobilised metal affinity chromatography (IMAC) was first coined by Porath [23] to encompass all modes of metal chelation interactions including ligand exchange. IMAC is a separation technique that uses covalently bound chelating compounds on solid chromatographic supports to immobilise divalent metal ions (electron pair acceptors) [23,24]. These cations serve as affinity ligands for various proteins via coordinative binding of surface exposed electron donating amino acid residues [12,23].

In sorption of proteins by metal affinity, the exposed electron-donating amino acid residues (affinity tags), such as the imidazole group of histidine, the thiol group of cysteine and the indoyl group of tryptophan coordinate with the metal ion through non-bonding lone pair electron coordination [12,13]. Other amino acid residues suitable for IMAC are tyrosine, aspartic acid and glutamic acid, which will also contribute to the binding of the immobilised metal ion. IMAC is most suitable for rapid, high throughput isolation of product, however it is not as highly specific as other affinity separation techniques using biological ligands. However, intelligent choice of metal cations, system buffers and the design of recombinant amino acid tags can increase the specificity of this widely used system.

Nevertheless, IMAC holds a number of advantages over biomolecule dependent affinity chromatography techniques, which have a similar order of affinity constants and exploit

affinities between enzymes and their inhibitors, receptors and their ligands or antigens and antibodies. The benefits of IMAC include:

- ligand stability and low cost;
- high protein loading;
- mild elution conditions and simple regeneration;
- quantifiable ligand capacity;
- stability under denaturing conditions.

2.3.2. Immobilised metal affinity membranes

Immobilised metal affinity membranes (IMAM) are one of the most widely used affinity membrane separation techniques [5]. IMAM designs basically follow the IMAC systems described above and hence the properties and applications are very similar. As with bioaffinity membranes, IMAM offers similar advantages to IMAC resins and from a down stream applications point of view, it has great potential for scale-up. Ligand stability and capacity are important parameters that require characterisation and quantification for successful scale-up or commercial applications. Determination of the ligand capacity of the IMAM requires an understanding of the chemistry of the membrane surface functional groups, the nature of the chelating agent, immobilisation method, types of metal ions, and metal ion concentration [13,19,25-27]. Table 2-2 summarises some of the IMAM systems that have used two or more metal ions for protein purification.

2.3.3. Metal chelating ligands

In aqueous environments, metal ions are solvated by surrounding water molecules. The metal ion serves as a Lewis acid and water as a Lewis base. However, when water is replaced by a stronger base, a coordination complex is formed [13]. A molecule with a single donor atom will form a mono-dentate ligand, resulting in a metal complex. A polydentate ligand formed by two or more atoms from the same molecule with a metal ion results in a metal chelate. The binding of a metal ion to a ligand is much stronger in a metal chelate than in a metal complex, due largely to the greater stability arising from the loss of free energy produced by ring formation from the polydentate ligand [28].

There are four different types of dentates that have been investigated as ligands for immobilised metal affinity separation [12,13,28], bidentates (e.g., salicylaldehyde, aminohydroxamic acid), tridentate [e.g., iminodiacetic acid (IDA), ortho-phosphoserine], tetradentate [e.g., nitrilotriacetic acid (NTA), carboxymethylated aspartic acid (CM-Asp)], pentadentate [e.g., *N,N,N'*-tris-carboxymethyl ethylene diamine (TED)]. Multidentates are the most popular chelating agents used in commercial applications and described in research reports [5]. Conventional coupling of reactive groups (such as hydroxyl, amine, etc.) on the membrane surface to dentate chelators usually occurrs via epoxide activation agents such as epichlorohydrin, epibromohydrin and bioxiranes [5,15]. Their chelating mechanism is presented in Figure 2-3.

Table 2-2: Characteristics of some immobilised metal affinity membranes reported in the literature that have investigated the chelation of two or more metal ions with the commercial chelating ligand IDA

Membrane material	Chelator	Ligand capacity	Metal ion	Metal ion capacity	Ligate	Reference
Sartorius hydrophilic copolymer	IDA	-	Cu^{2+} Ni^{2+} Zn^{2+} Co^{2+}	65.75 μmol.cm^{-2} 59.25 μmol.cm^{-2} - -	Lysozyme Myoglobin HSA	25
Glycidyl-4-oxoheptylether modified membrane	IDA	-	Cu^{2+} Ni^{2+} Zn^{2+}	0.48-0.75 mg.ml^{-1} 0.47-0.72 mg.ml^{-1} 0.47-0.73 mg.ml^{-1}	Histidine Tryptophan	27
Sartorius polysulphone membranes	IDA	-	Cu^{2+} Ni^{2+} Zn^{2+}	0.89-0.92 mg.ml^{-1} 0.88-0.93 mg.ml^{-1} 0.89-0.92 mg.ml^{-1}	Histidine Tryptophan	27
Polyglycidyl methacrylate-grafted cellulose membranes	IDA	15 - 150 μmol.g^{-1}	Cu^{2+} Ni^{2+}	- -	BSA, HSA, IgG, bovine liver catalase	8
Regenerated cellulose membranes	IDA	-	Cu^{2+} Ni^{2+} Zn^{2+} Co^{2+} Fe^{2+} Al^{2+} Ca^{2+}	33.4 μmol/disk - - - - -	Penicillin G acylase	29

According to the molecular structure and chelating mechanisms of multidentates, the order for affording a stronger immobilisation with the metal ions should be pentadentate > tetradentate > tridentate [2,13,15,24]. The stronger chelating ability for tetradentate and pentadentate ligands could induce a higher chelate complex stability, thus reducing metal ion leakage. However, the number of coordination sites on metal ions remaining for biomolecule binding will be reduced, causing weaker adsorption [5]. Therefore the order for biomolecule adsorption strength is tridentate > tetradentate > pentadentate.

Triazine dyes such as cibacron blue, cibacron red and procion brown etc., are also capable of chelating metal ions [30]. The immobilised metal ions using these dyes are not as stable as the dentate chelators and the chelator utilisation percentage (CUP) is usually lower. The CUP is defined as the immobilised metal ion capacity divided by the chelator capacity.

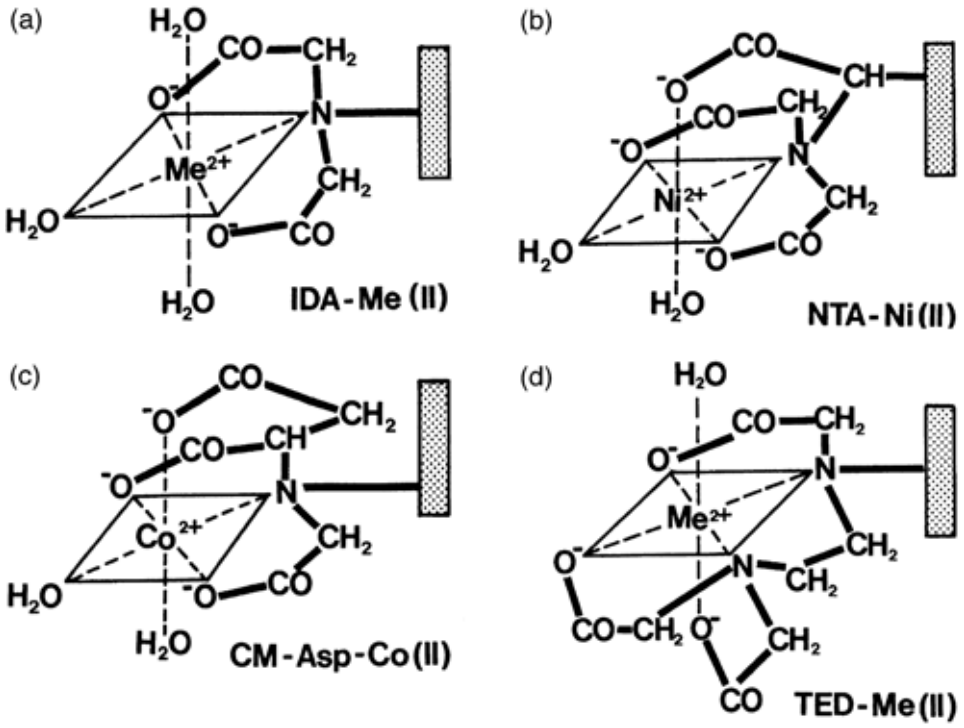

Figure 2-3: Putative structures of some representative chelators in complex with commonly used metal ions. Spacers to the various supports are not specified. [24].

2.3.4. Metal ions

Stable metal immobilisation is also dependent on the selection of a suitable metal ion. According to their reactivity to different nucleophiles, metal ions could be divided into three subcategories: soft, hard and intermediate [6,13]. The soft Lewis metal ions react better with the sulphur atom while the hard Lewis metal ions react better with oxygen-rich groups. Intermediate metal ions (such as Cu^{2+}, Ni^{2+}, Zn^{2+}, Co^{2+} and Fe^{2+}) include mostly the first transition metal series and could couple with S, O and N containing amino acids [5,12,13,24]. The intermediate metal ions Cu^{2+} and $Ni^{2+}$are the most commonly used for immobilised metal affinity separation. When IDA was applied as the chelator, the affinities to the retained biomolecules were in the following order: $Cu^{2+} > Ni^{2+} > Zn^{2+} > Co^{2+}$ [5,19].

2.3.5. Metal ion leaching and regeneration

Metal ion leakage and metal toxicity are important issues particularly with Ni(II) compounds being established as human carcinogens [24]. The role of Ni(II) in carcinogenesis is not clear but molecular models suggest interaction with histones in the cell nucleus, causing DNA damage [31]. Metal ion leaching occurs with every IMAC column, depending on the type of chelator, surface matrix and mode of elution [12,13,15,24,30,32]. In this respect, tetradentate chelators such as NTA or TALON are superior to tridentates. Ni-NTA was reported to exhibit low leaching in the range of up to 1 ppm [33].

The reasons for metal ion leakage at different stages of the affinity separation process differ. During adsorption and washing, the metal ions may be tightly captured by bio-molecules and released into solution, while during elution they may be displaced by salt ions in the elution buffer [5]. In most cases the immobilised metal ion capacity of a column is regenerated by incubation of the affinity membranes in a solution of the metal ion with excellent reusability for multiple experiments [5,33].

2.3.6. Purification of proteins

There are several factors to consider in protein-metal ion interactions [13,28]. The carboxyl, imidazole and sulfhydral side-chain groups are more important in metal ion coordination than are the terminal amino and carboxyl groups. The binding coefficient for metal ions decreases with decreasing pH, since protons begin to compete with the metal for binding to the functional ligand groups (NH_2, S^-, COO^-). The positive charge on the protonated amino group repels the positively charged metal ion, and protonation of sulphide and carboxylate ions negates the attractive force towards the metal ion [13]. Proteins can be released from their bound complexes by any mode which reduces the affinity constant between the immobilised metal ion and the protein such as changing the salt concentration, pH or displacement by a competitive agent that is similar in structure as the amino acid residues involved in the binding.

Many naturally occurring proteins contain histidine residues in their amino acid sequence, however these mildly hydrophobic histidine residues are rarely located on the protein surface. For proteins with known 3D structure, data regarding the number and arrangement of surface histidine residues can be obtained from protein data banks. This is potentially a very useful basis for predicting their behaviour in IMAM applications [24]. Due to the recent advances and successes in the field of proteomics the database of protein primary structure is constantly increasing, but there still remains too little published information regarding surface histidines, to be of immediate assistance in IMAC studies.

Protein purification using IMAC requires that the protein-surface histidine residues must be accessible to the metal ion and the comparatively bulky chelating compound [24]. Usually one histdine is enough for weak binding to IDA-Cu(II), while more proximal histidines are required for binding to Zn(II) and Co (II) [12,13]. A routinely-used strategy in recombinant protein affinity purification involves genetic engineering of a poly(histidine) tag to target proteins. The most popular IMAC approach involves histidine (His) tags of up to six consecutive histidine residues and NTA-Ni(II) columns [34,35].

The advantage of this system is that Ni(II) requires at least two surface histidine residues for efficient binding and since it is very rare to find two naturally occurring protein-surface histidine residues, this IMAC technology becomes much more selective. Histidine

tags are also compatible with all expression systems used today and have been produced in both procaryotic and eucaryotic organisms. The preferable position for the insertion of the His tag (N- or C- terminus) depends on the nature and intended use of the protein and must be determined experimentally [12,24,29]. In most cases His_6 tags are non-immunogenic and do not affect protein folding, nor interfere with the biological functionality of the target protein.

2.4. FUNCTIONALISED MEMBRANES AND BIOCOMPATIBILITY

2.4.1. Ligand coupling chemistry

Affinity matrices are usually hydrophobic and inert, thus requiring covalent attachment of ligands via reactive functional groups (carboxyl, amino and hyroxyl). However, anchoring the ligand molecule to the matrix reduces its freedom to interact with the ligate [13]. The tertiary structure of a native protein in solution also hinders the close approach of many functional ligands on the protein to a metal ion. To counteract this effect, a spacer arm is usually introduced between the matrix and the ligand [6].

There are usually two stages in preparing an affinity matrix; 1) the attachment of a spacer arm to the matrix and 2) the attachment of the ligand to the spacer [17]. The most commonly used strategy for spacer arm coupling to matrices is via cyanogen bromide activation of the vicinal diol groups on surfaces such as agarose, followed by coupling to popular spacer arms e.g. diamines (1,4-butanediamine) or polyhydrazides [36]. Radiation induced graft polymerisation is a popular method for forming polymeric brush layers such as glycidyl methacrylate (GMA) with reactive epoxy groups that can be ligand functionalised [37]. Epoxide activation of matrices is another commonly used method of ligand coupling to inert surfaces.

In most cases, the spacer molecules are pre-attached to the matrix. Choosing the attachment site to a biological ligand can be difficult, as the bound ligand must retain its original affinity for the ligate, so a non-essential reactive site on the biomolecule must be

found. The reaction chemistry employed for ligand coupling to spacer molecules or supports typically involves, 1) attachment by amide formation; 2) succinylation of amino alkyl termini and 3) nucleophilic attachment of a ligand to an activated carboxyl derivative [17].

2.4.2. Surface modification of membranes

The hydrophobic nature of a membrane can be changed into a more hydrophilic one by means of surface modification. A number of surface modification techniques can be applied, and most methods rely on post-treatments of an existing membrane [22]. These techniques include chemical reactions [38], grafting [37], crosslinking [39], plasma treatment [37], *in situ* polymerisation [40] and adsorption [41].

Chemical reactions introduce hydrophilic groups and ionic groups such as sulphonic and quaternary ammonium groups, whereas plasma treatment functionalises surfaces. Both techniques involve structural modification of surfaces and plasma treatment is particularly irreproducible [38,42,43]. However, membranes can also be non-permanently pre-treated with polymeric surfactants by physical adsorption of the polymer, either from a solution onto the membrane or by convective adsorption during filtration of the adsorbent [41,44].

2.4.3. Biocompatibility

Hydrophobic surfaces, associated with most commercial membranes are non-specifically active to the adsorption of a wide range of polymeric material such as biomolecules with hydrophobic components, proteins, lipids, etc. At the molecular level, these diverse bioadhesion manifestations condition the surface for the subsequent adhesion of other biopolymers [45]. As with conventional membrane filtration processes, much effort is being devoted to the development of protein shielding and biocompatible surfaces [46,47,48]. A protein shielding surface reduces non-specific and uncontrolled biomolecule adsorption, thereby increasing the signal to noise ratio for biosensors while maintaining the ligand capacity of affinity membranes.

Many strategies have been employed to produce protein shielding surfaces such as the development of polymer adducts such as poly(ethylene imine) and poly(ethylene glycol) [49]. Grafted poly(ethylene glycol) (PEG) chains [39] and tethered ligands have also been developed to improve the biocompatibility of potential colloidal drug carriers [43,50,51].

The use of PEG based non-ionic surfactants such as the Pluronic tri-block copolymers is also becoming popular. Pluronic® (BASF, Corp) are a group of poly(ethylene oxide) (PEO)-poly(propylene oxide) (PPO)-PEO surfactants that are being widely studied for applications in the pharmaceutical and medical industry because of their unique surfactant abilities and their low toxicity and immunogenic behaviour [52-54]. Pluronic copolymers also have the ability to suppress protein adsorption and platelet adhesion due to their PEO segments [54].

Several members of the Pluronic family have been reported to adsorb onto hydrophobic surfaces in a pseudo-irreversible way, forming complexes that have long term stability [9,55]. Despite the interest in numerous applications of this surfactant, few studies have dealt with the chemical modification and interfacial analysis of the resultant derivative. Studies by Li *et al.*, [9] and Ho *et al.*, [56] have demonstrated the covalent coupling of bioaffinity ligands to these surfactants and have studied the adsorption behaviour on solid matrices. A technique of adsorbing ligand derivatised Pluronic surfactants onto polystyrene latex spheres [9] has also opened an interesting research area to improve the biocompatibility of polymeric ligand-modified affinity-matrices.

2.5. REFERENCES

1. D.K. Roper, E.N. Lightfoot, J. Chromatograph. A. **702** (1995) 3.
2. M. Feins, K.K. Sirkar, J. Mem. Sci. **248** (2005) 137.
3. E. Lightfoot, J.S. Moscariello, Biotechnol. Bioeng. **87**(3) (2004) 259.
4. M. Martina, G. Subramanyam, J.C. Weaver, S. Valiyaveettil, Biomaterials **26**(28) (2005) 5609.
5. S-Y. Suen, Y-C. Liu, C-S. Chang, J. Chromatogr. B. **797** (2003) 305.
6. J. Porath, J. Chromatogr. **218** (1981) 241.
7. S. Govender, E.P. Jacobs, W.D. Leukes, V.L. Pillay, Biotechnol. Lett. **25** (2003) 127.
8. X.J. Yang, A.G. Fane, C. Pin, Chemical Eng. Journal. **88** (2002) 45.
9. J-T. Li, J. Carlsson, J-N. Lin, K.D. Caldwell, Bioconjugate Chem. **7** (1996) 592.
10. P. Cuatreccas, M. Wilchek, C.B. Anfinsen, Biochemistry **61** (1968) 636.
11. D.G. Castner, B.D. Ratner, Surf. Sci. **500** (2002) 28.
12. J. Porath, B. Olin, Biochemistry **22** (1983) 1621.
13. J.W. Wong, R.L. Albright, N-H.L. Wang, Separation Purif. Methods. **20**(1) (1991) 49.
14. K. Terpe, Appl. Micriobiol. Biotechnol. **60** (2003) 523.
15. G.S. Chaga, J. Biochme. Biophys. Methods. **49** (2001) 313.
16. E. Klein, J. Mem. Sci. **179** (2000) 1.
17. W.H. Scouten, Affinity Chromatography. John Wiley & Sons, New York, **49** 1981, p.20.
18. P. Matejtshuk. Affinity Separations: A practical approach. Oxford University Press, 1997, p.4.
19. J. Porath, J. Carlsson, I. Olsson, G. Belfrage, Nature **258** (1975) 598.
20. M.A. Teeters, T.W. Root, E.N. Lightfoot, J. Chromatogr. A. **944** (2002) 129.
21. Q.S. Yuan, A. Rosenfeld, T.W. Root, E.N. Lightfoot, J. Chromatogr. A. **831** (1991) 149.
22. K. Scott, Handbook of industrial membranes. Elsevier Science Publishers Ltd, Oxford, 1995, p.94.
23. J. Porath, Nature **218** (1968) 1302.
24. V. Gaberc-Porekar, V. Menart, J. Biochem. Biophys. Methods. **49** (2001) 335.
25. O-W. Rief, V. Nier, U. Bahr, Freitag, J. Chromatogr. A. **664** (1994) 13.

26. N. Labrou, Y.D. Clonis, J. Biotechnol. **36** (1994) 95.
27. K. Rodemann, E. Staude, Biotechnol. Bioeng. **46** (1995) 503.
28. J-C. Janson, L. Ryden, Protein purification: principles, high resolution methods and applications. VCH Publishers, USA, p.275.
29. Y-C. Liu, S-Y. Suen, C-W. Huang, J. Mem. Sci. **251** (2005) 201.
30. C-Y. Wu, S-Y. Suen, S-C. Chen, J-H. Tzeng, J. Chromatogr. A. **996** (2003) 53.
31. W. Bal, H. Kozlowski, K.S. Kasprzak, J. Inorg. Biochem. **1475** (2000) 163.
32. Y-H. Tsai, M-Y. Wang, S-Y. Suen, J. Chromatogr. B. **766** (2001) 133.
33. F. Schäfer, J. Blümer, U. Römer, K. Steinert, QIAGEN News. (2000) 11.
34. E. Hochuli, H. Doebeli, A. Schnacher, J. Chromatogr. **411** (1987) 177.
35. E. Hochuli, W. Bannwarth, H. Doebeli, R. Gentz, D. Stueber, Bio/Technology. (1988) 1321.
36. E.S. Severin, S.N. Kochetkov, M.V. Nesterova, N.N. Gulyaev, FEBS Lett. **49** (1974) 61.
37. T. Kawai, K. Sato, W. Lee, J. Chromatogr. B. **790** (2003) 131.
38. J.A. Howell, V. Sanchez, R.W. Field, Membranes in bioprocessing: Theory and applications. Chapman & Hall, Cambridge, 1993, p.25.
39. F-Q. Nie, Z-K. Xu, P. Ye, J. Wu, P. Seta, Polymer **45** (2004) 399.
40. C, Qiu, F. Xu, Q. Nguyen, Z. Ping, J. Mem. Sci. **255** (2005) 107.
41. A.G. Fane, C.J.D. Fell, K.J. Kim, Desalination. **53** (1985) 37.
42. W. Shi, F. Zhang, G. Zhang, J. Chromatogr. B. **819** (2005) 301.
43. W. Shi, F.B. Zhang, G.L. Zhang, D.T. Ge, Q.Q. Zhang, Polymer Internat. **54** (2005) 790.
44. K.J. Kim, A.G. Fane, C.J.D. Fell, Desalination **70** (1988) 229.
45. P. Kingshott, H.J. Grissier, Curr. Opinion Solid State Mat. Sci. **4** (1999) 403.
46. I.Y. Galaev, B. Mattiasson, Bio/Technology. **12** (1994) 1086.
47. A. Nilsson, C. Fant, M. Nyden, K. Holmberg, Colloids Surfaces B. **40** (2005) 99.
48. T. Segura, P.H. Chung, L.D. Shea, Biomaterials **26**(13) (2005) 1575.
49. B. Brink, E. Oesterberg, K. Holmberg, F. Tiberg, Colloids Surfaces B. **66** (1992) 123.
50. U. Rädler, J. Mack, N. Persike, G. Jung, R. Tampé, Biophysical Journal **79** (2000) 3144.
51. M. Malmsten, J.M. van Alstine, J. Colloid Inter. Sci. **177** (1996) 502.
52. H.J. Chung, D.H. Go, J.W. Bae, K.D. Park, Current Appl. Phys. **5**(5) (2005) 485.

53. R. Lin, L.S.Ng, C-H. Wang, Biomaterials **26**(21) (2005) 4476.
54. A. Higuchi, K. Sugiyama, T. Shirai, Biomaterials **24** (2003) 3235.
55. R. Veen, K. Fromell, K.D. Caldwell, J. Colloid Interface Sci. **288** (2005) 124.
56. C-H. Ho, L. Limberis, K.D. Caldwell, R.J. Stewart, Langmuir **14** (1998) 3889.

CHAPTER 3: FABRICATION AND CHARACTERISATION OF MODEL MEMBRANE AFFINITY MATRICES

3.1. INTRODUCTION

The choice of a polymer material for synthetic membrane fabrication is often based empirically, i.e. membranes have been developed for a wide range of applications, instead of developing a membrane for a certain class of applications, such as in bio-process applications [1]. A number of techniques are available to prepare synthetic polymeric membranes [2-4]. Some of these techniques can be used to prepare organic as well as inorganic membranes, but the choice of material limits the preparation technique employed [1]. Most commercial filtration membranes are prepared by phase inversion techniques, either by immersion precipitation or by thermal induced phase separation [4,5].

Developing membranes for specific applications requires an understanding of the material properties, and a study in relation to the intended application. However, the poor hydrophilicity and biocompatibility of many membranes limit their application in downstream bioaffinity processes [6]. Therefore the surface properties of a membrane, which is being used as an affinity matrix must be characterised to explain its interactions with polymers and its suitability for a particular application.

A distinction must be made between porous and nonporous membranes as these have different characteristics and fields of application [7]. Similarly, characterisation methods can be conveniently divided into two areas, for porous and nonporous membranes. For studying bioaffinity separation using Pluronic affinity linkers [8], membrane matrices should ideally be nonporous and inert with a well-defined surface structure before and after surface modification while exhibiting non-specific protein-shielding properties.

Typically a porous membrane will be characterised for its filtration properties while nonporous membranes are of dense polymeric composition, without pores and separation is thus dependent upon the material properties and morphology [4]. In chromatographic

applications porous membrane techniques involve the solid polymeric phase that usually has a liquid phase on either side, physically connected by the membrane pores. The transfer of macromolecules from one liquid phase (feed) to another (filtrate) is usually pressure driven and the target analytes such as biomolecules are concentrated in the filtrate [1]. However, nonporous membranes have many applications in techniques such as solid phase extraction chromatography and as affinity strips for protein immobilisation [7].

Several fundamental studies of polymer adsorption on membranes have investigated the effects of membrane surface properties such as pore size distribution, surface roughness and structure, electrokinetic characteristics, chemical properties and specific chemical structure [9,10,11]. A wide variety of analytical techniques have been used for elucidating specific chemical and physical properties of membranes and polymer films. Some of these include Raman spectroscopy (structure) [9], AFM (surface roughness, structure, topography) [12,13], electron microscopy (qualitative information on surface structure, pores, topography) [11,14], streaming potential measurements (membrane surface zeta potential) [9], XPS and FT-IR (surface chemical functional groups) [15] and surface tension (hydrophobicity) [16].

Although there are several robust techniques available for the characterisation of membrane surface morphology, no single technique can fully characterise membrane surface substructure [10]. Complete characterisation can only be achieved by a combination of techniques. To be of significance to the membrane industry these techniques should preferably be rapid, routinely available, inexpensive and non-invasive [9].

This study involved the preparation and partial characterisation of candidate polymeric membranes polysulphone (PSU), poly(vinylidene fluoride) (PVDF) and poly (ether imide) (PEI) for use as affinity adsorbent matrices. Detailed knowledge of the surface properties of these membrane supports would contribute to the understanding of the interactions of affinity ligands and biomolecules with the attendant membrane matrix.

3.2. EXPERIMENTAL

3.2.1. Reagents and chemicals

Pluronic® F108 with an average molecular mass of 14 600 daltons was obtained from BASF (Germany). Hexane, chloroform and 2-propanol were purchased from Merck NT laboratory suppliers, SA. Unless otherwise stated, all chemicals were obtained from Merck.

3.2.2. Membrane fabrication and module construction

Planar nonporous membranes were cast from solutions containing 27% [m/m] (PSU, PEI and PVDF) respectively and 73 % (m/m) *N*,*N*-Dimethylacetamide (DMAc). PSU and PEI were dissolved in DMAc by rotating the solution container for more than 48 h at room temperature to obtain a homogeneous solution. PVDF required sonication in an ultrasonic water bath for 30 min and further heat treatment at 55˚C for 48 h to dissolve. The solutions were then degassed before being used to cast the 200 μm planar membranes. Nonporous hollow fibre (HF) and hollow fine fibre (HFF) membranes and externally unskinned ultrafiltration (UF) membranes were produced by the phase inversion technique [3,4] using a dry-wet spinning process [2]. The dimensions of the capillary membranes were measured using an optical light microscope with a vernier scale and these measurements were verified with scanning electron microscopy (SEM).

The asymmetric nonporous HF capillary membranes were encased in a perspex shell. The multi-capillary membrane module (MCMM) was assembled by potting the capillary membranes and was left to set so that the capillaries were taut. An O-ring was inserted into the membrane module and then the end cap was threaded into the shell.

3.2.3. Solvent compatibility

The physical integrity of the membranes and the Perspex module was investigated in various commonly used cleaning and sterilisation solvents. This involved incubating each membrane in solutions of $CHCl_3$, hexane, 2-propanol, urea (8 M), formaldehyde (4 %), ethanol (40 %) and sodium hypochlorite (0.2 M) for ~30 min. The membranes were then analysed with SEM and FT-IR for morphological and chemical changes on the membrane surface.

3.2.4. Membrane coating

In order to compare the adsorption properties of the fibres with the 1 cm^2 flat sheets, the lengths of the fibres were prepared such that the external surface area was equivalent to 1 cm^2. Capillary and planar membranes (1 cm^2 external surface area) were stored in aqueous 0.04 M sodium azide solutions to prevent microbial growth. Prior to adsorption, membranes were washed overnight in sterile, deionised water, followed by three further washes with deionised water. Membranes were then sonicated three times in sterile deionised water in an ultrasonic bath for 5 min followed by drying in a laminar flow cupboard. Dry membranes were statically incubated in 5 $mg.ml^{-1}$ Pluronic F108 solutions in water at 20°C for 8 to 12 h. The coated membranes were then removed from solution, washed three times in deionised water and dried in a sterile laminar flow unit.

3.2.5. Infra-red spectroscopy

Photo-acoustic Fourier transform infra-red (FT-IR) spectroscopy is based on the principle that modulated infra-red (IR) radiation striking the sample surface causes the surface to alternately heat and cool with IR adsorption [17]. The advantages of using photo-acoustic spectroscopy for membrane analysis are that minimal sample preparation is required and the capability of studying opaque samples and depth profiling is also possible. The surface chemical composition of the membranes was verified using photo-acoustic FT-IR. Up to 128 scans at a scan range of 450 to 4000 cm^{-1}, were performed on each membrane

with a resolution factor of 8. A Perkin Elmer Paragon 1000 PC spectrophotometer was used for all solid-state infra-red analysis.

3.2.6. Scanning Electron Microscopy

Membranes were fixed for 2 h in 5 % (v/v) glutaraldehyde in 0.1 M phosphate buffer at 4°C and pH 7.5, after which the sections were dried in water:ethanol mixtures of 20, 40, 60, 80 and 100 % ethanol. Cross-sections of the membranes were prepared by freeze fracturing using liquid N_2. A Leo 1430VP SEM, fitted with backscatter, cathodoluminescence, variable pressure and energy dispersive detectors, as well as a Link EDS system and software for microanalysis and qualitative work was used to generate images of the membrane surfaces.

3.2.7. Atomic Force Microscopy

Atomic force microscopy (AFM) has been routinely used for the characterisation of filtration membranes, surface-colloid interactions and affinity ligands [13,14]. In the intermittent contact mode, the cantilever is oscillated vertically at high frequency during raster scanning. A topographical map was obtained by scanning with a silicon nitride tip attached to a cantilever over the membrane surface, while maintaining a constant force between the tip and the sample. The deflection of the tip and cantilever was measured optically using a reflected laser light beam off the back-face of the cantilever (AFM, TMX 2000 Explorer, Topometrix, Santa Barbara, CA).

3.2.8. Contact angle analysis

Contact angles for the planar membranes were calculated using the sessile drop technique. The measurement of contact angle, θ, provides information on the interaction of a liquid with a solid through Young's equation [18] $\gamma_{SV} = \gamma_{SL} + \gamma_{LV} \cdot \cos\theta$, where γ represents the interfacial tensions of solid and liquid. The experimental set-up incorporated a Nikon PUNiX video camera equipped with Nikon microscope objectives and adjustable vernier

scales. The camera was connected to a video recorder and the real-time image was provided on a monitor (Figure 3-1). The substrates were placed on an adjustable horizontal platform and droplets of water were deposited from a syringe. The narrow bore UF membranes; HF and HFF nonporous membranes were analysed using a Wilhelmy slide technique with deionised H_2O as the solvent.

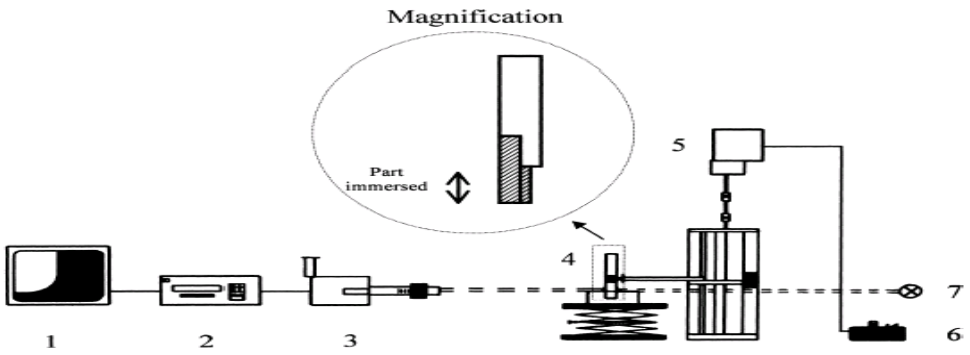

Figure 3-1: Experimental set-up of a movable platform and a CCD camera for static contact angle analysis. 1, computer; 2, video recorder; 3, camera; 4, chamber; 5, syringe facility; 6, adjustable stage; 7, optical windows.

3.3. RESULTS AND DISCUSSION

3.3.1. Planar nonporous membranes

When interactions between membranes and macromolecules are attractive, the latter adsorb on the pore walls, generally at a large number of interaction sites per molecule, which stabilise the molecule on the surface. The shear forces induced by conventional cross-flow filtration are generally not strong enough to overcome this attraction, hence the adsorbed macromolecules remain attached to the pore walls. This typical fouling mechanism, which is based on attractive interactions, could severely hamper reliable interfacial analysis of Pluronic-modified membrane-based affinity separation systems. Even if electrostatic repulsive interaction occurs between membranes and macromolecules, in practise proteins adsorb onto porous membrane material irrespective of the surface charge due to hydrogen bonding and hydrophobic attraction, which would overcome the electrostatic repulsion.

To avoid the aforementioned experimental bottlenecks, nonporous planar membranes were selected as potential affinity matrices for the study of Pluronic adsorption and affinity separation described in this and the following chapters. Using commercially available polymers such as PSU, PVDF and PEI, nonporous membranes were fabricated using a 27 % (m/m) solution of polymer in DMAc. Said membranes were prepared by an immersion precipitation technique [3] where a 27% (m/m) polymer solution was immersed in the non-solvent (deionised H_2O) bath and the composition shifted to the demixing region. By controlling these conditions, it was then possible to repeatedly produce asymmetric nonporous membranes with a characteristic dense top layer.

The PVDF polymer is of increasing scientific and industrial significance because of its outstanding electrical properties (piezoelectricity), chemical resistance, durability and its biocompatibility in soft tissue applications [19,20,21]. PVDF exists in at least three main crystalline forms, designated as α (form II), β (form I) and γ (form III), and also in a minor phase, designated as δ [20,21]. Each of these forms is distinguished by the conformation of the C-C bonds along the chain backbone. The α and γ phase can be

obtained from solution deposition while the oriented β phase can be produced by stretching a PVDF film [20].

The α phase of PVDF has a unique IR absorption band at 763 cm^{-1} (Figure 3-2), which was baseline separated from the other peaks. Other relevant peaks in Figure 3-2 that correlate to the α phase are the vibration bands at 532 cm^{-1} (CF_2 bending), 763 cm^{-1}, 613 cm^{-1} (CF_2 bending and skeletal bending), 792 cm^{-1} (CH_2 rocking). According to Benz and Euler [20] the β and γ crystalline phases resembled each other structurally and spectroscopically, making differentiation difficult. The vibration band at 840 cm^{-1} can be assigned to the β form.

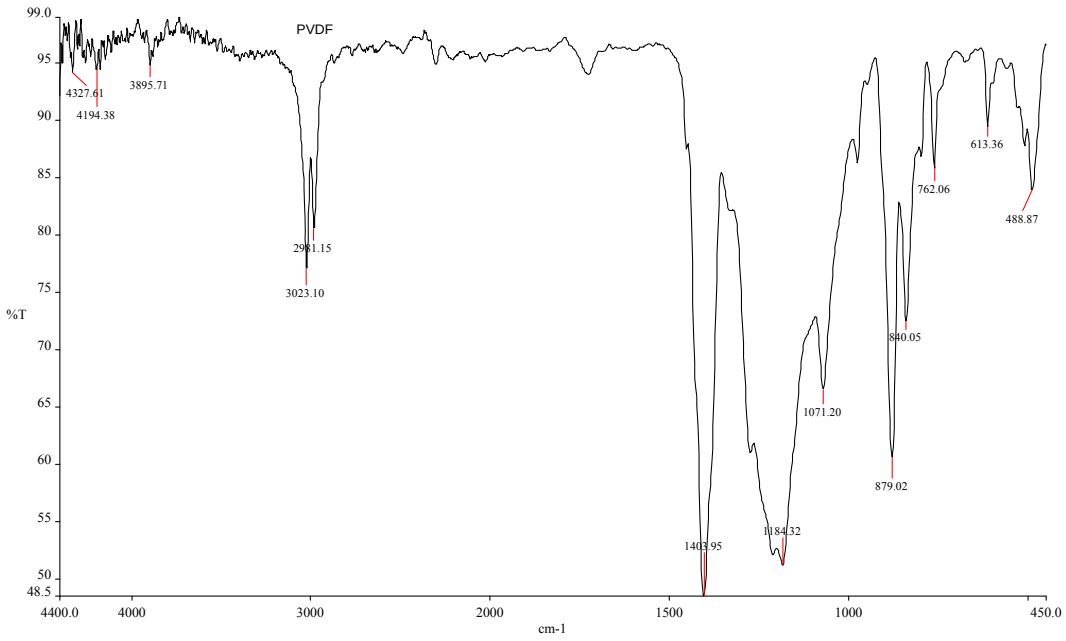

Figure 3-2: FT-IR spectrum of PVDF.

Photo-acoustic FT-IR spectra were also generated for PEI and PSU membranes (Figure 3-3). The imide group of PEI displayed four characteristic absorption bands at 1780 cm^{-1}, ν_s C=O 1725 cm^{-1}, ν_{as} C-O 1358 cm^{-1} and a possible ν C-N band at 745 cm^{-1}. The vibrations bands in the region 3700 to 2000 cm^{-1} were characteristic of PSU where the two triplet peaks around 3100 and 2950 cm^{-1} corresponded to the C-H stretching vibration of the carbon sp^2 and sp^3 hybrid in the aromatic system respectively [15].

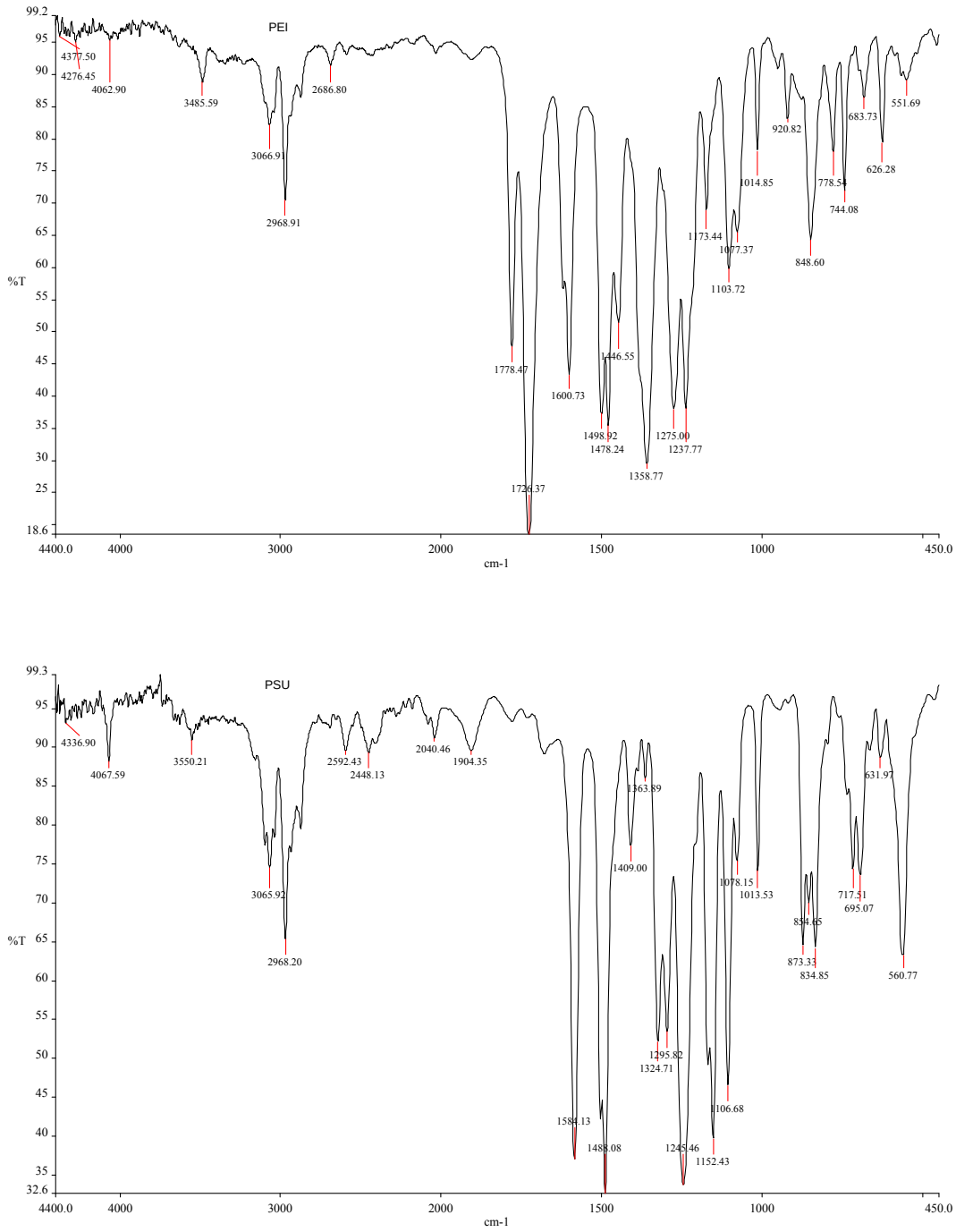

Figure 3-3: FT-IR spectra for native PEI and PSU membranes.

Membrane hydrophobicity can be determined by measuring the contact angle (θ) between the membrane and a solvent such as deionised H_2O (dH_2O). The angle, according to Young's equation depends on the interfacial tensions (γ) of the interfaces involved [1]. Contact angle analysis for native planar nonporous membranes is described in Table 3-1. Static contact angle measurements indicate that of the three candidate membranes under

investigation, PVDF appeared to be the most hydrophobic, while PEI was comparatively hydrophilic. It is expected that the surface hydrophobicity of the membranes would feature significantly in the development of affinity linkers using amphiphilic surfactants such as Pluronic® F108, which are based on non-covalent intermolecular interactions.

Table 3-1: Static contact angle analysis of native planar nonporous PVDF, PEI and PSU membranes

Polymer Type	Contact angle	±SD	*N*
PVDF	66.61°	2.35	6
PEI	51.38°	2.82	6
PSU	57.74°	1.81	6

Qualitative information on membrane surface structure, and the effect of solvents on membrane integrity was investigated by SEM imaging. Initial surface analysis was performed using the energy dispersive X-ray spectroscopy (EDX) feature of electron microscopy. While these planar membranes are difficult to distinguish from the Pluronic coated membranes at the microscopic level, SEM is still the standard analytical instrument for membrane morphology characterisation [22]. A low vacuum mode of operation was followed for much of the analysis to minimise artefacts.

The SEM images in Figure 3-4, depict fairly heterogeneous surfaces, with thin (nano scale) abrasions on the surface. This was a consequence of the fabrication process of the candidate planar membranes, where a stainless steel bar and a 2 mm spacer blade were used to spread the polymer films to form membranes. After coating with 5 $mg.ml^{-1}$ Pluronic solutions, more homogenous and smoother surfaces were noticed. The adsorbed Pluronic 'masking' of the inherent markings on the native membrane suggest that Pluronic adsorption was uniform over the 1 cm^2 membrane surface.

AFM analysis was performed under hydrated conditions, with the less destructive intermittent contact mode or 'tapping mode'. This involved performing vertical oscillations with the cantilever across the membrane surface using a constant force. The atomic force micrographs in Figure 3-5 and the attendant force curves suggest that the

average surface roughness decreases with Pluronic modification of the surface. A similar trend was observed with PVDF and PEI membranes.

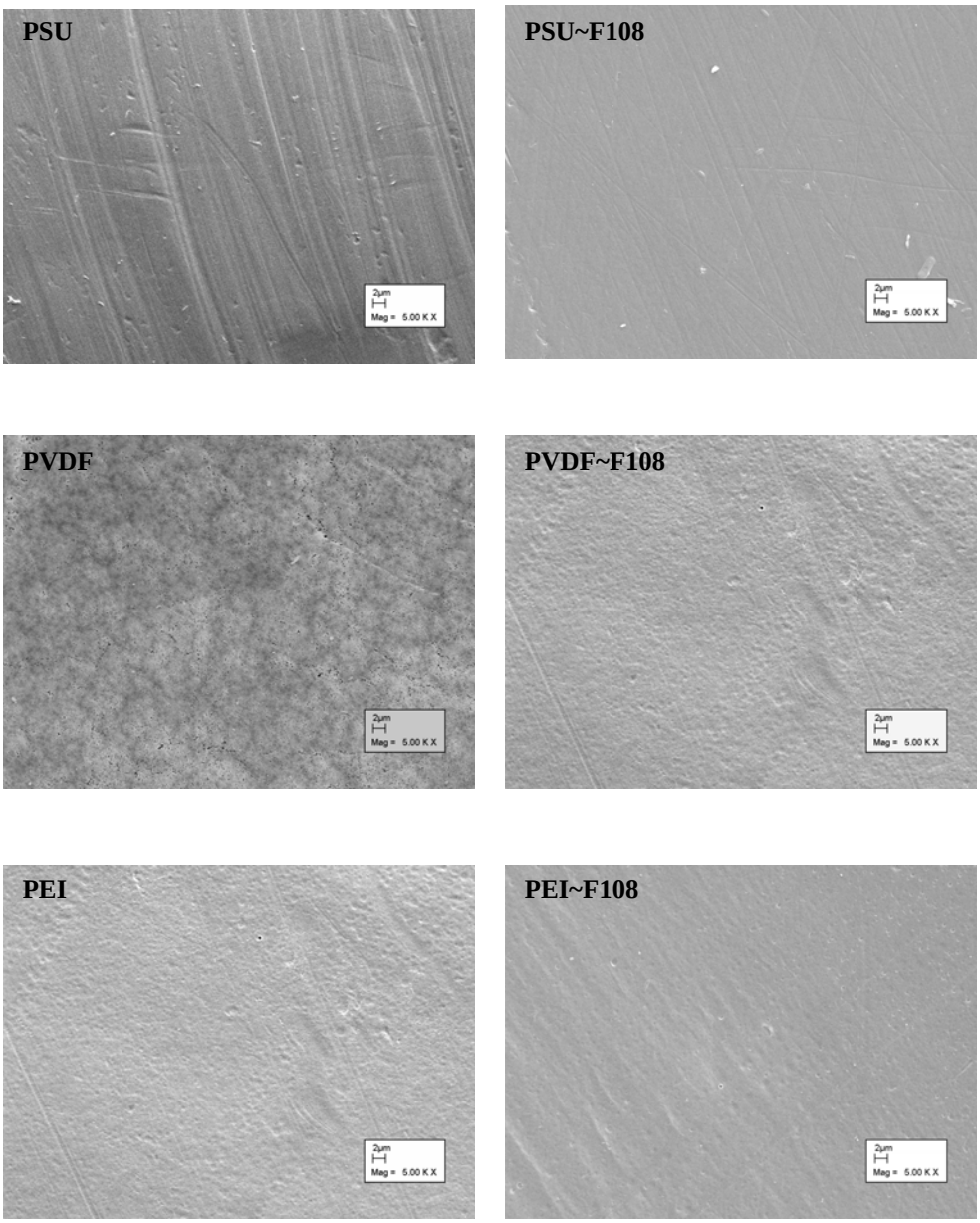

Figure 3-4 Electron micrographs showing native polymeric membranes (PSU, PVDF and PEI) and typical Pluronic coated membranes (PSU~F108, PVDF~F108 and PEI~F108). Bar = 2μm.

Production of smooth membranes, are not essential for affinity separation or filtration. Conversely, a rough surface is potentially more advantageous due to the larger surface area to volume ratio, which would favour surfactant adsorption. However, solid-state

analytical instruments (AFM, RBS and to a lesser extent XPS) are sensitive to rough surfaces that contribute background 'noise' which can hinder accurate measurements.

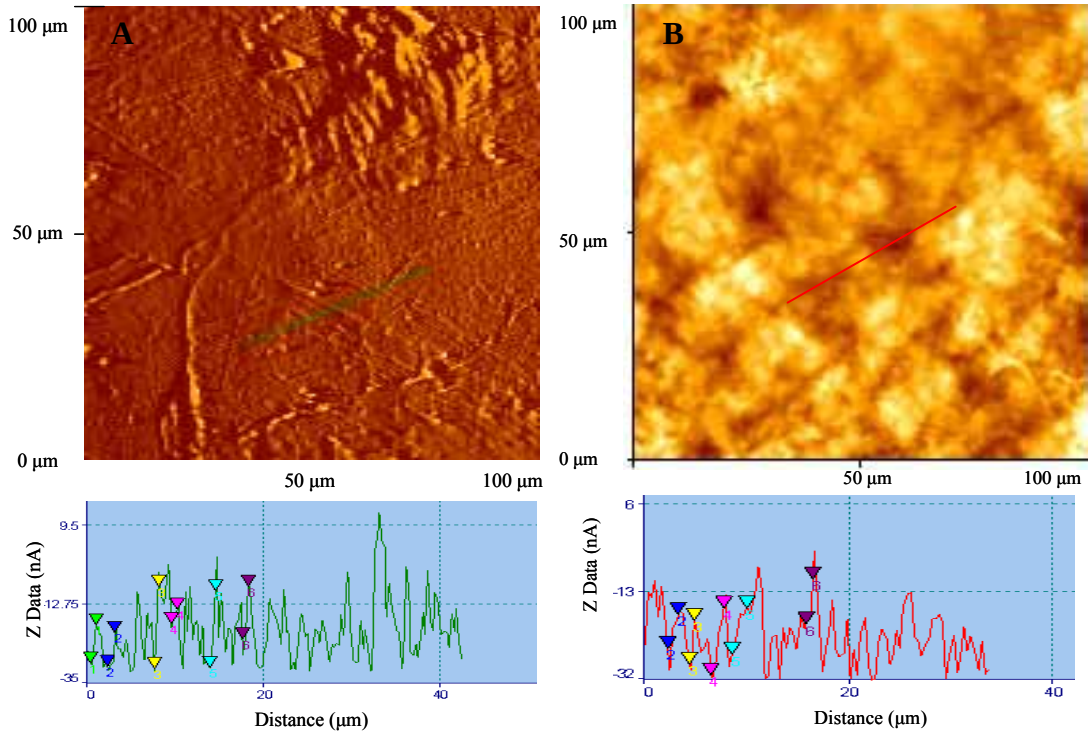

Figure 3-5: Atomic force topographical micrographs showing A) Native PSU membrane and B) Pluronic modified PSU surface. The insets beneath each figure represent force distance curves, which indicate the surface roughness.

The integrity of the native membranes was evaluated against organic solvents that were envisaged to be used during modification (displacement) of the surface adsorbed Pluronic or during affinity immobilisation of proteins. At the outset of the study solvents such as ethanol, urea, hexane, 2-propanol, chloroform and ethyl acetate were considered as agents or as buffer components for chemical treatment of surfactant-modified membranes.

Planar 1 cm^2 membrane sections were immersed in the different solvents at 20 and 70ºC, dried and examined with SEM. The membranes appeared to be stable in all of the solvents tested while PVDF and PSU showed similar characteristics except when incubated in $CHCl_3$. $CHCl_3$ treated PVDF membranes showed melting or widening of the nanometer size 'pores' detected on native PVDF surfaces (Figure 3-6). These results were similar to chemical reactivity assays performed by Momtaz *et al.*, [23] on commercial

"Durapore" PVDF microfiltration membranes. FT-IR analysis confirmed the stability of the native chemical groups on all the membranes subjected to solvent treatment.

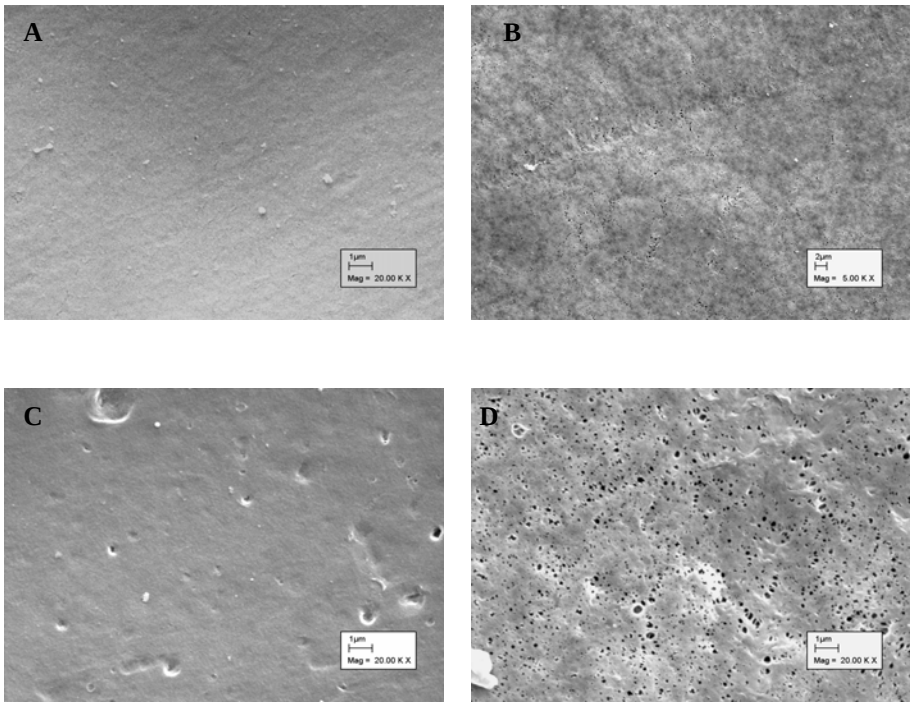

Figure 3-6: Hexane-isopropyl alcohol treated PSU and PVDF (A and B) and $CHCl_3$ treated PSU and PVDF (C and D) membranes. Bar = 1 μm.

3.3.2. Capillary membranes

The externally unskinned UF capillary membranes were produced according to the methodology of Jacobs and Leukes [2]. The fabrication conditions for the nonporous capillary membranes are listed in Table 3-2. These membranes (Figure 3-7) were spun into an aqueous solvent external contact bath containing a small percentage deionised water. The dimensions of the capillaries are listed in Table 3-3 and these membranes were stored in a cool dry cylinder at ambient temperature.

Surface tension analysis using a Wilhelmy slide technique was performed on the capillary membranes. Dynamic contact angle analysis (Table 3-4) revealed that the nonporous HF and HFF membranes were of similar surface hydrophobicity while the externally porous (unskinned) UF capillaries were slightly more hydrophobic, but with a larger discrepancy

between the advancing and receding contact angles. This dynamic contact angle hysteresis is typical of polymeric surfaces and the hysteresis described in Table 3-4 is most likely due to a combination of membrane surface roughness and porosity, particularly with the externally unskinned UF membranes.

Table 3-2: Parameters for nonporous capillary membrane production using the dry/wet spinning process

Parameter	Details
Spinning solvent	*N*,*N*-Dimethylacetamide
Coagulation solvent	94% solvent and 6% deionised water
Lumen solvent	Deionised water
Coagulation bath temperature	25 ºC
Extrusion rate of polymer	2.9 m.min^{-1}
Bore fluid flow rate	5.5 ml.min^{-1}
Residence time in air gap	2.5 s
Polysulphone concentration	27% (m/m)

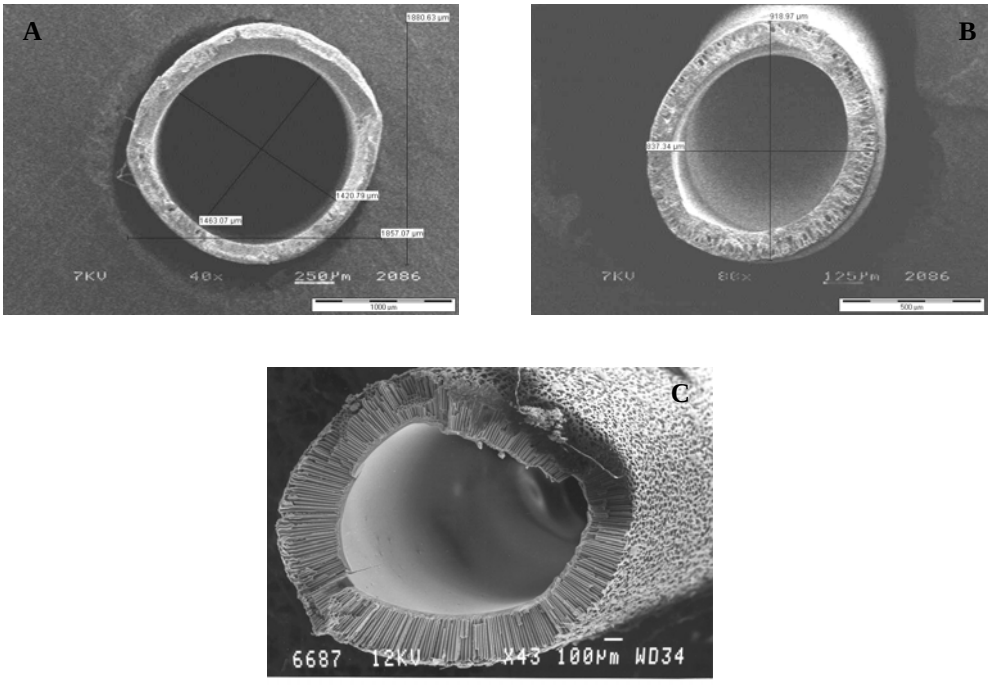

Figure 3-7: Electron micrographs of A) nonporous hollow fiber, B) nonporous hollow fine fiber and C) externally unskinned ultrafiltration PSU membranes.

Table 3-3: Dimensions and characteristics of the membranes used for construction of the capillary modules, with the external surface area (A_s), lumen surface area (A_L) and the volume (V_i)

Membrane Type	ID (mm)	OD (mm)	Wall (mm)	A_S (mm^2)	A_L (mm^2)	V_i (mm^3)
HFF	0.66	0.88	0.22	60.82	45.62	7.53
HF	1.44	1.87	0.43	129.15	99.66	35.83
UF	1.04	2.0	0.48	138.23	71.88	18.69

Table 3-4: Dynamic contact angle analysis of the capillary membranes

Membrane Type	$\theta_{advancing}$	±SD	$\theta_{receding}$	±SD	*N*
Hollow Fibre	79.69°	2.75	37.16°	2.72	3
Hollow Fine Fiber	79.32°	6.80	38.24°	3.78	3
UF Capillary	83.37°	5.08	26.42°	2.23	3

3.3.3. Construction of capillary membrane modules

Single-capillary membrane modules (SCMM) and multi-capillary membrane modules (MCMM) were constructed for two reasons:

1. to perform interfacial analysis of Pluronic adsorbed at curved interfaces [16] and
2. to enable testing of a laboratory scale multi-capillary membrane affinity separation system, coupled to an automated liquid chromatography system.

The SCMM (Figure 3-8A) was used to study the effects of interfacial curvature on Pluronic adsorption by slowly re-circulating a 5 $mg.ml^{-1}$ solution of Pluronic F108 within the lumen (concave interface) and the external wall of the membrane (convex interface).

These inexpensive membrane units were convenient to work with, easy to set up and dismantle and have a simple geometry that is well characterised [24,25].

The nonporous HFF and capillary membranes were encased in a clear Perspex shell and potted (glued) with a commercially available epoxy resin. The epoxy resin was allowed to set for at least 24 h before the membranes were pressure tested. The MCMM (Figure 3-8B) comprised 30 PSU HF capillary membranes with a total internal surface area of 3875.50 mm^2. The dimensions of the MCMM (Table 3-5) were compatible with a commercial fast protein liquid chromatography (FPLC) system, AKTA Prime (Amersham) such that it could be coupled to said FPLC as a column.

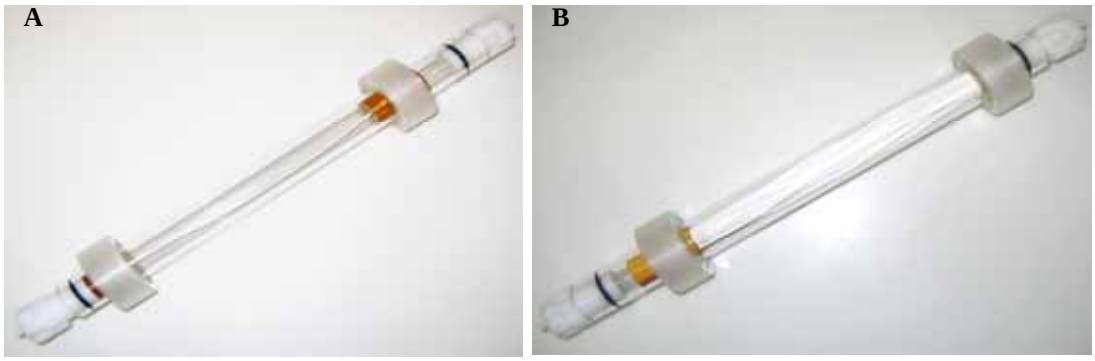

Figure 3-8: The single capillary membrane module (SCMM) and the multi-capillary membrane module (MCMM), A and B respectively.

Table 3-5: Dimensions of the Perspex capillary membrane module

Capillary membrane module	Dimensions
Shell Length	300 mm
Shell ID	19.5 mm
Shell OD	25.25 mm
Extra-capillary module volume	89594.30 mm^3

3.4. CONCLUSIONS

Synthetic polymeric membranes were fabricated using the immersion precipitation technique to manufacture nonporous planar and capillary membranes of reproducible physical and chemical composition. The surface chemistries of the membrane polymers were verified using photo-acoustic FT-IR analysis. Surface hydrophobicity was calculated using static and dynamic contact angle analysis for the planar and capillary membranes respectively. The membrane surface hydrophobicity was of the order PVDF > PSU > PEI. The candidate membranes chosen in this study have rough surfaces that are inherent to the fabrication conditions used. However, microscopy analysis (AFM and SEM) suggested that membrane surface roughness was found to decrease after surface modification in 5 $mg.ml^{-1}$ aqueous Pluronic F108 solutions.

PVDF membranes were found to be susceptible to damage after prolonged incubation in $CHCl_3$, while the membranes were relatively stable in the other solvents used in the investigation. The Perspex module used to encase the HF capillaries was unstable in solutions of hexane and 2-propanol. Using a Perspex shell and adjustable endcaps, single and multi-capillary membrane modules were constructed for interfacial curvature analysis and scale-up studies.

In summary, the partial characterisation using SEM, AFM, FT-IR and contact angle analysis, provided a better understanding of the mechanical and chemical properties of the affinity membrane matrix. This is of importance in future studies directed towards investigating the adsorption behaviour of Pluronic, bioligands and proteins at the membrane-liquid interface. Additionally, the physical and chemical nature of the membranes is also a factor that determines the success of solid-state spectrophotometric analysis.

3.5. REFERENCES

1. J.A. Howell, V. Sanchez, R.W. Field, Membranes in bioprocessing: Theory and Applications. Chapman and Hall. Cambridge, 1993, p.203.
2. E.P. Jacobs, W.D. Leukes, J. Mem. Sci. **121** (1996) 149.
3. S. Kazama, M. Sakashita, J. Mem. Sci. **243** (2004) 59.
4. A.M.W. Bulte, M.H.V. Mulder, C.A. Smolders, H. Strathmann, J. Mem. Sci. **121** (1996) 51.
5. L. Jiansheng, W. Lianjun, H. Yanxia, L. Xiadung, S. Xiuyun, J. Mem. Sci. **256** (2005) 1.
6. F-Q. Nie, Z-K. Xu, P. Ye, J. Wu, P. Seta, Polymer **45** (2004) 399.
7. J.Ä. Jonsson, L. Mathiasson, J. Chromat. A. **902** (2000) 205.
8. J-T. Li, J. Carlsson, J-N. Lin, K.D. Caldwell, Bioconjugate Chem. **7** (1996) 592.
9. E.M. Vrijenhoek, S. Hong, M. Elimelech, J. Mem. Sci. **188** (2001) 115.
10. S. Ramaswamy, A.R. Goldberg, M.L. Peterson, J. Mem. Sci. **239** (2004) 143.
11. R. Chan, V. Chen, J. Mem. Sci. **242** (2004) 169.
12. Y.F. Dufrene, Current Opinion in Microbiol. **6** (2003) 317.
13. S. Sagrin, S. Takac, T.H. Ozdamar, Sep. Sci. Technol. **40** (2005) 1191.
14. S. Govender, E.P. Jacobs, W.D. Leukes, B. Odhav, V.L. Pillay, J. Mem. Sci. **238** (2004) 83.
15. T. Steckenreiter, E. Balanzat, H. Fuess, C. Trautmann, J. Polymer Sci. **37** (1999) 4318.
16. S. Govender, E.P. Jacobs, M.W. Bredenkamp, P. Swart, J. Colloid Int. Sci. **282** (2005) 306.
17. J.L. Koenig, Spectroscopy of Polymers. American Chemical Scoiety, Washington DC, 1992, p.49.
18. A. Zdniennicka, B. Janczuk, W. Wojcik, J. Colloid Interface Sci. **281** (2005) 465.
19. D. Klee, Z. Ademovic, A. Bosserhof, H. Hoecker, G. Maziolis, H-J. Erli, Biomaterials. **24** (2003) 70.
20. M. Benz, W.B. Euler, J. Applied Polymer Sci. **89** (2003) 1093.
21. A. Salimi, A.A. Yousefi, J. Polymer Sci. **42** (2004) 3487.
22. H.K. Shon, S. Vigneswaran, I.S. Kim, J. Cho, H.H. Ngo, J. Mem. Sci. **234** (2004) 111.
23. M. Momtaz, J-L. Dewez. J.Marchand-Brynaert, J. Mem. Sci. **250** (2005) 29.

24. S.R. Reiken, D.M. Briedis, Biotechnol. Bioeng. **35** (1990) 260.
25. S. Govender, E.P. Jacobs, W.D. Leukes, V.L. Pillay, Biotechnol. Lett. **25** (2003) 127.

CHAPTER 4: A ROBUST APPROACH TO STUDYING THE ADSORPTION OF PLURONIC F108 ON NONPOROUS MEMBRANES

This chapter has been published in, Journal of Colloid and Interface Science in 2005, Volume 282, pages 306 – 313. S. Govender performed all the experimental work and data analysis detailed in this manuscript. The aim of this study was to develop a robust, extraction and detection system for Pluronic and to investigate the effects of membrane surface hydrophobicity and interfacial curvature on the adsorption process. The article as published is enclosed as Chapter 4 of this thesis.

Available online at www.sciencedirect.com
SCIENCE DIRECT
Journal of Colloid and Interface Science 282 (2005) 306–313
JOURNAL OF Colloid and Interface Science
www.elsevier.com/locate/jcis

A robust approach to studying the adsorption of Pluronic F108 on nonporous membranes

S. Govender [a,b], E.P. Jacobs [b,c], M.W. Bredenkamp [c], P. Swart [a,*]

[a] *Department of Biochemistry, University of Stellenbosch, Private Bag X1, Matieland 7602, South Africa*
[b] *UNESCO Associated Centre for Macromolecules and Materials, University of Stellenbosch, Private Bag X1, Matieland 7602, South Africa*
[c] *Department of Chemistry and Polymer Science, University of Stellenbosch, Private Bag X1, Matieland 7602, South Africa*

Received 17 May 2004; accepted 18 August 2004

Available online 5 November 2004

Abstract

A method for poly(ethylene oxide)–poly(propylene oxide)–poly(ethylene oxide) desorption from synthetic nonporous polymeric membranes, using hexane:isopropanol treatment and subsequent colorimetric quantification, is described. The polymers polysulfone, poly(vinyldiene fluoride), and poly(ether imide) were used to fabricate solid adsorption matrices. The desorbed Pluronic F108 forms a color complex with ammonium ferrothiocyanate (NH_4FeSCN) and is based on partitioning of a chromophore present in NH_4FeSCN from an aqueous phase to a chloroform phase in the presence of Pluronic. The protocols for Pluronic desorption and detection are simple, sensitive, inexpensive, rapid, and reproducible over a wide range of Pluronic coating concentrations and membrane surface chemistries. A linear response over the concentration range from 3 to 130 $\mu g\,ml^{-1}$ is obtained. The adsorption isotherms for flat sheet membranes are also described and the Langmuir equation provides the best fit for the adsorption data obtained within the concentration range studied. The absence of any significant interference from certain proteins, vitamins, carbohydrates, plasma, and halogenated derivatives makes the assay equally suitable for the estimation of Pluronic F108 in the attendant Pluronic conjugates or in biomedical applications. Using nonporous hollow fine fibers and capillary membranes as model curved substrates we were also able to correlate an increase in the radius of curvature with a corresponding increase in the surface interfacial adsorption of Pluronic F108.
© 2004 Elsevier Inc. All rights reserved.

Keywords: Pluronic F108; Nonporous membranes; Adsorption isotherms; Colorimetric detection; Interfacial curvature

1. Introduction

The advent of membrane technology in the past two decades has resulted in numerous applications in the fields of biotechnology, waste water treatment, and pharmaceutical and biomedical applications. The efficiency of membrane technology is highly dependent on its ability to resist the nonspecific adsorption of organic foulants due to protein and cell adhesion [1]. This often unwanted adsorption leads to decreased flux in water treatment [2], cytotoxicity in drug delivery, and increased thrombogenicity in biomaterial and cardiovascular therapeutics [3].

Poly(ethylene oxide)$_m$–poly(propylene oxide)$_n$–poly(ethylene oxide)$_m$ (PEO_m–PPO_n–PEO_m) triblock copolymers (Pluronics, BASF, Co) are water-soluble, nonionic amphiphilic surfactants. These compounds are surface active, form micelles and lyotropic crystalline phases [4], and have high chemical and thermal stability. These block copolymers of PEO and PPO are approved as thermoviscofying agents by the Food and Drug Administration and the Environmental Protection Agency as direct and indirect food additives, pharmaceutical ingredients, agricultural products and in biotechnological applications [5,6].

The interfacial adsorption behavior of Pluronic is receiving increasing attention due to its amphiphilic nature, which is attributed to the differing solubilities in water of the hydrophobic PPO and the hydrophilic PEO. This feature has

* Corresponding author. Fax: +27-21-808-5863.
E-mail address: pswart@sun.ac.za (P. Swart).

0021-9797/$ – see front matter © 2004 Elsevier Inc. All rights reserved.
doi:10.1016/j.jcis.2004.08.138

contributed to its emergence in the fields of polymer adsorption and steric stabilization [1,3,5,6]. It has also become a popular coating material because of its ability to noncovalently attach to hydrophobic surfaces and shield said surfaces from the nonspecific adsorption of macromolecules from the surrounding bulk phase [1,3–5]. This is a particularly attractive feature in applications using synthetic polymer membranes.

Pretreatment of membranes is an important strategy for the reduction of protein and cell adsorption. It is therefore important to understand the complex multiparameter process of polymer adsorption onto membranes. Pluronic pretreatment is achieved by passive adsorption of the hydrophobic PPO center block of the triblock copolymer onto the membrane surface, while the pendant hydrophilic PEO groups protrude out into the solution, forming a secondary hydrophilic layer that sterically hinders the adsorption of potential foulants.

A wide range of techniques such as small angle X-ray spectroscopy [5], sedimentation field flow fractionation [6], photon correlation spectroscopy [7], surface plasmon resonance spectroscopy [8], atomic force microscopy, ellipsometry, neutron scattering, and X-ray photoelectron spectroscopy [9] have been used to study Pluronic adsorption onto polymeric surfaces. It is to a large extent the physical and chemical properties of the adsorption matrix that determines the suitability of the attendant analytical methodology. Since most direct and indirect analytical instruments are not entirely suitable or routinely available for quantifying bound Pluronic, this study focused on a simple, inexpensive, and readily available protocol for Pluronic extraction and detection on synthetic membranes.

This work is aimed at developing a robust extraction and detection system for membrane-adsorbed Pluronic in order to investigate the interfacial properties of Pluronic and modified Pluronic, adsorbed onto flat-sheet or planar membranes and capillaries. Planar macroscopic surfaces such as membranes are ideal for fluid–solid systems since many experimental techniques are designed primarily for flat surfaces [10]. Polysulfone (PSU), poly(ether imide) (PEI), and poly(vinyldiene fluoride) (PVDF) were cast as dense-skinned or symmetrically homogeneous planar membranes, which resulted in three unique matrices that differed in their hydrophobicity, such that they could adsorb the amphiphilic Pluronic. Nonporous curved capillary membranes were also fabricated in order to investigate the possible contributions of interfacial curvature to Pluronic adsorption. We decided to base our assay on the phospholipid detection protocol described by Stewart [11] and the solvent extraction combination used for Pluronic extraction was hexane–isopropanol (3:2 v/v).

In this study we report a simple procedure for biphasic extraction and colorimetric detection of Pluronic F108 adsorbed onto dense-skinned membranes. The extraction and detection methods described were used to study interfacial adsorption onto capillary membranes and similar curved nonporous surfaces.

2. Experimental

2.1. Reagents and chemicals

Pluronic F108 was obtained from BASF (Germany). Unless otherwise stated, all chemicals and reagents were purchased from Merck NT laboratory suppliers, SA. The ammonium ferrothiocyanate assay solution was prepared by dissolving 30.4 g NH_4SCN (Protea Holdings Ltd., SA) and 27.03 g $FeCl_3 \cdot 6H_2O$ (Sigma–Aldrich Chemical Company, SA) in deionized water made up to 1 L. The deionized water was purified with a Milli-Q water purification system from Millipore.

2.2. Membrane matrix fabrication

Flat-sheet membranes were cast from a solution containing 27% (m/m) (PSU, PEI, and PVDF) and 73% (m/m) *N*,*N*-dimethylacetamide (DMAc). PSU and PEI were dissolved in DMAc by rotating the solution container for more than 48 h at room temperature to obtain a homogeneous solution. PVDF required sonication in an ultrasonic water bath for 30 min and further heat treatment at 55 °C for 48 h to dissolve. The solutions were then degassed before being used to cast the 200-μm planar membranes. Nonporous capillary and hollow fine fiber membranes were produced by the immersion precipitation technique using a dry–wet spinning process [12]. The dimensions of the capillary (1.8 mm) and HFF (0.9 mm) were measured using an optical light microscope with a vernier scale and these measurements were verified via scanning electron microscopy (SEM). In order to compare the adsorption properties of the fibers with the 1 cm^2 flat sheets used in previous experiments the lengths of the fibers were prepared such that the external surface area was equivalent to 1 cm^2.

2.3. Cleaning regime

Capillary and planar membranes (1 cm^2 external surface area) were stored in 0.04 M sodium azide to prevent microbial growth. Prior to adsorption, membranes were washed overnight in sterile, deionized water, followed by three further washes with deionized water. Membranes were then sonicated three times in sterile deionized water in an ultrasonic bath for 5 min, followed by drying in a laminar flow cupboard.

2.4. Synthesis of Pluronic iodide

p-Toluene sulfonyl chloride (19.06 g) was added to a solution of Pluronic F108 (14.6 g) in dry pyridine (50 ml) at ambient temperature. The reaction mixture was cooled

to 4 °C and retained for 7 days. The reaction mixture was slowly poured into rapidly stirred ice and water (150 ml). The mixture was then extracted with chloroform (4 × 100 ml). The combined chloroform ($CHCl_3$) extracts were then washed with hydrochloric acid (6 M, 150 ml) and deionized water (100 ml), dried over K_2CO_3–Na_2SO_4, and evaporated under high vacuum (0.04 mm Hg) at ambient temperature for 2 h to give Pluronic tosylate. Lithium iodide (2.658 g) was added to a solution of tosylated Pluronic (2.908 g) in dry DMF (20 ml) and heated to 100 °C under Ar for 3 h. The reaction mixture was treated with HCl (3 M; 50 ml) and extracted with $CHCl_3$ (3 × 100 ml). The combined $CHCl_3$ extracts were evaporated overnight in a freeze dryer to give polyoxyethylene (diiodide)–block–polyoxypropylene (Pluronic iodide). The structure of Pluronic iodide was confirmed by ^{13}C nuclear magnetic resonance (NMR) spectroscopy using a Varian VXR 300 NMR spectrometer. All samples were analyzed in deuterated chloroform at 25 °C.

2.5. Pluronic adsorption onto nonporous membranes

A dilution series of Pluronic F108 in deionized water was made, from 7 mg ml^{-1} Pluronic down to 0.125 mg ml^{-1}. Membrane sections (1 cm^2) were incubated into each solution for 8 to 12 h at room temperature to ensure that the adsorption reaction reached equilibrium. After incubation the membranes were washed three times with deionized water and allowed to air-dry for 30 min.

2.6. Hexane:isopropanol extraction of Pluronic F108

Dried Pluronic-coated membranes were then submerged in 25 ml hexane–isopropanol (3:2 v/v) mixture and incubated for 1 h at room temperature. The mixture containing the membranes was subsequently boiled for 15 min and washed twice with 10 ml preheated hexane–isopropanol (3:2 v/v). The mixture was then filtered through Whatman No. 1 filter paper. The hexane–isopropanol filtrate was subsequently evaporated under N_2 gas and slight heat until complete dryness. The extracted Pluronic was redissolved in 10 ml $CHCl_3$. Native or uncoated membranes were used as controls.

2.7. Assay procedure

A dilution series of Pluronic F108 in $CHCl_3$ was prepared and an assay was performed on each dilution in order to generate a standard curve. The Pluronic–$CHCl_3$ standard solution (3 ml) was added to NH_4FeSCN solution (3 ml) and the mixture was vortexed thoroughly for 2 min. The resultant two phases were then allowed to separate. The bottom $CHCl_3$ phase was carefully pipetted out and the absorption was measured spectrometrically at 510 nm using a 1 cm beam cuvette in a CARY 100 spectrophotometer. The average optical density (OD) was plotted for Pluronic F108 and its halogen derivative. A curve of absorption at 510 nm vs Pluronic concentration was determined.

The robustness of this assay was experimentally verified by adding human plasma (1.5 mg ml^{-1}), biotin from Sigma–Aldrich Chemical Company, SA (1 mg ml^{-1}), bovine serum albumin from Sigma–Aldrich (1 mg ml^{-1}), dextran (1 mg ml^{-1}), 34 mM sodium dodecyl sulfate (SDS), and lysozyme from Sigma–Aldrich (1 mg ml^{-1}) directly into the cuvette used for the Pluronic assay. Any interference or change in the stable OD reading at 510 nm would be attributable to the presence of the attendant additive.

2.8. Pluronic adsorption at curved interfaces

Studies were conducted on PSU capillaries and hollow fine fibers (HFF) by adsorbing 5.0 mg ml^{-1} Pluronic F108 onto the convex external surface of the membranes and measuring the adsorbed fraction using the hexane:isopropanol desorption approach previously discussed. The effect of the concave inner surface of the fibers was not considered at this stage, due largely to the difficulty in accurately extracting the adsorbed Pluronic layer from the lumen (tube side) of the membrane.

2.9. Contact angle analysis

Contact angles for the planar membranes were calculated using the sessile drop technique. The measurement of contact angle, θ, provides information on the interaction of a liquid with a solid through Young's equation [10], $\gamma_{SV} = \gamma_{SL} + \gamma_{LV}\cos\theta$, where γ represents the interfacial tensions of solid and liquid. The experimental setup incorporated a Nikon PUNiX video camera equipped with Nikon microscope objectives and adjustable vernier scales. The camera was connected to a video recorder and the real-time image was provided on a monitor. The substrates were placed on an adjustable horizontal platform and droplets of water were deposited from a syringe.

2.10. Atomic force microscopy

Atomic force microscopy (AFM) has already been applied extensively for the characterization of surface adsorbed Pluronic [9] and of hydrophobic surfaces [13]. In the tapping mode, the cantilever is oscillated vertically at high frequency during raster scanning. A topographical map was obtained by scanning a silicon nitride tip attached to a cantilever over the air-dried membrane surface, while maintaining a constant force between the tip and the sample. The deflection of the tip and cantilever was measured optically by reflecting a laser light beam off the back face of the cantilever (AFM, TMX 2000 Explorer, Topometrix, Santa Barbara, CA).

3. Results and discussion

3.1. Colorimetric estimation of Pluronic using the biphasic assay system

Most of the existing colorimetric methods for measuring PEO-based surfactants in biological samples require the removal of proteins, lipids, and sugars by precipitation and or filtration [14]. Colorimetric estimation of PEO-based surfactants and Pluronics have been based on the formation of a complex with cobalt thiocyanate [15], the Wickbold method [16], or titration with tetrakis(4-halophenyl) borate [17]. The cobalt thiocyanate assay required repeated centrifugation steps, while the Wickbold method involved the use of a specifically designed apparatus for concentrating the color complex.

In this study the extracted Pluronic formed a color complex with NH_4FeSCN. This is based on partitioning of a chromophore present in NH_4FeSCN from an aqueous phase to a $CHCl_3$ phase in the presence of Pluronic. A pink to purple color development occurs rapidly after mixing at room temperature with λ_{max} at 505 to 510 nm. The $Fe(SCN)_3$ chromophore on its own does not partition into the chloroform layer in the biphasic assay system, so it is highly likely that the amphiphilic Pluronic solvates the $Fe(SCN)_3$ complex due to its solubility in both water and $CHCl_3$.

A linear response over a concentration range of 3 to 130 $\mu g\,ml^{-1}$ is obtained (Fig. 1). Beyond 130 $\mu g\,ml^{-1}$ the Beer–Lambert law is not obeyed and the concentration curve deviates progressively from linearity. The robustness of this assay was tested with a halogenated Pluronic F108 derivative, which had been used in another study for solid-state detection of Pluronic on membranes (results not shown). Pluronic iodide was characterized with ^{13}C NMR (Table 1) and showed similar linearity at 510 nm (Fig. 1) and the linear response was also within the dilution range of 3 to 130 $\mu g\,ml^{-1}$. In comparison to the systems described in [14–17], both the protocols for Pluronic desorption and detection are relatively simple, sensitive, inexpensive, quick, and reproducible over a wide range of Pluronic coating concentrations and membrane surface chemistries.

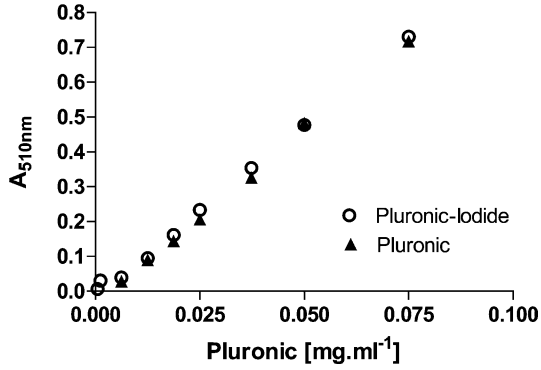

Fig. 1. Typical standard curves for Pluronic F108 ($r^2 = 0.9985$) and for Pluronic F108 iodide ($r^2 = 0.9966$).

Table 1
^{13}C NMR chemical shifts (δ) of Pluronic–I in $CDC1_3$ at 25 °C

Carbon	Pluronic–I
$–CH_2–CH(CH_3)–O$	17.05; 17.18
$–CH_2–I$	29.44
$–CH_2–CH_2–I$	70.46
$–CH_2–CH(CH_3)–O$	72.74; 72.78; 72.82; 72.87; 73.28
$–CH_2–CH(CH_3)–O$	75.03; 75.24; 75.27; 75.44
o-Ts	–
m-Ts	–
p-Ts	–
$Ts–CH_3$	–

Table 2
Effects of bioadditives on the $NH_4FeSCN–CHCl_3$ assay for Pluronic

Additive	Concentration ($mg\,ml^{-1}$)	Change in OD
None	–	0
Human plasma	1.5	<2–5%
Biotin	1.0	0
Bovine serum albumin	1.0	0
Dextran	1.0	0
Sodium dodecyl sulfate	34 mM	>70%
Lysozyme	1.0	>90%

In an attempt to further test the versatility of this method of Pluronic estimation in the presence of common biological materials such as plasma, sugars, proteins, and vitamins, the effect of these additives on the recovery of Pluronic was investigated. Table 2 shows the effect of bioadditives on the quantification of Pluronic F108. Biotin, BSA, and dextran had no effect on Pluronic recovery, while the presence of human plasma had a minor impact on the assay. SDS and lysozyme however were incompatible with the assay.

3.2. Efficacy of hexane:isopropanol extraction of Pluronic

Both hexane and isopropanol have been used for lipid extraction from plant tissue with an efficacy of 52 and 45%, respectively [18]. A binary solvent system using hexane:isopropanol was considered for Pluronic desorption from polymer membranes due to its proven efficacy with lipids and oils [19].

The atomic force micrographs in Fig. 2 serve as a macroscopic indicator of the extent of Pluronic desorption with the hexane:isopropanol solvent system. A typical native, untreated PSU planar membrane is shown in Fig. 2a, while Fig. 2b shows a Pluronic-coated membrane with bright clusters suggesting micelle formation [13]. AFM analysis indicated uniform adsorption of Pluronic onto flat sheet PSU membranes, while native membranes were characterized by rough and extremely heterogeneous surfaces, irrespective of the polymer used in its preparation. Typical membrane treatment with hexane:isopropanol for Pluronic desorption is shown in Figs. 2c and 2d. Figs. 2c and 2d are micrographs showing hexane–isopropanol extraction below the melting point of Pluronic F108 (55 °C) and at ~70 °C, respectively. The color intensity shows the vertical profile of

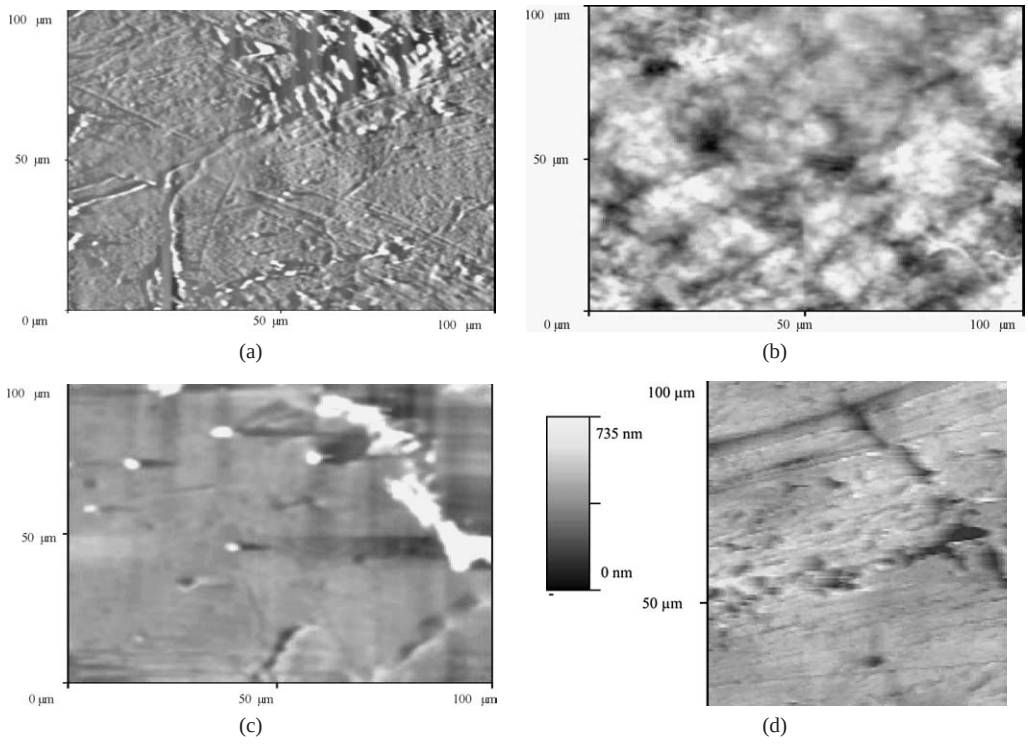

Fig. 2. (a) Atomic force micrographs showing a native PSU flat sheet membrane, (b) Pluronic F108-coated flat sheet PSU membrane, (c, d) typical planar Pluronic-coated PSU membranes that were treated with hexane:isopropanol at 50 and ∼70 °C, respectively. The inset in (d) correlates the surface-peak differences on the hexane–isopropanol-treated membranes with respect to color intensity.

the membrane surface, with light regions indicating the highest points (micelles), the dark regions being the depressions inherent to the fabrication process, while the intermediate region is the membrane surface. The variation in light intensity or "brightness" of the adsorbed Pluronic, suggests that Pluronic aggregation occurred on the membrane surface. A similar profile for native, Pluronic-coated, and hexane–isopropanol-treated membranes was observed with an environmental scanning electron microscope (results not shown).

Since the extraction kinetics and the extraction efficiency of a suitable solvent are positively influenced by temperature, methods based on extraction at elevated temperatures are in common use. This is also applicable to hexane–isopropanol extraction of membrane-adsorbed Pluronic. Bi-solvent extraction at 65–70 °C (above the melting point of Pluronic F108) was comparatively much more effective in desorbing the surfactant coating (Fig. 2d) than treatment at lower temperatures (Fig. 2c). The robust membrane and the low-melting-point Pluronic F108 are an ideal adsorbent and adsorbate system for this binary solvent extraction protocol.

3.3. Interfacial analysis of Pluronic adsorption on planar membranes

The saturation curves for the adsorption of Pluronic F108 onto PSU, PVDF, and PEI are shown in Fig. 3. The results presented in Fig. 3 were analyzed in terms of the Langmuir isotherm. The adsorption/desorption data of Pluronic F108 on dense skin planar membranes was fitted to the Langmuir

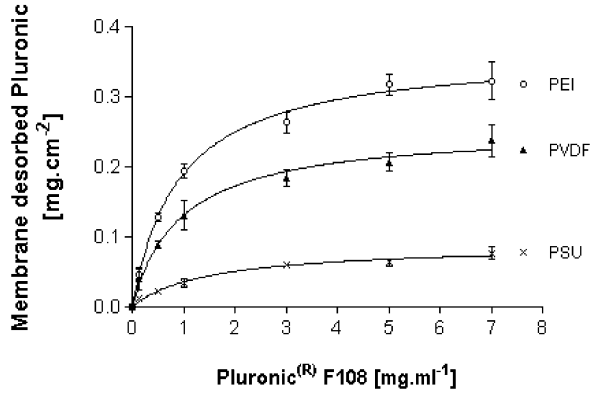

Fig. 3. Saturation curves for Pluronic F108 adsorbed on candidate planar membranes.

isotherm,

$$Q = Q_{\max} KC(1 + KC)^{-1}, \tag{1}$$

where Q and $Q_{\max}$ are the equilibrium amount and adsorption capacity of Pluronic F108 adsorbed per 1 cm^2 of adsorbent, respectively. C is the liquid phase adsorbate concentration at equilibrium and K is the binding constant.

The isotherms obtained followed a Langmuir type profile as characterized by a steep initial slope at a low copolymer equilibrium concentration (<1 mg ml^{-1}) and an adsorption plateau was reached above a bulk Pluronic coating concentration of 5 mg ml^{-1}. Since the adsorption capacity of the different membrane substrates differ due to their inherent

Table 3
Static contact angle measurements for 1 cm^2 planar membranes; N is the sample number, which indicates the number of measurements made on each sample

Polymer type	Native membranes			Pluronic-coated membranes		
	Contact angle	N	±SD	Contact angle	N	±SD
PEI	51.38	6	2.82	61.84	6	1.85
PSU	57.74	6	1.81	40.29	6	1.69
PVDF	66.61	6	2.35	51.34	6	2.84

surface chemistries, the equilibrium adsorption concentration also differed for all the membrane matrices under investigation. The critical micelle concentration of the Pluronic F108 used in this study was calculated from surface tension measurements to be 7 mg ml^{-1} [20], so the plateau does deviate from linearity for coating solutions greater than 5 mg ml^{-1} Pluronic, due to the formation of micelles in the bulk coating solution.

From the saturation curves in Fig. 3, the curve for Pluronic adsorption onto PEI lies above the isotherm plots for both those of PVDF and PSU. This suggests that Pluronic adsorbs more strongly to PEI than it does to PVDF and PSU. The slopes of the isotherms for PVDF and PSU appear steeper than that for PEI, which indicates that the adsorptive capacity of PVDF and PSU increases at higher equilibrium solute concentrations.

Contact angle measurements for both native and Pluronic-coated flat sheet membranes are shown in Table 3. Static contact angle measurements show that native PEI membranes are relatively hydrophilic and Pluronic adsorption could result in a reversal of the surface properties to that of a relatively hydrophobic membrane. This could be due to the self-assembly of the hydrophilic PEO segments as trains in contact with the membrane surface, with the PPO loops sticking out. This scenario differs markedly from the hydrophilic brushes formed by PEO chains on the hydrophobic PSU and PVDF membranes, which form a hydrophilic layer that can potentially sterically hinder the adsorption of proteins and cells [3,5].

Langmuir isotherms for planar PSU, PVDF, and PEI nonporous membranes are described (Fig. 4) and the corresponding adsorption isotherms (Figs. 4a and 4c) obey the Langmuir equation. The isotherms generated on PEI membranes (Fig. 4b) showed the greatest deviations from linearity. This could be attributed to the conformational self-assembly of the PEO groups on the surface such that the PPO center block served as a matrix for multilayer Pluronic adsorption. This was undesirable from a membrane pretreatment perspective since the Pluronic adsorption process would be more complex. This also reduces the sterically repulsive forces provided by the highly hydrated PEO layer at high surface coverage that allows the stabilization of colloidal dispersions, which enable resistance to fouling. The linear fit of the Langmuir isotherms for PSU and PVDF suggests that the adsorption of Pluronic F108 onto these membranes is due to monolayer formation, since there may be minimal Pluronic–Pluronic interaction.

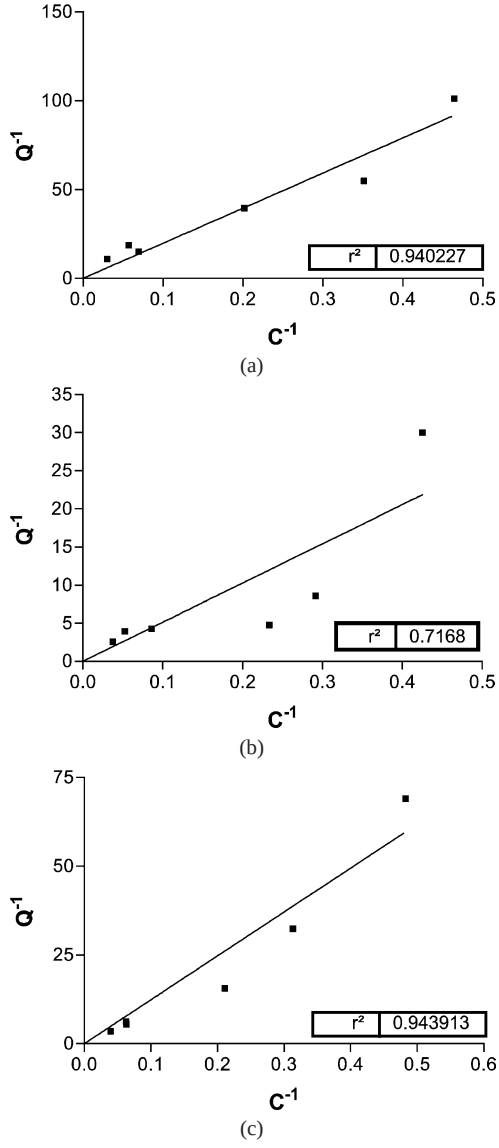

Fig. 4. Typical Langmuir isotherms for (a) PSU flat sheet membranes at 25 °C, (b) PEI flat sheet membranes at 25 °C, and (c) PVDF flat sheet membranes at 25 °C. The interfacial adsorbed amount of Pluronic (Q) and the liquid phase equilibrium concentration of Pluronic (C) were used to construct the Langmuir isotherms.

3.4. Influence of interfacial curvature on Pluronic adsorption

Curved capillaries with their defined radii can easily be used for studying adsorption under controlled flow conditions and as models for adsorption on porous substrates. When previous studies [20] were conducted with flat sheets it was assumed that the radius of curvature was large with respect to the thickness of the adsorbed layer.

However, according to Fleer et al. [10], in order to describe the adsorption of polymers on small spherical parti-

Table 4
Data for Pluronic desorption from 1 cm^2 curved surfaces (experiments were conducted in triplicate)

PSU membrane	Desorbed Pluronic (mg ml^{-1})	±SD	*N*
Capillary	0.14	0.0025	3
Hollow fine fiber	0.055	0.0010	3
Planar	0.063	0.0084	3

cles or in pores, or to model the self-assembly of surfactants or block copolymers into spherical or cylindrical micelles, a flat lattice geometry is inadequate. According to theoretical studies by Wijmans et al. [21], curvature effects become important when the radius of curvature of the substrate is of the same order of magnitude as the adsorbed layer thickness. These authors predicted an increase of the adsorbed amount of diblock copolymer and the hydrodynamic layer thickness with increasing curvature. Baker and Berg [22] measured the layer thickness for various Pluronic surfactants on polystyrene particles and concluded that the specific adsorption was independent of particle size while the adlayer thickness decreased with an increase in particle radius. Considering these and many other conflicting reports on Pluronic adsorption on curved polymeric surfaces an experimental study of Pluronic adsorption on capillary membranes was undertaken.

Measurements of the adsorbed amount of Pluronic on each of the model membrane matrices are summarized in Table 4. The results show an increase in Pluronic adsorption (0.055 to 0.14 mg ml^{-1}) with an increase in membrane radius (0.9 to 1.88 mm). The capillaries with a larger lumen diameter, hence less convex than the HFF, showed greater Pluronic adsorption. This correlates with the trend seen with Pluronics adsorbed onto polystyrene lattices of varying thickness [22]. However, reported results in the literature appear to be plagued with inconsistencies [5–9], and this is due to a combination of the instability of the adsorption matrix used and the constraints imposed by the analytical instrumentation or technique [5]. The reliable hexane:isopropanol protocol and the sensitive biphasic $NH_4FeSCN/CHCl_3$ assay system is well suited to Pluronic analysis on synthetic polymer membranes, which limits the possibility of drawing convoluted conclusions from the interfacial curvature data.

The larger interfacial curvature of HFF membranes causes additional lateral crowding in the adsorbed layer, which might sterically hinder the adsorption of further PPO chains. The capillary membrane has a larger radius of curvature thus limiting lateral crowding and this is reflected in the much greater amounts of Pluronic adsorbed per cm^2 of membrane. On theoretical grounds, it can be expected that an increase in particle size would provide an increase in the adsorbed layer thickness up to the point where the curvature of the surface was essentially the same as a planar surface. The progression from capillary to flat sheet did not show a similar increase in Pluronic adsorption. This was most likely due in large part to the surface physicochemical properties that arose due to the differing membrane fabrication protocols that are inherent to the manufacture of capillary and planar membranes.

4. Summary

Biphasic colorimetric quantification using NH_4FeSCN and $CHCl_3$ was sensitive to Pluronic F108 (3–130 µg ml^{-1}) and insensitive to dextran, biotin, human plasma, and halogenated Pluronic derivatives. Modification of the hydroxyl end groups of Pluronic F108 to Pluronic iodide showed a similar linearity within the described dilution range.

The bisolvent extraction of Pluronic F108 using hexane: isopropanol treatment at ∼70 °C, was highly reproducible for a wide range of Pluronic coating concentrations and surface chemistries in addition to being relatively effective as a desorbent based on AFM and electron microscopy analysis. The saturation curves followed Langmuir-type adsorption and the corresponding Langmuir isotherms correlated to the current understanding of the adsorption of Pluronic onto hydrophobic surfaces such as the candidate membranes.

The specific spectrophotometric detection of Pluronic in the presence of some common bioadditives such as human plasma, serum albumin, and dextran, suggest that this assay system could also be used to quantify Pluronic and poly(ethylene oxide) based surfactants in biomaterial studies and drug delivery devices. The methods described in this study for the extraction and detection of Pluronic were also successfully used for studying interfacial curvature and the results were in good agreement with many other reports concerning surfactant adsorption onto curved polymer surfaces.

Acknowledgments

Financial support was provided by the Water Research Commission and the National Research Foundation.

References

[1] J.-T. Li, J. Carlsson, S.-C. Huang, K.D. Caldwell, Adv. Chem. Ser. 248 (1996) 67.
[2] J.A. Howell, V. Sanchez, R.W. Field, Membranes in Bioprocessing: Theory and Applications, Chapman & Hall, London, 1993, p. 203.
[3] F. Ahmed, P. Alexandridis, S. Neelamegham, Langmuir 17 (2001) 537.
[4] C.R.E. Mansur, M.P. Barboza, G. Gonzalez, E.P. Lucas, J. Colloid Interface Sci. 27 (2004) 232.
[5] S. Stolnik, B. Daudali, B. Arien, J. Whetsone, C.R. Heald, M.C. Garnett, S.S. Davis, L. Illum, Biochim. Biophys. Acta 1514 (2001) 261.
[6] M. Bohner, T.A. Ring, K.D. Caldwell, Macromolecules 35 (2002) 6724.
[7] S.M. O'Connor, S.H. Gehrke, G.S. Retzinger, Langmuir 15 (1999) 2580.
[8] R.J. Green, S. Tasker, J. Davies, M.C. Davies, C.J. Roberts, S.J.B. Tendler, Langmuir 13 (1997) 6510.

[9] K. Eskilsson, L.M. Grant, P. Hansson, F. Tiberg, Langmuir 15 (1999) 5150.
[10] G.J. Fleer, M.A. Cohen-Stuart, J.M.H.M. Scheutjens, T. Cosgrove, B. Vincent, Polymers at Interfaces, Chapman & Hall, London, 1993, p. 45.
[11] J.C.M. Stewart, Anal. Biochem. 104 (1980) 10.
[12] E.P. Jacobs, W.D. Leukes, J. Membr. Sci. 121 (1996) 149.
[13] V.M. De Cupere, J.F. Gohy, R. Jerome, P.G. Rouxhet, J. Colloid Interface Sci. 271 (2004) 60.
[14] A. Nag, G. Mitra, P.C. Ghosh, Anal. Biochem. 237 (1996) 224.
[15] A.M. Tercyak, T.E. Felker, Anal. Biochem. 187 (1990) 54.
[16] H. Ghebeh, A. Handa-Corrigan, M. Butler, Anal. Biochem. 262 (1998) 39.
[17] M. Tsubouchi, N. Yamasaki, K. Yanagisawa, Anal. Chem. 57 (1985) 783.
[18] A. Hara, N.S. Radin, Anal. Biochem. 90 (1978) 420.
[19] K. Schafer, Anal. Chim. Acta. 358 (1998) 69.
[20] C. Yanic, M.W. Bredenkamp, E.P. Jacobs, P. Swart, Bioorg. Med. Chem. Lett. 13 (2003) 1381.
[21] C.M. Wijmans, F.A.M. Leermakers, G.J. Fleer, Langmuir 10 (1994) 1331.
[22] J.A. Baker, J.C. Berg, Langmuir 4 (1988) 1055.

CHAPTER 5: SOLID-STATE ANALYSIS OF MEMBRANE COUPLED LIGAND-MODIFIED PLURONIC

5.1. INTRODUCTION

Polymeric membranes are widely used in chromatographic applications such as affinity separation for the isolation and purification of proteins from biological fluids [1,2]. The performance of an affinity membrane is greatly dependent on its surface properties exhibited at the solid-liquid interface. The surface properties of an affinity membrane may affect the adsorption capacity and its behaviour by controlling adsorption of proteins present in the liquid phase [3,4]. In particular, surfactant self-assembly, non-specific protein adsorption and bio-specific affinity separation is dependent on the surface composition and morphology of the affinity membrane.

There are numerous reports that protein and cell adsorption on affinity membrane surfaces are quantitatively changed, depending on the type of ligands immobilised [5,6]. The adsorption of polymers onto surfaces is a complex and poorly understood process, which can be influenced by several factors. Among these the chemical structure, surface roughness, degree of surface hydrophobicity, electrostatic interactions of the polymer molecules with each other and with the surface and the structural stability of polymer molecules are the most significant [7]. The study of such factors has been of great interest in the last four decades [8]. The benefits in the understanding of these problems have found their applications in bioengineering, colloid stabilisation, materials science and biophysics, etc. [9].

In membrane affinity chromatography, membrane matrices are usually surface functionalised with ligands [1,10,11] and in many cases the chemical nature of this functional layer or surface is not precisely known, thus surface analysis is normally required. In general, the field of surface analysis is vast and rapidly growing, requiring specialised equipment and skilled operators. It is largely the surface matrix under investigation and the information required that determines the surface analysis technique

to be used. These techniques include proximal probes, electron microscopy, electron spectroscopy, ion beam analysis, X-ray techniques [12] and optical analysis [13].

The surface analysis of ligand-modified and unmodified nonporous membranes in this study attempts to use solid-state techniques to generate information that can contribute to the understanding of both the native membrane surface and the chemical state of the ligand termini of Pluronic. Ligand modification of the PEO terminus of Pluronic frequently involves the conversion of the hydroxyl end groups of the hydrophilic brush layer to primary amine equivalents for the covalent attachment of an affinity ligand [11,14]. Synthesis of ligand terminated Pluronic also involves the activation of the oxygen functionality to enhance its capacity as a leaving group.

Aminated Pluronic F108 was initially synthesised in this group [15] for the coupling of the non-specific protein binding ligand, cibacron blue 3GA. Although this amine derivative of Pluronic was an excellent nucleophile, the amino terminus was not a suitable chemical constituent for solid-state analysis due to its low backscattering potential and the atomic similarity of the amino N to O and C in both the membrane and Pluronic. Therefore, in order to 'model' a covalently attached affinity ligand, halogen derivatives of Pluronic were synthesised for both adsorption experiments and ion beam and X-ray analyses. It was hypothesised that accurate surface quantification of the PEO coupled halogens would correspond to potential ligand binding sites per unit area of membrane.

In this study, Langmuir adsorption isotherms were determined and saturation curves for Pluronic adsorption at different temperatures were constructed. Halogenated Pluronic derivatives (Pluronic bromide and Pluronic iodide) were synthesised to mimic affinity ligands, and to facilitate solid-state analysis using X-ray photoelectron spectroscopy (XPS), Rutherford backscattering spectroscopy (RBS) and protein induced X-ray emission (PIXE). Three candidate membranes (PSU, PVDF and PEI) were non-covalently modified with a halogenated Pluronic derivative and nuclear microprobe and X-ray analysis were performed on these surfaces so that solid-state measurements could be obtained that would generate reliable and accurate data. Of particular interest were the coating homogeneity of the derivatised Pluronic, the layer thickness and the potential number of ligand binding sites per cm^2 of membrane surface.

5.2. EXPERIMENTAL

5.2.1. Reagents and chemicals

Unless otherwise stated all reagents and chemicals used in this study were purchased from Merck NT laboratories, South Africa.

5.2.2. Pluronic adsorption

A dilution series comprising Pluronic F108 in deionised water was made from 7 $mg.ml^{-1}$ to 0.125 $mg.ml^{-1}$. Three batches of PVDF, PSU and PEI membrane sections (1 cm^2) were incubated in all the respective coating solutions for 8 h at 25°C, 35°C and 45°C respectively. After incubation the membranes were washed three times in deionised water and dried in air for 30 min. Membrane adsorbed Pluronic was subsequently extracted and quantified [16], and Langmuir isotherms were calculated.

5.2.3. X-Ray Photoelectron Spectroscopy

The XPS instrument used in this study was a PH1 5300. An Al Kα with a radiation of 1486.6 eV was used as the primary X-ray source, which was obtained by an acceleration voltage of 15 keV and an emission current of 20 mA. Two different angles (20 and 70°) between the sample surface and the position of the analyser were used to measure the photoelectrons. At low angles the analyser only detects the photoelectrons coming from the outermost surface, while at larger angles (70°) information from those electrons that are coming from regions deeper inside the surface layer, is also detected [17]. In this way no sputter coating is required to obtain depth information and thus eliminates the possibility of sputter-induced modification of the surface layer.

5.2.4. Rutherford Backscattering Spectroscopy

A Varian sputter coater with a high vacuum evaporator system and a control unit for online thickness monitoring was used to coat the samples with 900 Å Ti at a rate of 4.6 $Å.s^{-1}$ with a current strength of 100 mA. The beam energy used for RBS was 1 MeV with the He^{2+} backscattering measured at an incident angle set at 0° with the backscattering angle at 15°. SiO_2 and Pt/Si were used as reference standards. The Rutherford universal modification program (RUMP) source code was used to analyse the RBS data.

5.2.5. Proton Induced X-Ray Emission

PIXE was used to quantify the number of Br atoms on the surface of Pluronic-Br coated membranes. Measurements were performed using a nuclear microprobe at Materials Research Group (iThemba LABS, South Africa) [18]. A 3.0 MeV H^+ beam was focused and collimated to a 5 μm x 5 μm spot and scanned on the membrane surface. PIXE spectra were recorded with a Si(Li) detector positioned at 135º to the beam direction. Data were collected using XSYS data acquisition system in list mode. GUPIX software [19,20] was used for the evaluation of the concentration of metals on the membrane surface from the PIXE spectra. PIXE elemental maps were obtained with GeoPIXE-II software and generated using the *dynamic analysis* method [21]. Proton backscattering spectra were used for evaluation of the depth distribution of metal atoms.

5.2.6. Atomic Force Microscopy

The surface topography of Pluronic coated membranes was analysed with intermittent contact mode AFM as described in Section 3.2.5.

5.2.7. Synthesis of halogenated Pluronic derivatives

p-Toluene sulphonyl chloride (19.06 g) was added to a solution of Pluronic® F108 (14.6 g) in dry pyridine (50 ml) at ambient temperature. The reaction mixture was cooled to 4°C and retained for 7 d. The reaction mixture was slowly poured into rapidly stirring ice and water (150 ml). The mixture was then extracted with chloroform (4 x 100 ml). The combined chloroform ($CHCl_3$) extracts were then washed with hydrochloric acid (6 M, 150 ml) then deionised water (100 ml), dried over K_2CO_3-Na_2SO_4, evaporated under high vacuum (0.04 mmHg) at ambient temperature for 2 h to give Pluronic – tosylate. Lithium bromide (2.658 g) was then added to a solution of tosylated Pluronic (2.908 g) in dry DMF (20 ml) and heated to 100°C under Argon for 3 h. The reaction mixture was treated with HCl (3 M; 50 ml) and extracted with $CHCl_3$ (3 x 100 ml). The combined $CHCl_3$ extracts were evaporated overnight in a freeze dryer to give Pluronic-Br. The reaction schematic is detailed in Figure 5-1.

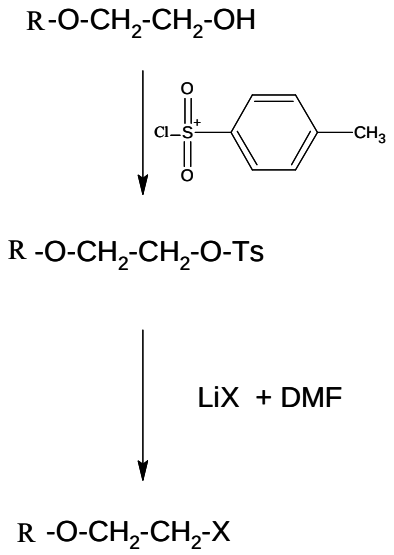

Figure 5-1: Reaction schematic for the halogenation of Pluronic® F108.

5.2.8. Nuclear Magnetic Resonance Spectroscopy

NMR analysis was performed with a Varian VXR 300 NMR spectrometer. 40.2 mg Pluronic-bromide was dissolved in deuterated chloroform and subjected to ^{13}C analysis.

5.3. RESULTS AND DISCUSSION

5.3.1. Adsorption isotherms

The adsorption profile of Pluronic on nonporous membranes at high temperature (25 to 45°C) was investigated. Adsorption studies were performed on planar membranes using 5 $mg.ml^{-1}$ Pluronic F108 at 25°C, 35°C, and 45°C. The melting point of Pluronic® F108 is ~55°C. The adsorption/desorption data of Pluronic at said temperatures were fitted to the Langmuir isotherm $Q = Q_{max}.K.C(1 + KC)^{-1}$. Typical Langmuir isotherms for planar PVDF, PEI and PSU membranes are shown in Figure 5-2 and the corresponding adsorption isotherms at 35°C and 25°C obey the Langmuir equation.

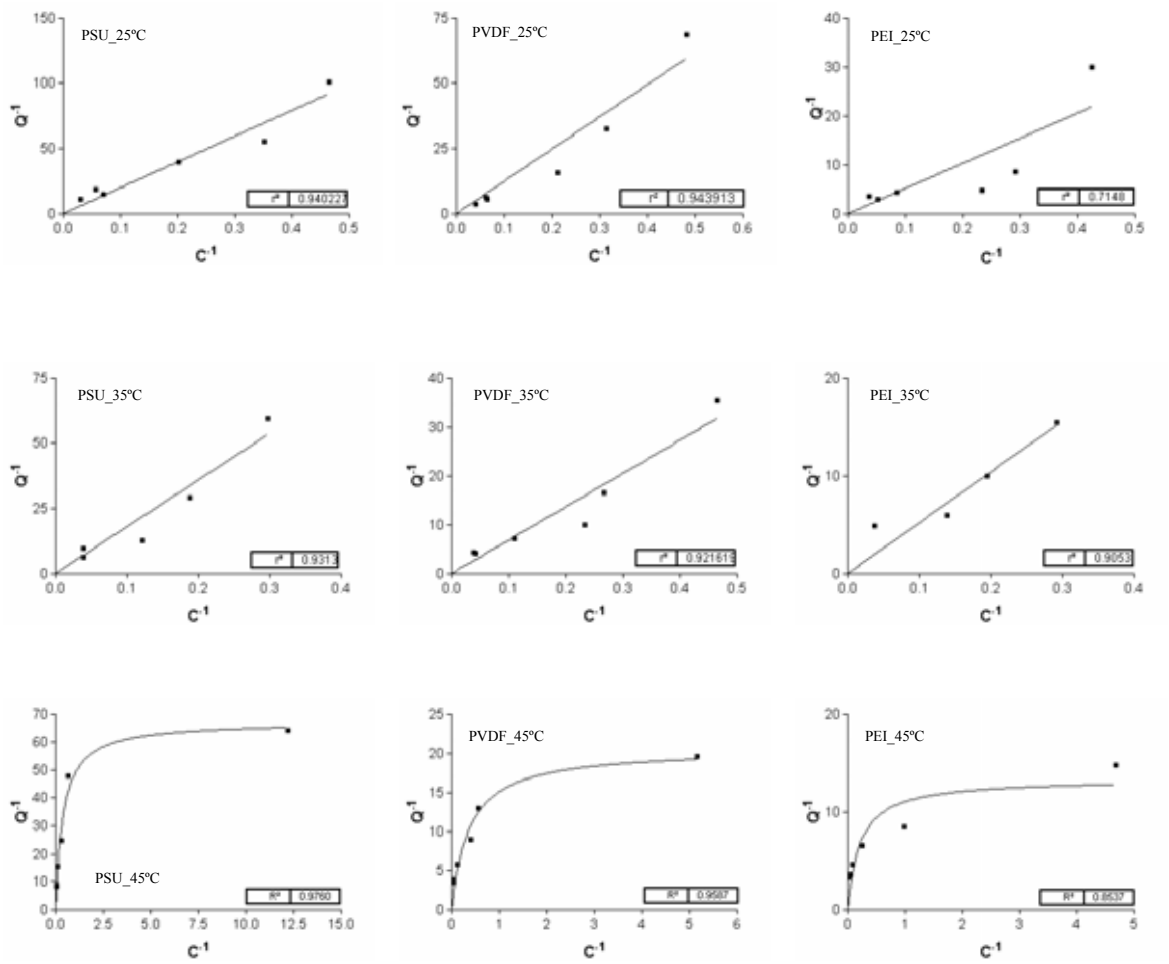

Figure 5-2: Langmuir isotherms for the candidate membranes at 25°C, 35°C and 45°C. The interfacial adsorbed amount of Pluronic (Q) and the liquid phase equilibrium concentration of Pluronic (C), were used to construct the Langmuir isotherms.

The isotherms generated at 45°C, however show the greatest deviation from the Langmuir requirements for monolayer formation at specific constant temperature. From the non-linear isotherms in Figure 5-2, it is likely that Pluronic did not form monolayers on the surfaces of all the candidate membranes during incubation at 45°C. An increase in Pluronic adsorption is also evident, which could be a consequence of multi-layer formation or aggregation. Nevertheless, the amount of Pluronic adsorbed on membranes was found to increase from 25°C to 45°C. A requirement for the efficient functioning of Pluronic as an affinity linker is that the pendent hydroxyl termini are accessible to the bulk solution for ligand attachment or ligate retrieval. Hence, multi-layer formation would suggest that surfactant aggregation could occur on the membrane surface. The AFM micrographs in Figure 5-3 suggest that it is also possible that, upon aggregation from solution at 45°C, there may also be Pluronic coating inhomogeneity.

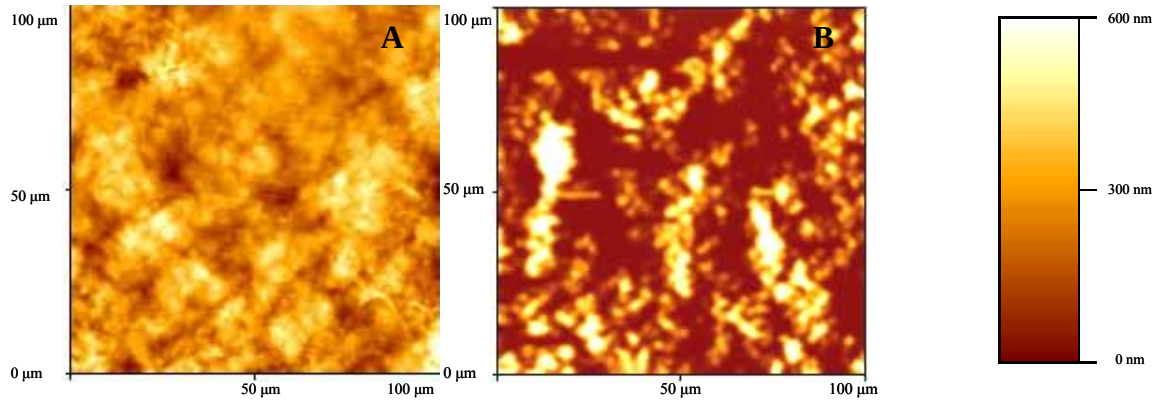

Figure 5-3: AFM analysis of PSU membranes at 25°C and 45°C respectively. The inset correlates the surface peak differences between the A and B.

The non-linearity at high temperature makes it difficult to reliably study Pluronic adsorption using the data generated for the Langmuir model. A study on the melting endotherm of Pluronic using differential scanning calorimetry might offer a better explanation for the adsorption of Pluronic at higher temperatures. Additionally, solid-state analytical techniques such as RBS and PIXE utilise high energy beams that cause sample heating, and this becomes a consideration later in this study, where the stability of the adsorbed Pluronic layer and the membrane integrity need to be monitored during solid-state analysis.

5.3.2. Pluronic activation and modification

As the candidate membranes are chemically inert and contain no reactive functional groups relevant to its ligand coupling ability, the Pluronic affinity linker had to be functionalised before membrane coating. The reactive functional group on Pluronic F108 is the terminal hydroxyl group on the PEO chain that can be functionalised by:

- activation of the oxygen functionality to enhance its capacity as a leaving group or
- increasing the electrophilicity of the carbon atom to which the oxygen functionality is attached, making it a better alkylating agent.

Activation of hydroxyl groups to enhance nucleophilic substitution was accomplished by their transformation into sulphonic esters, using *p*-toluenesulphonyl chloride (TsCl), which is selective towards oxygen containing functional groups. Since the reactivity of sulphonyl chloride is strongly solvent dependent, the reaction with TsCl was conducted in the presence of one equivalent of dry pyridine. The completion of the reaction was indicated by the cessation of pyridinium chloride precipitation. The characterisation of Pluronic-tosylate was described in detail by Yanic *et al*., [22] using ^{1}H and ^{13}C NMR spectroscopy. This was a challenging task that was complicated by the high molecular mass of Pluronic F108. The indirect conversion of Pluronic to the halide derivative was completed with the displacement of the tosylate by the halide. Pluronic-Br was characterised with ^{13}C NMR spectroscopy (Table 5-1).

Table 5-1: ^{13}C NMR chemical shifts (δ) of Pluronic-Br in $CDCl_3$ at 25°C

Carbon	Pluronic-Br
-CH_2-CH(**C**H_3)-O	17.23; 17.4
-**C**H_2-Br	30.35
-**C**H_2-CH_2-Br	70.48
-**C**H_2-CH(CH_3)-O	72.74; 72.78; 72.82; 72.87; 73.28
-CH_2-**C**H(CH_3)-O	75.03; 75.24; 75.27; 75.44
o-Ts	-
m-Ts	-
p-Ts	-
Ts-CH_3	-

5.3.3. X-RAY PHOTOELECTRON SPECTROSCOPY

The surface composition of the membrane adsorbed Pluronic films were investigated by XPS measurements. By fitting carbon 1s spectra, the ratio of ether carbons (C-O) to total carbon atoms (C-O + C-H + C-C) can be calculated for PSU, which has by comparison with Pluronic, very few surface ether groups and no ester and hydroxyl groups. The activity of this membrane for different interfacial layers such as Pluronic F108, brominated Pluronic and or a metal chelating Pluronic can be estimated. XPS was therefore used to quantify the O_{1s}/C_{1s} ratios, which indicate the C-O bonds in the sample.

With respect to adsorbed Pluronic-Br, the C-O bonds could be attributed to C-OH and C-O-C (i.e. the hydroxyl carbons and ether carbons respectively). Changes in O_{1s}/C_{1s} ratios would then indicate the amount of OH groups that were derivatised to form the Br terminus. This is due to C-OH and C-O-C.

Typical XPS spectra are described in Figure 5-4 where the expected C_{1s}, O_{1s}, S_{1s} and N_{1s} peaks are observable. Hydroxyl carbon terminated Br (Br_{1s}) however, was not detected using XPS. By subtracting the O_{1s}/C_{1s} ratios calculated in Figure 5-4B from those in Figure 5-4A (negative control with most of the background ether groups), an indirect indication of the extent of ligand modification with the bromine derivative is possible. The O_{1s}/C_{1s} ratios calculated from XPS analyses are listed in Table 5-2.

Table 5-2: O_{1s}/C_{1s} ratios calculated from XPS analysis of PSU surfaces

Membrane Description	Surfactant Coating Concentration	O_{1s}/C_{1s} ratio
PSU	-	23.25 %
PSU~Pluronic	5 mg.ml^{-1}	29.66 %
PSU~Pluronic-Br	5 mg.ml^{-1}	26.97 %

The increase in the O_{1s}/C_{1s} ratio (23.25 %) for native PSU (spectra not shown) to Pluronic F108 coated PSU (29.66 %) suggests that Pluronic coating increases the hydrophilicity of the hydrophobic PSU membrane. This increase in the hydroxyl carbons and ether carbons is attributed to the PPO and PEO chains of Pluronic that self-assemble onto the membrane by adsorption. These results also support the surface tension analysis described in chapter 3. However, the O_{1s}/C_{1s} ratio for Pluronic-Br coated PSU membranes were lower than that of unmodified Pluronic coated PSU membranes. The change from 29.66 % to 26.97 % indicates that there was a decrease in the number of hydroxyl carbons (CH_2-OH) that were converted to CH_2-Br.

XPS detection of specific levels of Br was inconclusive as the only Br signals observable were the Br_{3d} lines, which was less than 0.1 %. It is likely that the CH_2-Br signals were extremely small in comparison to the larger C and O related signals of the large Pluronic molecule, and consequently Br levels were below the detection limit for XPS. XPS does, however, provide information on the chemical state of the C, O and S content of the surface and adsorbed film but is not sensitive enough as an analytical tool for quantitative detection of ligand-coupled Pluronic adsorbed on membrane surfaces.

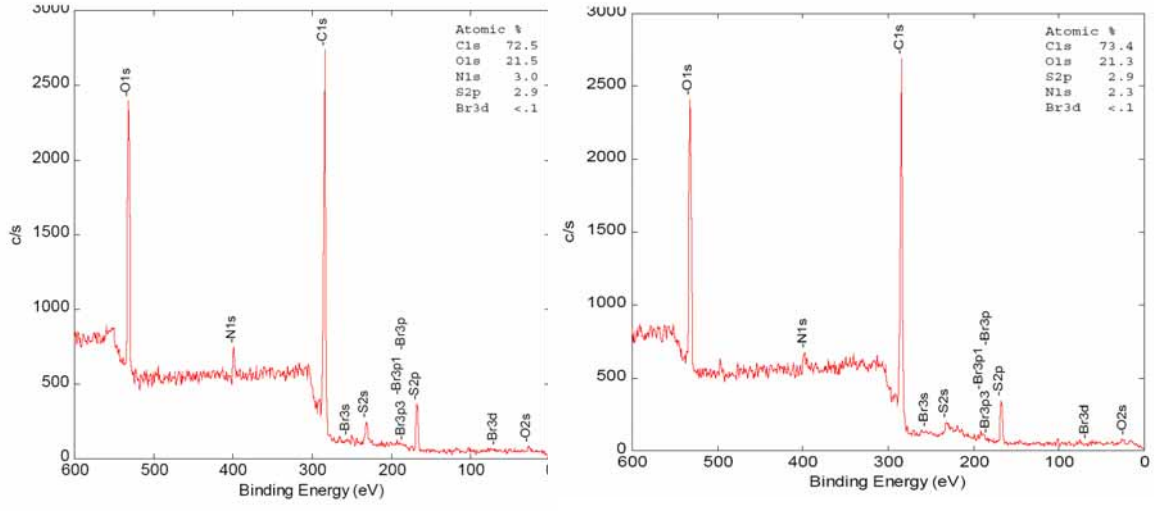

Figure 5-4: X-Ray analysis of PSU membranes modified with A) Pluronic and B) Pluronic-Br.

5.3.4. Nuclear microprobe analysis

Nuclear microprobe analysis (NMA) enables quantitative detection of any element of the periodic table that is immobilised on a solid surface [23]. Mircobeams of protons, deuterons and alpha particles with energies varying from 0.5 to 3.7 MeV can be focused on an area as small as 1 μm^2, to produce atomic or nuclear interactions with the elements of the target sample placed in an analysis chamber under vacuum. Under optimised conditions NMA can also generate accurate information on characteristics of a thin film adsorbed onto a sample surface with no sample damage. Popular NMA techniques include nuclear reaction analysis (NRA), proton induced γ-ray emission (PIGE), PIXE, RBS and non-Rutherford backscattering spectrometry using resonances. Due to the lack of sensitivity of XPS for the detection of Br terminated Pluronic, RBS and PIXE were investigated as possible analytical tools for the study of ligand modified Pluronic (Pluronic-*X*) adsorbed onto synthetic membranes.

From an analytical point of view, RBS compatible materials are heavier thin-films on lighter substrate materials. Heavier thin films give high intensity RBS signals free of background. RBS measurements of 'lighter' elements such as the C and O in Pluronic and the sulphur (PSU), fluorine (PVDF) and nitrogen (PEI) in the respective membranes are more difficult due to low signal to background ratio. Since samples need to be conductive to generate RBS spectra, a thin layer of Ti (15 nm) was coated onto inert planar membranes preadsorbed with Pluronic F108 as described in section 5.2.2. Since the chemical composition of unmodified Pluronic® F108 (C, H, O) and the membranes C, H, O and S, F and N respectively) were so similar with little elemental variation, a problem for measuring the adsorbed layer thickness using conventional RBS analysis arose.

Backscattering spectra of Ti was measured in relation to the S, F and N in the three types of membranes. All experiments were conducted in triplicate and an uncoated membrane was used as a control. Differences in eV readings could thus be used to measure the adsorbed layer thickness of Pluronic. Other quantitative information expected to be generated using this modified approach was the coating homogeneity of the adsorption process. Computer simulations with a Rutherford universal modification program, which is a standard program specifically designed for analysis and simulation of RBS data, was

used to calculate the optimum coating for 'soft', non-homogenous nonporous membranes. Titanium was found to give the best simulation with a thickness of 90 nm and accurate coating was achieved with a sputter coater coupled to an electronic thickness monitor. Figure 5-5 represents an RBS spectrum of a Ti coated Pluronic modified PSU membrane. RBS could not generate reliable data to measure the layer thickness on PVDF and PEI membranes due in large part to the difficulty in discriminating the F and N peaks from the C and O background in the Pluronic.

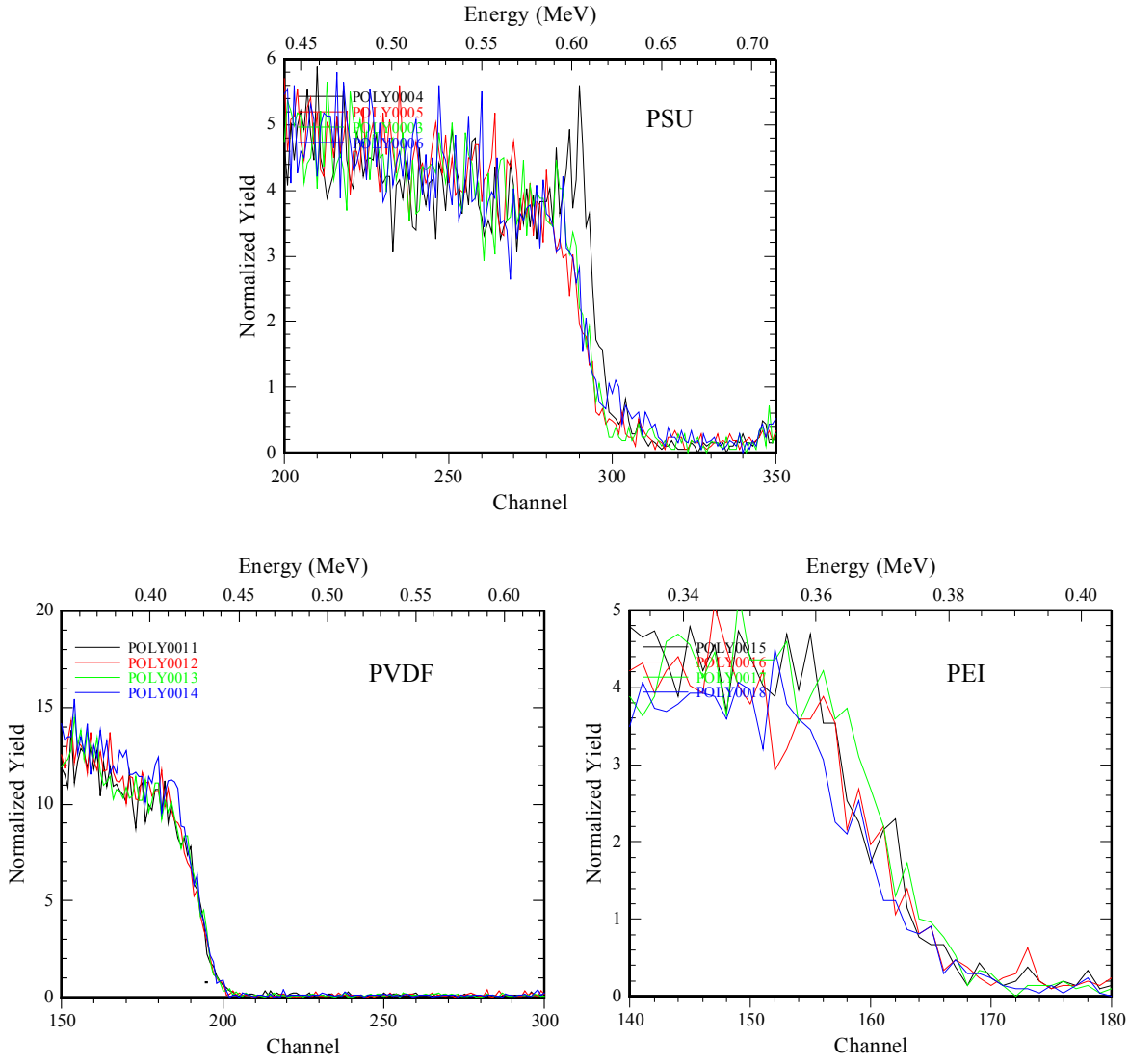

Figure 5-5: RBS spectra on Pluronic® F108 modified PSU, PVDF and PEI membranes in an attempt to measure adsorbed layer thickness. The black spectra (poly 004, poly 011 and poly 015) are native membrane samples while the other spectral lines in each RBS spectrum were generated from membranes coated with Pluronic® F108.

However, if we assumed that Pluronic formed a monolayer after adsorption and washing in deionised water, the thickness would have to be in the order of micrometers to be reliably measured. This assumption is based on convincing microscopy analysis and Langmuir adsorption isotherms (chapters 3 and 4 respectively), which reliably indicated the formation of Pluronic monolayers on membrane surfaces at ambient temperature. RBS, however, is generally not suited to measuring depths in the nm range [24] and in attempting to quantify the S signals in PSU membranes, the detection limits of RBS were being tested.

Coating homogeneity data was only generated for PSU since the S was able to give an appreciable backscattering yield compared to the lighter elements F and N where no significant energy loss was detected. To explain the 157.07 keV difference (612.6-606.4 keV) in Figure 5-5, between PSU (poly 004 , control) and the Pluronic F108 coated PSU membranes, requires a layer with a calculated average composition of (C:H:O = 7:16:5) to be 157 x 10^{15} atoms.cm^{-2} thick. Thus for an assumed densely packed mono-layer this would suggest the presence of PPO strands with a nearest neighbour distance of about 4.7 nm.

In order to verify these data for PSU and to develop a NMA protocol for ligand quantification, coating the membranes with derivatised Pluronic carrying a 'heavy' element such as Br covalently coupled to the hydroxyl terminus of PEO was attempted. This high atomic mass halogen should theoretically give a higher signal to background ratio than the elements C, H, O, N, F or S found on most conventional affinity ligands and in the candidate membranes in this study. Another advantage would be that the Br moiety is covalently coupled to the hydroxyl group of Pluronic, which is the functional group that is modified to accept a ligand in affinity chromatography. Thus RBS could be a possible tool to accurately determine the number of ligand binding sites on a saturated 1 cm^2 membrane by measuring the energy loss of the Br atom.

A method for the direct solid-state quantification of ligand binding sites on derivatised Pluronic, using a halogenated derivative of Pluronic could then also be used to quantify the metal affinity of a chelating Pluronic ligand described in Chapter 8. Halogenation of Pluronic was accomplished by covalently coupling the halogens Br and I to the terminal hydroxyl group of Pluronic, which was conventionally used for ligand attachment [11].

The protocols developed in this study were based on initial experiments performed under empirical conditions. Generally the counts per channel were too low to give statistically reliable data. The best fit in Figure 5-6, was 1 – 5 x 10^{14} Br atoms.cm^{-2} using backscattered αHe particles. This equates to a nearest neighbour Br distance of 0.8 nm under optimised conditions determined by RUMP simulations.

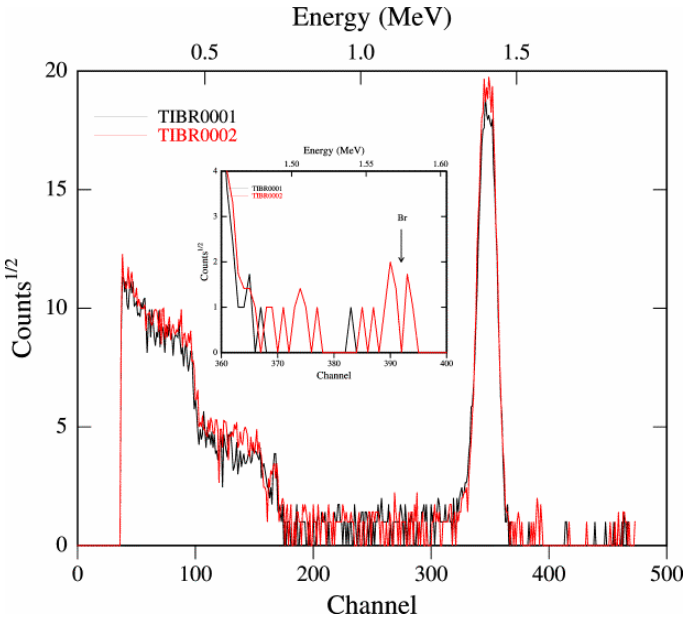

Figure 5-6: Rutherford backscattering spectrum showing the potential number of ligand binding sites on derivatised Pluronic using the model affinity ligand Pluronic-Br.

Figure 5-7 represents a RUMP simulated RBS spectrum performed under the optimised conditions calculated from data generated with Figure 5-6. The conditions used to generate data with up to 95 % confidence levels was achieved using a current of 2 nA, a charge of 20 000 μC and 1 MeV voltage. Higher currents initially caused overheating of the polymer so the reduced current of 2nA (which also prevented damage to the adsorbed Pluronic film) extended the analysis time to 167 min per sample. This was very labour intensive and could be viewed as a practical difficulty with RBS analysis of Pluronic modified polymers.

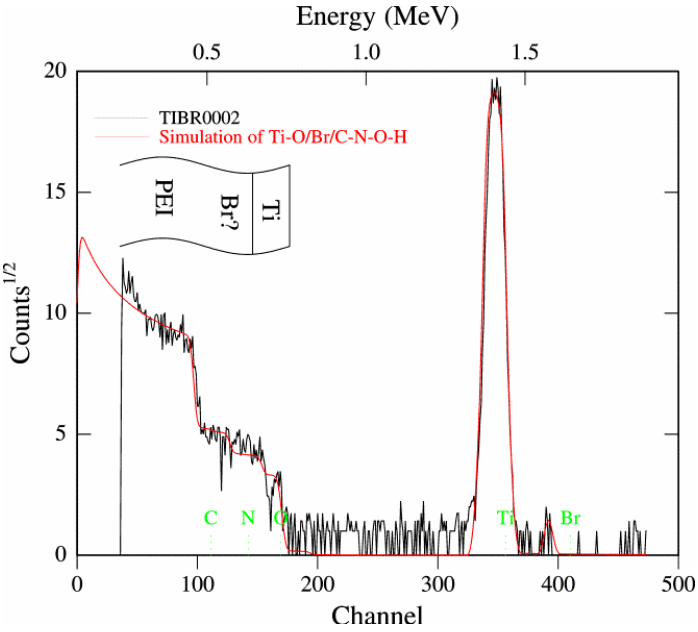

Figure 5-7: RBS spectrum under 'optimised' conditions of a PSU membrane coated with Pluronic-Br (5.0 $mg.ml^{-1}$). This was achieved with a current of 2 nA, a charge of 20 000 μC and 1 MeV voltage.

PIXE analysis using proton beams was another NMA technique considered for solid-state analysis of surface adsorbed Pluronic derivatives. The advantages of PIXE analysis are that surface roughness or homogeneity is not as critical during analysis compared to RBS. PIXE cannot reliably be used for depth profiling of the adsorbed Pluronic film but it can be used for accurate elemental quantification and to create X-ray images of the sample. Samples were made conductive by sputter coating a thin layer of C onto the membrane surface, prior to analysis.

The PIXE spectra in Figure 5-8 show the elements detected on halogenated Pluronic treated PSU and PVDF membranes. The corresponding ^{35}Br and ^{53}I Kα lines were quantified and the concentrations were expressed as $ng.cm^{-2}$ in Table 5-3. As concluded in chapter 4 and observed at higher temperatures in Figure 5-2, PVDF adsorbed more Pluronic than PSU and this could explain the larger amounts of halogenated Pluronic detected on PVDF membranes. The synthesis protocol for Pluronic-I was similar to Pluronic-Br but it is also possible that incomplete tosylation of Pluronic or Br displacement could also explain the lower amounts of Br on PSU membranes. The surface concentration of iodine on the PVDF membrane (33950.6 $ng.cm^{-2}$) is an indication of the amount of ligand on the Pluronic coated surface. This also corresponds to 2.68 x

10^{-7} mol I atoms or 1.61 x 10^{17} I atoms.cm^{-2}. The more hydrophobic PVDF membranes were therefore considered for use as the affinity matrices in forthcoming studies on membrane affinity binding.

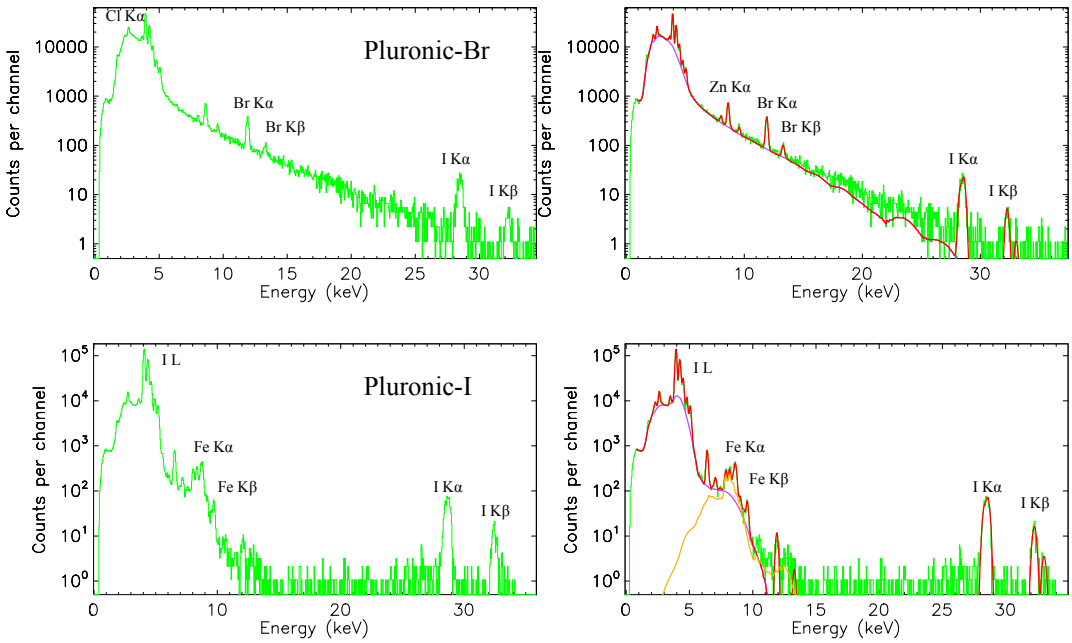

Figure 5-8: PIXE spectra for halogenated Pluronic adsorbed onto candidate membranes. Pluronic-Br was adsorbed onto PSU membranes while Pluronic-I was adsorbed onto PVDF membranes. The Iodine derivative was chosen because of its larger atomic number, which generated a stronger signal thus reducing analysis time. The figures on the right of the PIXE spectra for Br and I spectra show the superimposed element standards as a verification of the accuracy of PIXE analysis of the respective Pluronic coated membranes.

Table 5-3: Summary of PIXE analysis of PSU membranes modified with Pluronic-Br

Membrane Details	^{35}Br *K* [ng.cm^{-2}]	^{53}I *K* [ng.cm^{-2}]	N	SD
PSU~Pluronic	27.25	5722.70	2	4.89 and 1741.32
PSU~Pluronic-Br	1395.15		2	277.16
PVDF~Pluronic-I		33950.60	2	7230.51

5.4. CONCLUSIONS

Adsorption isotherms generated from adsorption studies at elevated temperatures suggest that Pluronic F108 adsorption does not exhibit the typical Langmuir characteristics above 35°C. It is thus likely that non-uniform, multi-layer coating occurs at this temperature. In addition to adsorption, surface analysis should be monitored to minimise instrumentation induced heating and prolonged exposure above 35°C. Halogenated Pluronic-F108 derivatives were synthesised via indirect coupling of bromine (LiBr) and iodine (LiI) to Pluronic via a tosylated intermediate. The resultant halogenated Pluronic was used as a high molecular mass 'marker' to mimic an affinity ligand coupled Pluronic for quantitative solid-state analysis. XPS analysis was found to be unsuitable for solid-state detection of halogenated Pluronic adsorbed to membranes, due to the low signal intensity of the Br_{3d} lines. XPS can, however be used to study the chemical states of surface adsorbed C,O, S and N. Optimum conditions for RBS analysis of Pluronic modified membranes were with a current of 2 nA, a charge of 20 000 μC and 1 MeV voltage. Reliable RBS spectra were generated on PSU membranes where a Pluronic layer thickness of 157 x 10^{15} atoms.cm^{-2} was measured, which suggested an arrangement of PPO strands with a nearest neighbour distance of 4.7 nm. RBS analysis of a Pluronic-Br coated membrane yielded ~ 2.5 x 10^{14} Br atoms.cm^{-2} of PSU membrane. Iodine terminated Pluronic was synthesised due to its higher atomic mass that generated stronger nuclear microprobe signals, subsequently reducing analysis time and possible sample heating. Iodine coupled Pluronic was detected on the surface of PVDF membranes at a concentration of 33.960 μg.cm^{-2}. This also correlates to 2.68 x 10^{-7} mol I atoms or 1.61 x 10^{17} I atoms.cm^{-2}. In summary, the protocols developed in this study to measure the Pluronic layer thickness and the concentration of the surface halogen, could be adopted for the investigation of new Pluronic ligands (detailed in chapter 8). The stability and adsorption properties of the PVDF polymeric membrane studied thus far make it the ideal affinity matrix for affinity separation studies.

Acknowledgements

XPS analysis was performed by Dr. Martin van Staden at CSIR, Pretoria.

5.5. REFERENCES

1. G.A. Platanova, T.B. Tennikova, J. Chromatogr. A. **1065** (2005) 19.
2. Y-C. Liu, S-Y. Suen, C-W. Huang, J. Mem. Sci. **251** (2005) 201.
3. M.Y. Arica, G. Bayramoglu, J. Chromatogr. B. **805** (2004) 315.
4. G. Bayramoglu, M.Y. Arica, Coll. Surf. A. **243** (2004) 11.
5. S. Belfer, Y. Purinson, O. Kedem, J. Mem. Sci. **172** (2000) 113.
6. C. Zhao, X. Liu, N. Nishi, J. Mem. Sci. **214** (2003) 179.
7. K. Eskilsson, L.M. Grant, F. Tiberg, Langmuir. **15** (1999) 5150.
8. F. Tiberg, J. Brink, L. Grant, Curent Opinion Colloid Interface Sci. **4** (2000) 411.
9. A.V. Dobrynin, E.B. Zhulina, M. Rubinstein, Macromolecules **34** (2001) 627.
10. Y-C. Liu, S-Y. Suen, C-W. Huang, J. Mem. Sci. **251** (2005) 201.
11. J-T. Li, J. Carlsson, J-N. Lin, K.D. Caldwell, Bioconjugate Chem. **7** (1996) 592.
12. Z.F. Li, E. Ruckenstein, J. Colloid Interface Sci. **264** (2003) 362.
13. E.M. Vrijenhoek, S. Hong, M. Elimelech, J. Mem. Sci. **188** (2000) 115.
14. L.Liauszki, L. Howard, L. Savati, P.J. Tarcha, J. Biomedical Materials Res. **35** (1997) 1.
15. C. Yanic, M.W. Bredenkamp, E.P. Jacobs, P. Swart, Bioorganic Medicinal Chem. Lett. **13** (2003) 1381.
16. S. Govender, E.P. Jacobs, M.W. Bredenkamp, P. Swart, (2005). J. Colloid Interface Sci. **282** (2005) 306.
17. J.Y. Li, S. Ichizuri, Y. Tabata, M. Washio, Appl. Surf. Sci. **245** (2005) 260.
18. V.M. Prozesky W.J. Przybylowicz, Nucl. Instrum. Meth. B **104 (**1995) 36.
19. J.A. Maxwell, J.L. Campbell, W.J. Teesdale, Nucl. Instr. and Meth. B **43** (1989) 218.
20. J.L. Campbell, T.L. Hopman, J.A. Maxwell, Z. Nejedly, Nucl. Instr. and Meth. B **170** (2000) 193.
21. C.G. Ryan, D.N. Jamieson, C.L. Churms, J.V. Pilcher, Nucl. Instr. and Meth. B **104** (1995) 157.
22. C. Yanic, M.W. Bredenkamp, E.P. Jacobs, H.S.C. Spies, P. Swart, J. Appl. Polymer Sci. **78** (2000) 109.
23. F. Mercier, V. Moulin, M.J. Guittet, N. Barre, M. Gauteir-Soyer, P. Trocellier, P. Toulhoat, Organic Geochemistry **33** (2002) 247.
24. H. Metzner, M. Gossla, T. Hahn, Nucl. Instr and Meth. **124** (1997) 567.

CHAPTER 6: AFFINITY IMMOBILISATION OF PROTEINS ON RE-USABLE LIGAND-MODIFIED MEMBRANES

This chapter has been submitted for publication in Journal of Biotechnology. S. Govender performed all the experimental work described in this manuscript.

Coupled with an understanding of the interfacial adsorption of halogenated Pluronic, this study uses a new biotinylated Pluronic for testing both the bio-specificity of membrane adsorbed, ligand-modified Pluronic and its ability to simultaneously inhibit non-specific protein adsorption. A strategy for membrane regeneration and re-use was also investigated.

S. Govender [1,2], E.P. Jacobs [2], M.W. Bredenkamp [3], P. Swart [1*]

[1]Department of Biochemistry, [2]UNESCO Associated Centre for Macromolecules and Materials, [3]Department of Chemistry and Polymer Science, University of Stellenbosch, Private Bag X1, Matieland, 7602, South Africa,

* To whom all correspondence should be addressed
Pieter Swart
Department of Biochemistry, University of Stellenbosch, Private Bag X1, Matieland, 7602, South Africa
Email: pswart@sun.ac.za
Tel: +2721 808 5865
Fax: +2721 808 5863

Abstract

A membrane based affinity immobilisation system was developed, that has the properties of bio-specific affinity immobilisation, protein shielding and regeneration. The amphiphilic surfactant Pluronic® F108 was used as an affinity linker, by non-covalent coupling to nonporous membrane matrices. The terminal hydroxyl groups of Pluronic were covalently coupled to the ligand biotin. Planar nonporous membranes of varying surface chemistry were fabricated to test the affinity adsorption of biotinylated Pluronic and its ability to resist non-specific protein adsorption. Solutions of lysozyme and bovine serum albumin (0.25 $mg.ml^{-1}$) were used as model protein adsorbates. Pluronic F108 coated membranes offered 98% shielding of lysozyme adsorption and 75% shielding of BSA adsorption respectively. Anionic sodium dodecyl sulfate (SDS) formed the basis of a displacement solution intended to regenerate the affinity membrane matrix by desorbing both membrane bound Pluronic and protein foulants. A membrane regeneration strategy using SDS was capable of displacing both adsorbed proteins and Pluronic. SDS micelles (34 mM) were most effective in desorbing membrane bound protein while 5 mM SDS removed > 85% of the adsorbed Pluronic F108 after 20 h incubation at 20°C. Biotinylated Pluronic modified PVDF membranes specifically immobilised avidin-peroxidase, and the resultant affinity membrane system was regenerated and re-used with no significant change in performance for up to five cycles.

Key Words

Affinity membranes, avidin-biotin, Pluronic® F108, regeneration, SDS

6.1. INTRODUCTION

Synthetic polymeric membranes are becoming increasingly popular as solid adsorption matrices in biological applications ranging from enzyme immobilisation for biosensors [1] to separation and filtration in downstream bio-processing [2]. As with all types of membranes, the interaction between the surface properties of the membrane and the molecules in solution determine the extent of fouling and flux through the membrane. Bio-fouling is usually characterised by the uncontrolled, irreversible adsorption or adhesion of macromolecules such as proteins, lipids and cells [3]. The extent of biochemical diversity in different biological processes severely complicates the manufacture of the perfect membrane for biological processes. Surface protection or 'shielding' is afforded by either pre-filtration of the macromolecular solution and or membrane surface modification to prevent bio-fouling.

Protein adsorption and interactions on surfaces is a common phenomenon and is of considerable technological concern [4,5]. Thus the prevention of protein adsorption on surfaces influences the design and viability of biomaterials including membranes. *In vitro* experiments have also shown that cell behaviour is influenced by the physicochemical properties of polymer surfaces [6]. In recent years a popular approach to enhancing surface bio-compatibility was to graft polymeric molecules such as poly(ethylene oxide) chains [4], betaines, phospholipids, poly(acryl amide) and polysaccharides [7,8]. An alternative to this covalent coupling is the physisorption of surfactants onto these polymer surfaces to alter adsorption properties.

In protein-surface interactions, the governing factors are determined by both the physical state of the adsorption matrix, protein surface and the solution environment. These factors include bound ions, surface charge, roughness, surface elemental composition and surface energetics. The interactions of polymers and surfactants, mainly in oppositely charged polymer-surfactant systems have also received much attention [2,9]. Many reports focus on the interaction of Pluronic® F108 (a non-ionic surfactant) and SDS (an anionic surfactant) since they are much studied and from a process application point of view are amongst the few thermo-viscofying materials approved as direct and indirect food additives, pharmaceutical ingredients and agricultural products [2].

Pluronic® F108 surfactants are poly(ethylene oxide) (PEO)-poly(propylene oxide) (PPO)-poly(ethylene oxide) tri-block copolymers, that are important to many bio-medical and biotechnological applications [2,9,10,11]. These commercially available, amphiphilic, non-ionic surfactants self-assemble onto hydrophobic surfaces via the hydrophobic PPO centre block, while the longer hydrophilic PEO chain forms a flexible tether that terminates in a functional hydroxyl moiety. This hydroxyl group has also been targeted for the covalent attachment of ligands [9,10]. A ligand of particular interest is biotin which ligates strongly and specifically to the protein avidin [12]. Interactions between biotin and avidin represent one of the strongest non-covalent coupling processes in nature, (K_d = 10^{15} M^{-1}), and has been used as a model for biosensor development, usually via surface immobilisation of biotin onto a transducer [13].

This study is directed towards an effort to produce a robust, re-usable, membrane based affinity separation system for the specific immobilisation of avidin peroxidase using a novel biotinylated Pluronic as a model affinity ligand. The use of biotinylated derivatives as ligands on affinity matrices provides an attractive approach for the specific isolation of biochemical ligates such as hormones and receptors [14]. Candidate planar, nonporous membranes of varying surface chemistry were fabricated and the capability of these membrane matrices to resist non-specific protein adsorption and of being efficiently regenerated for reliable re-use was also investigated. A procedure for Pluronic pre-treatment of membranes to inhibit non-specific protein adsorption is described, and attempts to regenerate said membranes with sodium dodecyl sulfate (SDS) are discussed. Experimental results also describe the synthesis and interfacial adsorption of the novel biotinylated ligand for avidin immobilisation and will contribute to the understanding of surfactant displacement of Pluronic modified membranes.

6.2. EXPERIMENTAL

6.2.1. Reagents and chemicals

Bovine serum albumin (BSA) and lysozyme (Roche, Penzberg Germany) were used as model protein adsorbates and were reconstituted as 0.25 $mg.ml^{-1}$ solutions in 0.1 M phosphate buffer, pH 7.4. SDS (Merck, Darmstad, Germany) was used as a desorption agent. Pluronic® F108 (14 600 $g.mol^{-1}$) was obtained from BASF corporation (New Jersey, USA) and biotinamidohexanoic acid *N*-hydroxysuccinimide ester (NHS-Biotin) from Sigma chemical company, South Africa. Streptavidin-peroxidase conjugate and ABTS were purchased from Roche. Unless otherwise stated, all other reagents were purchased from Merck (Darmstad, Germany).

6.2.2. Pluronic assay

A biphasic colorimetric assay for Pluronic quantification was performed as described by Govender *et al.,* [10]. A plot of absorbance at 510 nm *versus* Pluronic concentration yielded a linear standard curve.

6.2.3. Protein assay

Protein concentration was measured using a bicinchoninic acid protein assay kit from Pierce™, (Rockford, USA), with bovine serum albumin as a protein standard.

6.2.4. Membrane matrix fabrication

Planar nonporous membranes were cast from solutions containing 27% (m/m) [Udel P3500 polysulphone (PSU), poly(ether imide) (PEI) and poly(vinylidene fluoride) (PVDF)] respectively and 73% (m/m) *N*,*N*-Dimethylacetamide (DMAc). PSU and PEI were dissolved in DMAc by rotating the solution container for more than 48 h at room temperature to obtain a homogeneous solution. PVDF required sonication in an ultrasonic

water bath for 30 min and further heat treatment at 55˚C for 48 h to dissolve [10]. All solutions were degassed before being used to cast the 200 μm flat-sheet membranes. To ensure that all membrane surfaces were free of contaminating adsorbents, membranes were washed overnight in sterile deionised water. The membranes were then sonicated three times in sterile deionised water in an ultrasonic bath for 5 min followed by drying in a laminar flow cupboard prior to surfactant and protein adsorption. The surface hydrophobicity of PVDF and PSU membranes was verified using static contact angle analysis, while PEI membranes were confirmed to be hydrophilic [10].

6.2.5. Protein adsorption on membrane

67 000 Da Bovine serum albumin (BSA) and lysozyme (14 700 Da) solutions [0.25 $mg.ml^{-1}$] in 0.1 M phosphate buffer (PB), pH 7.4 were prepared and stored at 4°C. Membranes were non-covalently modified with Pluronic by static incubation in 5 $mg.ml^{-1}$ Pluronic at 20°C for 8 h. Membranes (native and Pluronic coated) were statically incubated for 120 min at 20°C in 10 ml of the respective protein solutions. The membranes were then rinsed three times in PB and then inserted into a vial containing 10 ml of 1.0 % (w/v) SDS. These vials were then shaken for 120 min and the protein concentration in the SDS solution was measured using a Pierce™ protein assay reagent kit. In a conventional protein adsorption experiment [3], also called the depletion method, the amount of adsorbed proteins was determined based on the decrease in protein concentration in the solution after contacting with the solid surface.

6.2.6. Membrane regeneration

Pluronic modified membranes were stripped of adsorbed Pluronic using a 34 mM aqueous SDS solution. Pluronic coated membranes were initially statically equilibrated in 10 ml of the SDS solution for 1 h and then transferred to a Stoval Belly Dancer™ shaker for 2 h of vigorous shaking. In an attempt to determine if this was a time dependent process, the shaking incubation period was increased from 2 h to 4 h, 20 h and 48 h respectively. A concentration range of SDS (5 mM, 8 mM and 34 mM) was also investigated in order to ascertain if SDS micelles facilitated Pluronic desorption from candidate membranes of

varying surface chemistry. The critical micelle concentration of SDS is 8 mM. After incubation in SDS, the membranes were washed in a solution of 100 ml dH_20 for 12 h and finally rinsed three times in dH_2O. Pluronic was separated from SDS after solvent evaporation, followed by the addition of 10 ml $CHCl_3$. SDS is insoluble in $CHCl_3$ and can be separated from Pluronic by filtration through Whatman filter paper.

6.2.7. Synthesis of biotinylated Pluronic

The terminal hydroxy groups of Pluronic were modified in a two-step reaction to yield an amine terminated Pluronic (Figure 6- 1). Pluronic F108 (2g) [I] was dissolved in benzene (6 ml) and then added dropwise to 4-nitrophenyl chloroformate in 6 ml of benzene. After 24 h of stirring, the reaction product [II] was precipitated with excess ether, filtered, dried under high vacuum and redissolved in benzene. This procedure was repeated at least 3 times [9]. The dried activated Pluronic (1.5 g) was then dissolved in 6 ml methanol, with slow dropwise addition of 1 ml hydrazine (NH_2NH_2). The molar ratio of hydrazine to Pluronic was kept at 100:1. After an 8 h reaction period, the product was precipitated with an excess of ethyl ether. Precipitation from methanol was repeated at least three times, and the final product [III] was dried under high vacuum overnight. Hydrazine Pluronic (40 mg) and NHS-biotin (12.5 mg) were then dissolved in 5 ml dry DMF. This reaction mixture was stirred for 48 h at 20°C, followed by drying under high vacuum. The dry product [IV] was re-dissolved in deionised water to a final concentration of 5 $mg.ml^{-1}$.

The structure of the biotinylated Pluronic derivative was confirmed by ^{13}C nuclear magnetic resonance (NMR) spectroscopy using a Varian VXR 400 NMR spectrometer. All samples were analysed in deuterated chloroform (Sigma) at 25˚C with tetramethylsilane as the internal standard.

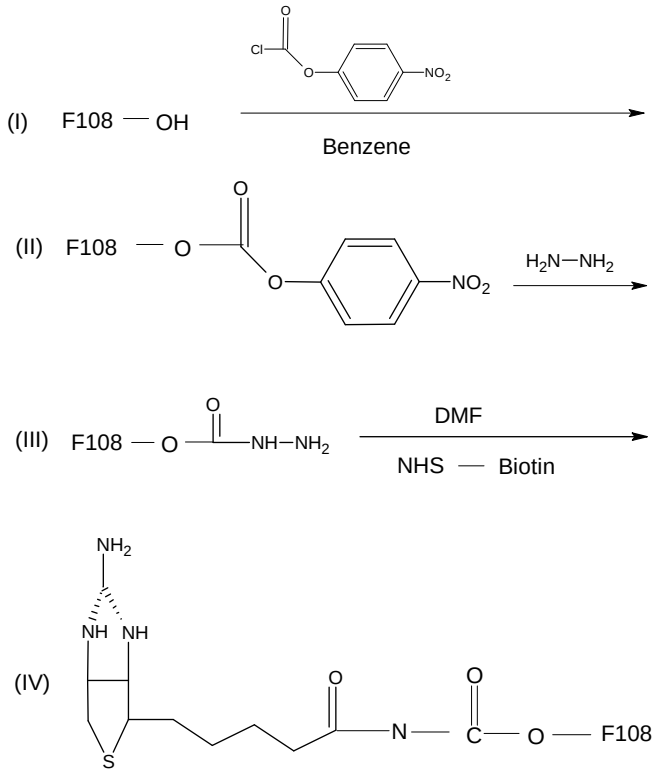

Figure 6-1: Modification of Pluronic® F108 for imino-biotin coupling.

6.2.8. Membrane affinity immobilisation of avidin-peroxidase

Membrane surfaces were modified by static adsorption for 8 to 12 h at 25°C, in 5 mg.ml^{-1} solutions of Pluronic F108 and biotinylated Pluronic respectively. Membranes incubated in unmodified Pluronic were used as negative controls. The two sets of eight membranes were then transferred to glass scintillation vials containing a dilution series of avidin-peroxidase in phosphate buffered saline, pH 7.4 (serial dilution series from 1 U.ml^{-1} to 0.0156 U.ml^{-1}) in a total reaction volume of 2 ml for 60 min with vigorous shaking. Membranes were then washed three times in dH_2O, air dried and transferred to a 8 x 12 well NUNC^{TM} microtitre plate. An ABTS solution (300 µl of 0.5 mg.ml^{-1}) in citrate buffer, pH 5 and 1µl.ml^{-1} H_2O_2, was added to each well. Plates were immediately shaken at 37°C for 30 min before removing 150 µl of the ABTS solution for analysis at 405 nm. In the presence of sufficient peroxidase, the ABTS solution undergoes a distinct colour change from yellow/green to dark green/blue indicating peroxidase activity. The log of avidin-peroxidase dilution was plotted against absorbance to illustrate specific binding of

avidin-conjugated peroxidase to membrane bound biotinylated Pluronic. To demonstrate competitive avidin-peroxidase binding to biotinylated membranes, studies were also performed with 0.2 $mg.ml^{-1}$ of a model protein contaminant cocktail comprising 0.1 $mg.ml^{-1}$ BSA and 0.1 $mg.ml^{-1}$ lysozyme.

A schematic illustration of the process from membrane surface modification and avidin-peroxidase immobilisation to regeneration is illustrated in Figure 6-2.

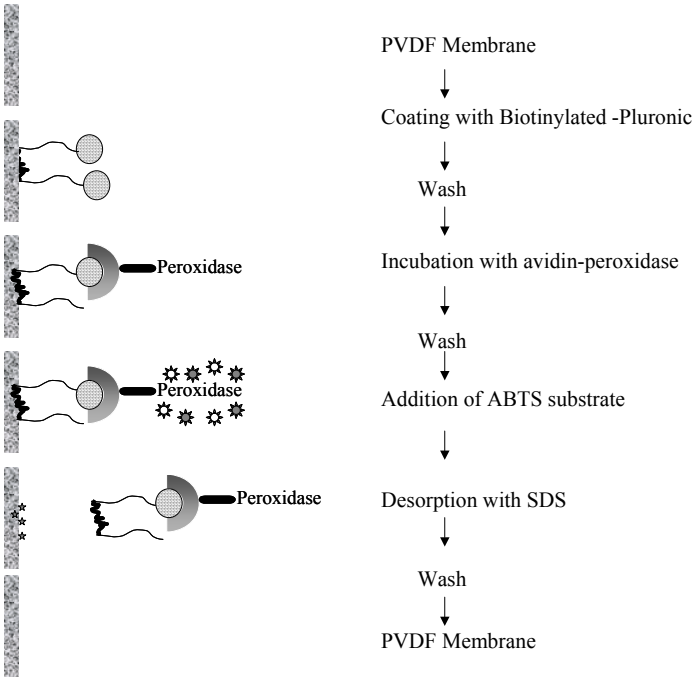

Figure 6-2: Schematic illustration of affinity immobilisation of avidin-peroxidase and membrane regeneration with SDS.

6.3. RESULTS AND DISCUSSION

6.3.1. Protein shielding ability of Pluronic modified membranes

Nonporous planar membranes are becoming increasingly popular in the development of 'strip tests' where they are used as affinity chromatography matrices [15]. A solid-liquid interface usually has a higher standard free energy than the bulk phase and as a result, this interface is apt to be thermodynamically stabilised by adsorbing any substances that are different from the solvent molecules [3]. The secondary, tertiary and quaternary structures of proteins and polypeptides can deviate significantly from their conformation in free solution upon adsorption onto a hydrophobic surface. The interactions between proteins and surfactants are generally described as arising because of both electrostatic and hydrophobic interactions [16].

The pI values of BSA and lysozyme are 4.8 and 10.45 respectively, and after correcting the pH to 7.4, a negative charge was conferred to BSA while lysozyme was rendered positive. Between proteins such as lysozyme (+) and BSA (-) or polyelectrolytes and an oppositely charged surfactant, the attractive interaction is in general very strong, and the initial binding is more site specific than in the case of inert (uncharged) polymers such as Pluronic and the candidate native membranes used in this study.

From the data in Table 6-1, it was observed that Pluronic coated membranes offer as much as 98% shielding of lysozyme adsorption and up to 75% shielding of BSA adsorption from a high protein coating concentration of 0.25 $mg.ml^{-1}$. Typically, the higher the bulk concentration of the protein the greater the adsorbed amount at the membrane surface [3,17]. Since PVDF is more hydrophobic than PSU [10], it adsorbed Pluronic more efficiently and was therefore most effective in shielding both BSA and lysozyme adsorption from solution. Although PEI membranes are fairly hydrophilic, they were found to adsorb Pluronic almost as effectively as PVDF [10] but were however not as effective in reducing BSA adsorption. This was most likely due to the polar PEO chains of Pluronic self-assembling onto the hydrophilic PEI surface such that the centre PPO block was exposed to the liquid phase. This could reduce the steric hindrance offered by PEO, thereby encouraging hydrophobic interactions between PPO blocks from different

Pluronic molecules, resulting in multi-layer formation. The Langmuir isotherms describing Pluronic F108 adsorption onto PEI [10] suggest possible micelle formation on hydrophilic surfaces while monolayer coverage on hydrophobic surfaces was observed.

Table 6-1: Lysozyme and bovine serum albumin adsorption onto membranes from a bulk equilibrium protein solution of 0.25 $mg.ml^{-1}$. The protein shielding ability of Pluronic F108 modified membranes was determined after measuring the amount of protein adsorbed onto native membranes. Analysis was based on the depletion method of estimating protein adsorption [3]

	Lysozyme		Bovine Serum Albumin		
	$\mu g.cm^{-2}$	SD	$\mu g.cm^{-2}$	SD	N
PEI	113.58	4.43	66.44	0.017	3
PSU	109.46	5.57	67.87	11.89	3
PVDF	121.46	6.71	54.15	17.09	3
PEI~~Pluronic	5.76	1.80	65.14	1.75	3
PSU~~Pluronic	4.49	1.78	54.95	1.92	3
PVDF~~Pluronic	0.78	0.33	44.76	5.82	3

In general, the amount of adsorbed proteins is dependent on various factors including the surface matrix, protein internal stability energy, tertiary conformation and ionic strength of the buffer [3,18]. Proteins such as BSA have a lower structural stability or a low internal stability energy, which facilitates adsorption onto surfaces under seemingly unfavourable conditions [3,17]. This factor contributes significantly to the relatively high non-specific adsorption of BSA on all Pluronic-modified membranes in this study (Table 6-1), where adsorption is favoured because of a gain in conformational entropy upon adsorption. Lysozyme has a stronger internal coherence and this higher internal stability energy does not favour adsorption on hydrophilic surfaces, as observed by the lower adsorption of lysozyme on Pluronic hydrophilised membranes.

Typical Pluronic modified and unmodified PSU membrane surfaces are depicted in the electron micrographs in Figure 6-3. The native PSU membrane in Figure 6-3A is characteristic of the planar nonporous membranes prepared in this study. The membrane

surface morphology is typically rough, and this was found to be inherent to the fabrication protocol. This phenomenon is however not an undesirable factor for membrane adsorption where a rough surface has more surface area available for adsorption of macromolecules from solution. Figure 6-3B suggests that Pluronic coating of the PSU surface changes the microscopic appearance of the membrane surface and the coating at 5 $mg.ml^{-1}$ appeared uniform over the surface. Intermittent contact mode atomic force analysis of membrane surfaces (Figure 3-5) confirmed the decrease in surface roughness after Pluronic coating.

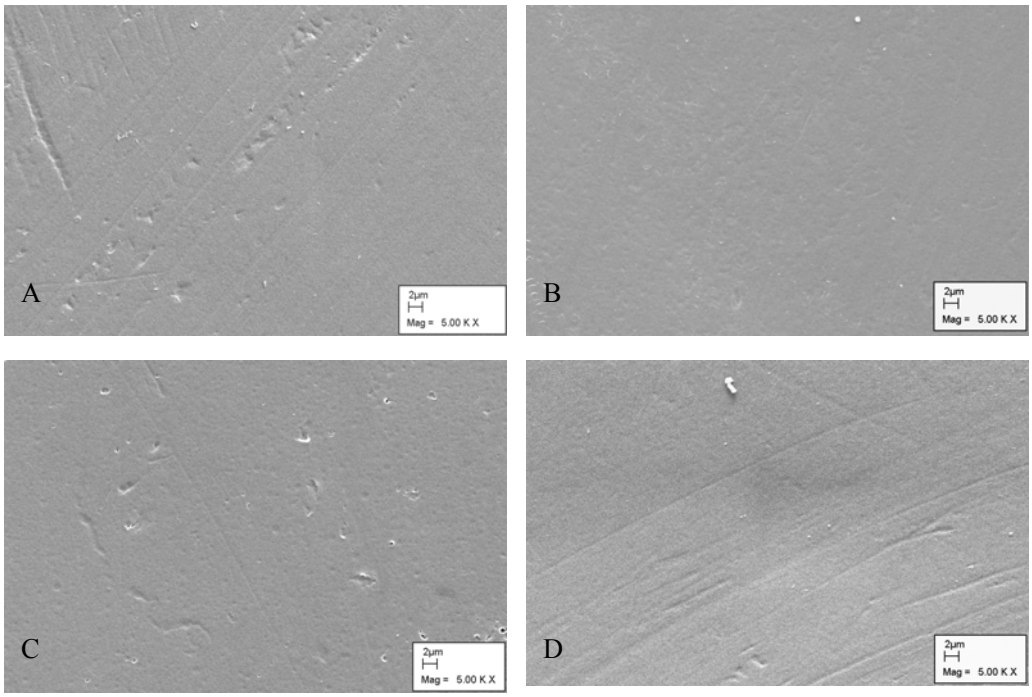

Figure 6-3: Electron micrographs showing typical planar nonporous PSU membranes that were used in Pluronic coating and desorption. A) Native or virgin PSU membrane surface; B) Pluronic coated PSU, C) SDS displacement of Pluronic treated membranes, D) Hexane-isopropanol treated membranes modified with Pluronic. Magnification = 5000X and bar = 2 µm.

6.3.2. Regeneration of Pluronic modified membranes

An important practical consideration for the implementation of membrane affinity technology is its lifetime and regeneration capacity [19]. Regeneration was investigated by SDS treatment of Pluronic coupled affinity membranes. SDS was used because it is non-toxic, water soluble, economic from a process point of view and is a known competitive displacer of adsorbed polymers that can bind organics in solution in the micellar form [16,20,21]. SDS treatment was performed at room temperature (20°C) and its efficacy was compared with that of high temperature (70°C), biphasic (hexane:isopropanol) solvent extraction of Pluronic (Figure 6-4) described in another study [10]. This biphasic solvent system poses potential problems with degradation of polymers such as perspex and polyvinyl chloride (PVC) that are routinely used in laboratory scale membrane module manufacture.

SDS treatment was considered as a non-solvent based Pluronic desorption alternative. It has been reported that the phase behaviour and microstructure of Pluronic block copolymers are affected by SDS micelles [5]. 34 mM SDS displacement of Pluronic appeared effective as the native membrane surface could once again be observed (Figure 6-3C), however, the electron dense structures observed on the surface suggested the possible remnants of SDS deposits. The *ex situ*, energy intensive but highly efficient hexane-isopropanol extraction of Pluronic depicted in Figure 6-3D appeared more effective, since it lacked the apparent electron dense structures in Figure 6-3C. A 'cleaning in procedure' or a more rigorous wash process after SDS treatment, should remove possible micelles or aggregates, as SDS is water-soluble. This is important since most surfaces acquire some surface charge when exposed to ionic solutions and in such situations long-range electrostatic interactions will dominate protein adsorption. Most physiological buffers such as PB will confer a charge to proteins (except at the isoelectric point, where the net charge on the protein is zero) and this can orient the protein towards an oppositely charged surface.

Figure 6-4 illustrates the typical Pluronic displacement trends observed with hexane:isopropanol and SDS respectively. Importantly it was noted that SDS was efficiently separated from Pluronic prior to biphasic colorimetric analysis, where SDS was found to interfere with the spectrophotometric assay [10]. In general SDS was not as

effective as high temperature bi-solvent extraction of Pluronic from hydrophilic PEI membranes and hydrophobic PVDF and PSU membranes. However, the empirically selected SDS desorption parameters were far from optimised with respect to incubation time, shaking and temperature.

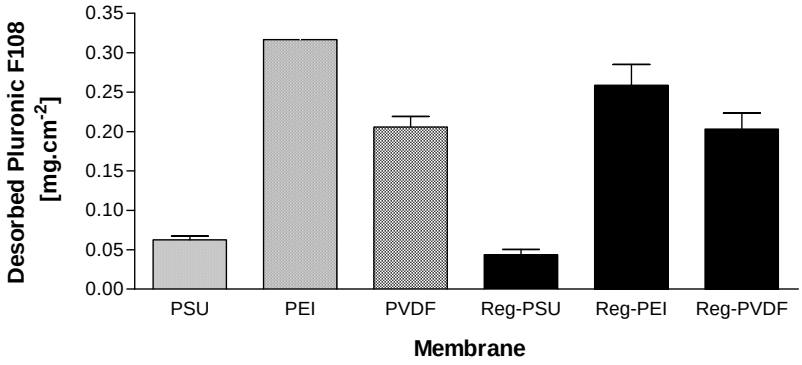

Figure 6-4: A comparison between typical hexane-isopropanol desorption of Pluronic F108 from native planar membranes and membranes that were regenerated (Reg-) with 5 mM SDS. N = 3.

The data in Figure 6-5 suggests that 5 mM SDS was more effective in displacing Pluronic from the membrane surface than at concentrations at or above the 8 mM critical micelle concentration (cmc). These results were comparable with trends observed with hexane:isopropanol extraction and were similar to findings by Cosgrove *et al.,* [20], where the same trend was observed with SDS and poly(ethylene glycol) (PEG) adsorbed on polystyrene beads. In said paper, it was found that the PEO served as a nucleation centre for the formation of micelles at SDS concentrations above the cmc of the surfactant. These authors concluded that the driving force for SDS displacement of PEG from solid supports was due to polymer-surfactant interactions and not competitive adsorption for sites. It can be argued that membrane bound Pluronic would behave differently than the extremely hydrophilic PEG with the SDS micelles forming a solution complex with the PPO centre block of Pluronic at high SDS concentrations (34 mM).

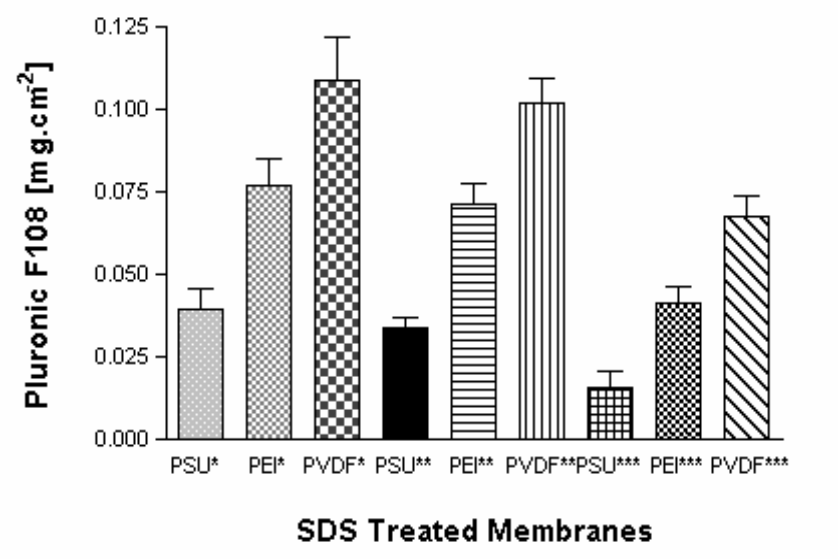

Figure 6-5: Influence of SDS concentration on Pluronic desorption. (* 5 mM, ** 8 mM and *** 34 mM). Pluronic® F108 desorption occurred at 20°C for 2 h with gentle shaking. N = 3.

A contradiction to the observed displacement of membrane adsorbed Pluronic layers in this study and also in other reports [20], was noted in a study by Ma and Li [21]. These authors showed a reverse trend, where SDS above its cmc of 8 mM was more effective in displacing a pre-adsorbed layer of PVP while the layer thickened at lower SDS concentrations (below its cmc). It was suggested that increasing the SDS concentration close to and above the cmc, results in micellisation of SDS and the micelle association number decreases until pure SDS micelles and individual Pluronic macromolecules saturated with SDS are present [2].

Table 6-2 shows the time dependent nature of SDS displacement of Pluronic. Initially experiments were performed under empirical conditions with 2 h incubation at room temperature. Much more Pluronic was displaced after a 20 to 40 h incubation period, but the desorbed amount from all candidate membranes was at least 20 % less than the amount of Pluronic that can be desorbed by high temperature (70°C) solvent extraction. The time dependence of SDS desorption was most significant for hydrophilic PEI membranes rather than hydrophobic PSU and PVDF. It is possible that the multi-layer formation of Pluronic at the PEI interface compared to the Langmuir type monolayer coverage observed with PSU and PVDF complicated the association of SDS micelles with the PPO blocks of Pluronic.

Studies have also shown that this bi-solvent extraction protocol is temperature dependent [10], such that incomplete desorption is observed below 65°C. Although the empirically selected conditions for SDS displacement are far from optimised, this remains a promising approach for Pluronic displacement from nonporous membranes. Future work could involve using varying SDS concentrations at higher temperatures with a range of incubation times and with the membrane also under shear stress.

Table 6-2: Time dependent displacement of Pluronic F108 coated membranes at 20°C using 5mM SDS. The amount of SDS displaced Pluronic [$\mu g.cm^{-2}$] was measured after varying the incubation period from 2 h to 40 h. N = 3

	Incubation Time in 5 mM SDS							
	2 h		4 h		20 h		40 h	
	$\mu g.cm^{-2}$	SD	$\mu g.cm^{-2}$	SD	$\mu g.cm^{-2}$	SD	$\mu g.cm^{-2}$	SD
PEI	0.077	0.013	0.13	0.020	0.18	0.009	0.181	0.018
PSU	0.039	0.011	0.042	0.010	0.047	0.0059	0.045	0.0071
PVDF	0.11	0.022	0.14	0.017	0.19	0.014	0.19	0.013

6.3.3. Desorption of model protein foulants

At membrane surfaces, additional interactions between the adsorbed molecules and the surface come into play. These interactions are both hydrophobic and electrostatic in nature and the interactions between the protein, surfactant and copolymer, can be affected by the presence of the surface. Furthermore the relation between the properties of the complex will determine whether the surfactant will be able to displace the protein [16]. The ability of SDS to displace membrane-adsorbed proteins is depicted in Table 6-3.

A comparison of the desorbed protein data in Table 6-3 with Table 6-2 indicates that even after SDS treatment, a large amount of protein (over 80 % for native membranes) remains adsorbed to the membrane. BSA was also found to be more difficult to displace than lysozyme. The physical displacement of proteins is most likely due to the conformational

change in the protein structure after denaturation by SDS micelles. Stigter [22] showed that for different head-groups on the same surfactant alkyl chain, it is usually found that the binding again follows the micellisation, where the higher the tendency to form micelles the stronger the interaction with proteins. Recent work has also verified that the protein repellent properties of the membrane were still retained after re-coating with Pluronic.

Table 6-3: SDS (34 mM) displacement of pre-adsorbed polymers on native and Pluronic modified membrane surfaces after 20 h of incubation at 20°C

	Lysozyme		Bovine Serum Albumin		Pluronic F108		
	$\mu g.ml^{-1}$	SD	$\mu g.ml^{-1}$	SD	$\mu g.cm^{-2}$	SD	N
PEI	9.30	1.98	9.55	1.12			3
PSU	8.23	1.54	8.56	0.98			3
PVDF	7.18	1.27	6.33	1.00			3
PEI~~Pluronic	1.081	1.25	11.96	1.06	0.26	0.05	3
PSU~~Pluronic	6.063	1.00	11.67	1.47	0.04	0.01	3
PVDF~~Pluronic	0.512	0.09	11.14	2.20	0.20	0.04	3

At low SDS concentrations (5 mM), binding is thought to take place via electrostatic interactions between the charged headgroup of the anionic surfactant and the oppositely charged residues in the protein molecule. As a result of this initial binding, the protein-surfactant complex becomes less charged and more hydrophobic than the protein itself, which may lead to aggregation and precipitation. At higher surfactant concentrations (> 8 mM), binding most likely occurs via hydrophobic interactions, with the SDS headgroups pointing out from the protein surface [23]. At this stage the hydrophobicity of the protein-surfactant complex decreases and it becomes more hydrophilic and re-dissolves into the polar bulk equilibrium solution, eventually acquiring a negative charge like the SDS molecule [16].

6.3.4. Membrane immobilisation of avidin-peroxidase

In an attempt to conceive a re-usable bioaffinity membrane separation technology, we used the biotin-avidin system as a model of biological (ligand-receptor) interaction. Biotin is an imidazolone ring *cis*-fused to a tetrahydrothiophene ring substituted at position 2 by valeric acid. It is the essential coenzyme for carboxylation reactions, where it is covalently bonded to proteins by an amide linkage between its carboxyl group and a lysyl-ε-NH_2 group in the polypeptide chain. However, the strength of the non-covalent interaction between biotin and avidin can pose problems for ligate retrieval. In this study a weaker binding biotin ligand was used, that was displaceable by biotin. One such potential ligand is the *N*-hydroxysuccinimido ester of (iminobiotinylamido)hexanoic acid [24]. Coupling was achieved by displacement of the NHS group in the conjugated biotin by the amine group in hydrazide Pluronic in a DMF solution (Figure 6- 1).

The structure of biotinylated Pluronic was confirmed with ^{13}C NMR. The similarities in the saturation curves in Figure 6-6 indicate that biotin coupling to the hydroxyl terminus of Pluronic did not affect its adsorption affinity for hydrophobic surfaces via the unmodified PPO moiety.

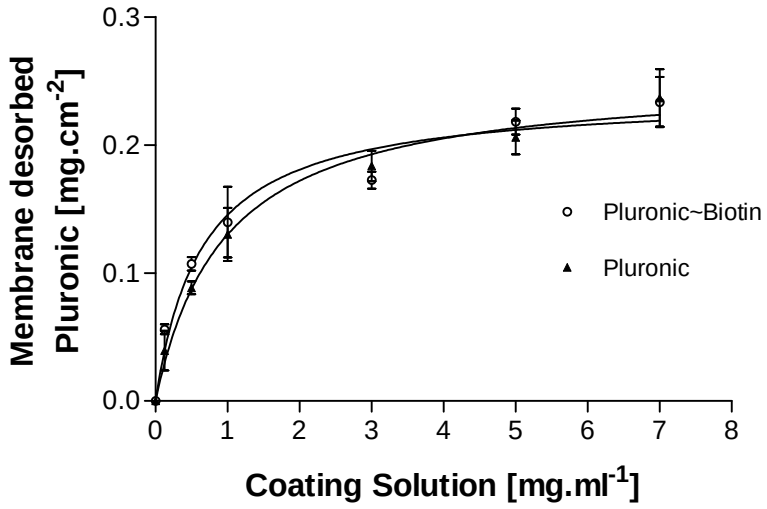

Figure 6-6: Saturation curves for biotinylated Pluronic (r^2 = 0.9162) and unmodified Pluronic F108 (r^2 = 0.9307) on planar PVDF membranes. Both Pluronic F108 and biotinylated Pluronic were desorbed from PVDF surfaces using the optimised hexane-isopropanol extraction method described in [10].

Protein adsorption isotherms using lysozyme and BSA (results not shown) also indicate that the covalently modified biotinylated Pluronic retains the protein shielding ability described in this study (Table 6-1). The adsorption of biotinylated Pluronic (Figure 6-6) showed a typical Langmuir type adsorption profile at 25°C with a plateau at ~ 5 $mg.ml^{-1}$. Pluronic F108 and its derivatives were also only found to form micelles on membranes at coating solutions approaching 7 $mg.ml^{-1}$ [10].

PVDF was selected as the substrate affinity membrane in this study because of its high hydrophobicity, protein shielding ability (Table 6-1), mass transfer properties as hollow fibers [25] and because it is a popular piezoelectric, electro-active polymer in biosensor development. Dose response curves were obtained that related the solid phase biotinylated Pluronic to concentration of avidin conjugated peroxidase (Figure 6-7). The normalised curves follow a typical inverted sigmoidal shape, reaching a plateau when all the available binding sites on the membrane are occupied by the enzyme conjugate.

The typical dose-response effect in Figure 6-7A suggests that there is a specific link between avidin-peroxidase binding to surface immobilised Pluronic-biotin, and the response is proportional to the concentration of avidin-peroixdase used in the binding assay. The curves in Figure 6-7B however, are of the interaction between Pluronic and avidin-peroxidase. Interactions producing a signal in Figure 6-7B are due to non-specific binding of protein to Pluronic. The highest response is at the highest enzyme concentration (1 $U.ml^{-1}$) where protein saturation of the surface at high concentration occurred. The subsequent dilution steps yielded a much lower signal or response suggesting that there was comparatively low non-specific binding.

Pluronic coated membranes that were repeatedly regenerated appeared to lose their protein shielding properties as observed by the increase in the signal intensity with the fourth regeneration cycle. SDS displacement of Pluronic is not 100 % efficient as depicted in Figures 6-4 and 6-5, and if avidin bound Pluronic remained on the surface after SDS regeneration, then there could be an increased tendency for the conjugated avidin to non-specifically bind more protein from solution via hydrophobic interactions, eventually forming protein multi-layers at the interface.

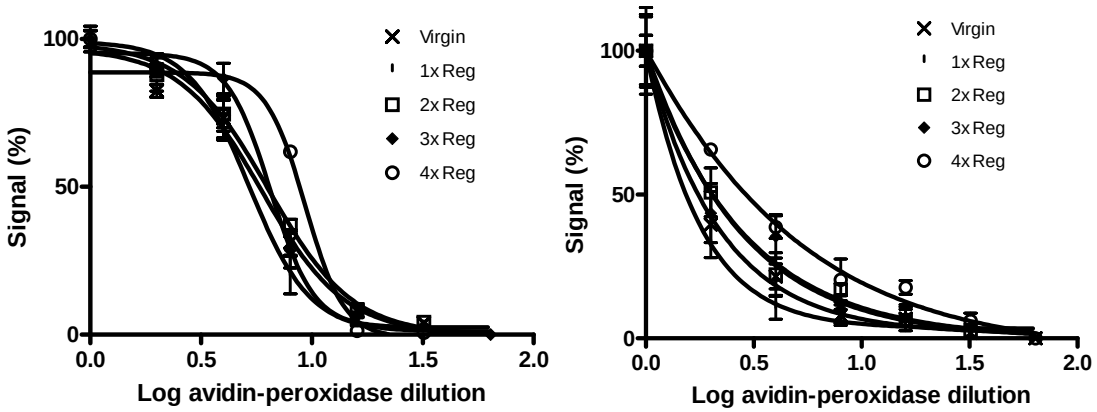

Figure 6-7: Dose-response obtained with A) biotinylated membranes and B) unmodified Pluronic treated membranes incubated with a serial dilution of avidin-peroxidase. Avidin-peroxidase was serially diluted from 1 $U.ml^{-1}$ to 0.0156 $U.ml^{-1}$. Biotinylated membranes and Pluronic coated membranes were subjected to four regeneration cycles and each experiment was performed in triplicate. To make comparisons possible, all curves have been normalised so that their highest signal corresponds to 100%. Baselines are less than 10 % of the maximum and were not subtracted when calculating EC_{50} values using GraphPad Prism® for the biotin-avidin-peroxidase interaction.

The regenerated membranes treated with biotinylated Pluronic (Figure 6-7B), still produced characteristic dose-response curves, but EC_{50} analysis revealed that with increasing regeneration cycles, the concentration of avidin-peroxidase required to induce a response halfway between the maxima and the baseline decreased. EC_{50} data for the virgin PVDF through to the four regenerated cycles described in Figure 6-7A are 5.95, 5.923, 6.358, 6.506 and 9.231 respectively. This is most likely due to incomplete regeneration of the membranes with SDS-treatment, where protein-protein interactions progressively increased resulting in higher EC_{50} values. However, this colorimetric avidin-peroxidase assay is extremely sensitive, and the consistent shapes of the binding curves warrant further investigation of SDS treatment of affinity membranes to increase their capacity and performance.

The specificity of avidin-peroxidase binding to membrane immobilised biotin and the protein shielding ability of the ligand-modified Pluronic, were tested with a competitive binding assay where 0.2 $mg.ml^{-1}$ of model protein contaminants were incubated with each of the serially diluted avidin-peroxidase containing vials. In Figure 6-8 the presence of 0.2 $mg.ml^{-1}$ of lysozyme did not cause a significant change to the typical dose response

effect (EC_{50} = 5.414) suggesting that the hydrophilic PEO tether of Pluronic F108 shielded the membrane surface from non-specific lysozyme adsorption, whilst freeing the biotinylated ligand binding sites to recognise avidin-peroxidase. However, a mixed solution of BSA and lysozyme did not yield a similar trend with a dramatic shift in the EC_{50} from 5.414 to 0.88. It is postulated that since BSA adsorbs on both hydrophobic and hydrophilic surfaces [3], such as Pluronic F108 coated membranes (Table 6-1), BSA blocked many of the avidin binding sites on the biotinylated PVDF membrane. This would cause a reduction of the avidin-peroxidase binding capacity of the membrane resulting in lower signal intensity. The adsorbed BSA could also serve as a nucleation centre for further protein adsorption if the reaction incubation times were extended.

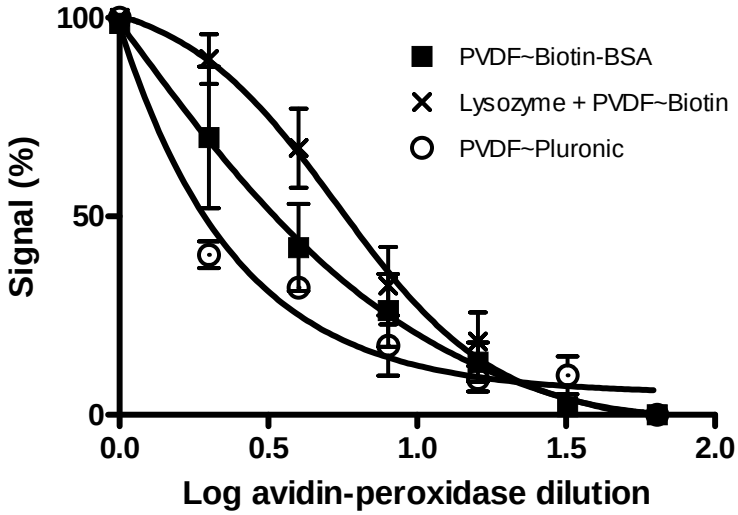

Figure 6-8: Normalised competitive binding assay for avidin–peroxidase in the presence of 0.2 $mg.ml^{-1}$ model protein contaminants. ■ Represents biotinylated PVDF membranes that were incubated with 0.1 $mg.ml^{-1}$ BSA and 0.1 $mg.ml^{-1}$ lysozyme, × represents biotinylated PVDF membranes incubated with 0.2 $mg.ml^{-1}$ lysozyme while o represents a non-derivatised Pluronic coated membrane with 0.1 $mg.ml^{-1}$ BSA and 0.1$mg.ml^{-1}$ of lysozyme. N = 3.

6.4. CONCLUSIONS

The amphiphilic surfactant Pluronic® F108 and the attendant covalently modified biotin derivative, coupled to synthetic polymeric membranes via predominantly hydrophobic interactions. The protein shielding ability of membrane bound Pluronic F108 was dependent on its adsorption capacity on the membranes, which was influenced by the surface hydrophobicity conferred by the fabrication polymer. These properties in addition to its ability to be displaced by SDS make this affinity membrane technology possible to regenerate thus improving its process lifespan and capacity.

This study has also shown specific affinity immobilisation of the protein conjugate, avidin-peroxidase onto biotinylated PVDF membranes using a novel ligand (Pluronic-biotin). Biotin coupling to the hydroxyl terminus of the PEO moiety of Pluronic did not affect its adsorption profile on the electroactive polymer PVDF, thus making it an attractive option for use in biosensor development. Competitive binding assays also suggest that this specific binding is not influenced by up to 0.2 $mg.ml^{-1}$ of lysozyme. However large amounts of the globular protein BSA (0.1 $mg.ml^{-1}$) does affect the competitive affinity binding sites for avidin-peroxidase, with a significant decrease in the EC_{50}.

The dose response curves for regenerated biotinylated membranes followed the same shape as that of the virgin PVDF membrane, with the EC_{50} values increasing with each corresponding regeneration cycle. Pluronic displacement was favoured at lower SDS concentrations (5 mM) while SDS micelles (> 8 mM) were more effective in desorbing adsorbed proteins. The SDS regeneration protocol developed in this study can be incorporated into both *in situ* and *ex situ* membrane systems by utilising existing equipment for re-circulation of the various system components.

Acknowledgements

The Water Research Commission and the National Research Foundation provided financial support for this study.

6.5. REFERENCES

1. N. Wisniewski, M. Reichert, Colloids Surf. B. **18** (2000) 197.
2. R. Ivanova, P. Alexandridis, B. Lindman, Colloid Surf. A. **183-185** (2001) 41.
3. K. Nakashini, T. Sakiyama, K. Imamura, J. Biosci. Bioeng. **91**(3) (2001) 233.
4. M.A. Carigano, I. Szeifer, Colloids Surf. B. **18** (2000) 169.
5. N.V. Efremova, S.R. Sheth, D.E. Leckband, Langmuir **17** (2001) 7628.
6. J-L. Dewez, A. Doren, Y-J. Schneider, P.G. Rouxhet, Biomaterials **20** (1999) 547.
7. P. Kingshott, H.J. Griesser, Curr. Opin. Solid State Mat. Sci. **4** (1999) 403.
8. A. Nilsson, C. Fant, M. Nyden, K. Holmberg, Colloids Surf. B. **40** (2005) 99.
9. J-T. Li, J. Carlsson, J-N. Lin, K.D. Caldwell, Bioconjugate Chem. **7** (1996) 592.
10. S. Govender, E.P. Jacobs, M.W. Bredenkamp, P. Swart, J. Colloid Int. Sci. **282** (2005) 306.
11. L. Kong, J.K. Beattie, R.J. Hunter, Colloids Surf. B. **27** (2003) 11.
12. T. Segura, B.C. Anderson, P.H. Chung, R.E. Webber, K.R. Shull, L.D. Shea, Biomaterials **26** (2005) 359.
13. G. Karlstrom, H-O. Johansson, Colloids Surf. B. **20** (2001) 245.
14. B-S. Lee, S. Gupta, S. Krishnanchettier, S.S. Lateef, Anal. Biochem. **334** (2004) 106.
15. J. Ballesta-Claver, M.C. Valencia-Miron, L.F. Capitan-Vallvey, Anal. Chim. Acta **522** (2004) 267.
16. J.C. Froberg, E. Blomberg, P.M. Claesson, Langmuir **15** (1999) 1410.
17. J.J. Ramsden, Chem. Society Rev. **24** (1995) 73.
18. W. Norde, A.C.I. Anusiem, Colloids Surf. **66** (1992) 73.
19. M.C. Duke, J.C. Diniz da Costa, G.Q. Lu, M. Petch, P. Gray, J. Mem. Sci. **241** (2004) 325.
20. T. Cosgrove, S.J. Mears, T. Obey, L. Thompson, R.D. Wesley, Colloids Surf. B. **149** (1999) 329.
21. C. Ma, J. Li, J. Colloid Int. Sci. **131** (1993) 485.
22. D. Stigter, J. Colloid Int. Sci. **47**(2) (1974) 473.
23. M.N. Jones, P. Manley, P.J.W. Midgeley, J. Colloid Int. Sci. **82** (1981) 257.
24. C-M. Pradier, M. Salmain, L. Zheng, G. Jaouen, Surface Science **502-503** (2002) 193.
25. H-F, Fu, W.S. Lim, H-Q. Mao, Biomaterials **24** (2003) 4893.

CHAPTER 7: CLONING AND EXPRESSION OF HISTIDINE TAGGED HUMAN CYTOCHROME b5

7.1. INTRODUCTION

Immobilised metal affinity separation is one of the most popular methods for the isolation and purification of recombinant proteins using an engineered histidine affinity tag. In this study (detailed in chapter 8) we aim to show the bio-specific immobilisation of soluble *E. coli* histidine tagged proteins under native conditions. However, therapeutically relevant biomolecules such as the frequently reported recombinant eukaryotic proteins tend to be sequestered into insoluble aggregates or inclusion bodies when expressed in bacterial hosts [1,2]. This is particularly endemic to integral membrane proteins that have a hydrophobic membrane binding domain and a hydrophilic portion.

Cytochrome b5 (cytb5) is a ubiquitous membrane bound, amphipathic electron transfer hemoprotein that is found mainly in the endoplasmic reticulum and mitochondria of many mammalian cells [3,4,5]. It has a molecular mass of approximately 16 000 Da comprising 134 amino acids [6]. Cytb5 participates in a number of electron transport reactions and is required for the function of a number of cytochrome P450 catalysed reactions, for fatty acid desaturation and for the sythesis of plasmalogens [6-8].

The polypeptide consists of two distinct domains linked by a trypsin sensitive region: a short hydrophobic C-terminal membrane binding domain comprising approximately 40 amino acid residues which anchors the protein to the endoplasmic reticulum membranes and a larger globular segment containing the heme catalytic domain that projects into the cytosol [5]. In liver microsomes cytb5 is an integral part of a system responsible for oxidative conversion of stearyl-CoA to oleoyl-CoA and has been implicated as a participant in the cytochrome P-450 dependent hydroxylation reactions [9].

The different forms of cytb5 all show a high degree of sequence identity (Figure 7-1), while the carboxyl-terminal domains show somewhat lower identity. Additionally, different mammalian species show over 80 % identities with substitutions being very

conservative [9]. Due to its high solubility and its ease of isolation the heme-binding domain has been the subject of most structural and functional studies. The sequence of this cytosolic amino terminal heme domain, residues 1 – 96, is highly conserved [10]. By contrast little definitive structural data is available for the membrane-binding domain. Progress in this area has been hindered due to difficulties encountered during the isolation of full-length cytb5, where the hydrophobic membrane-binding domain promotes aggregation [9,11].

The primary goal of this study, within the context of the overall objectives of this dissertation, was to test the efficacy of an IMAM system (described in chapter 8) for the bio-specific immobilisation of a typical insoluble membrane protein. This could involve the purification of the histidine tagged cytb5 under denaturing conditions with buffers containing urea and guanidine HCl and surfactants to solubilise the protein. Thus the biochemical behaviour of the Pluronic affinity chelator in this buffer system would be of practical interest when applied to the purification of proteins that tend to form aggregates.

The choice of the target protein was based on its physical and chemical behaviour in solution and because of the ferric heme domain, which has one Fe^{2+} per protein molecule. The heme group could thus potentially be used as an 'intramolecular marker' to quantify the number of affinity adorbed protein molecules per cm^2 of membrane using PIXE (protocols described in chapter 5), and to relate the ratio of chelated Ni^{2+} ions to bound protein.

Thus the aim of this study is to clone human cytb5 into a commercial plasmid vector pET22b that allows the intracellular expression of histidine tagged cytochrome b5. Typically the strategy will involve insertion of the cytb5 DNA upstream of the hex histidine tag of pET22b located on the COOH terminus. The expression hosts for these plasmids are *E. coli* mutants such as BL-21(DE3). The histidine tagged cytb5 can be purified with commercial Ni-NTA columns, while the presence of the soluble folded target protein was investigated using labelled polyclonal antibodies (Ab) raised against sheep liver cytb5 and with a horse radish peroxidase conjugated-Ni chelating probe.

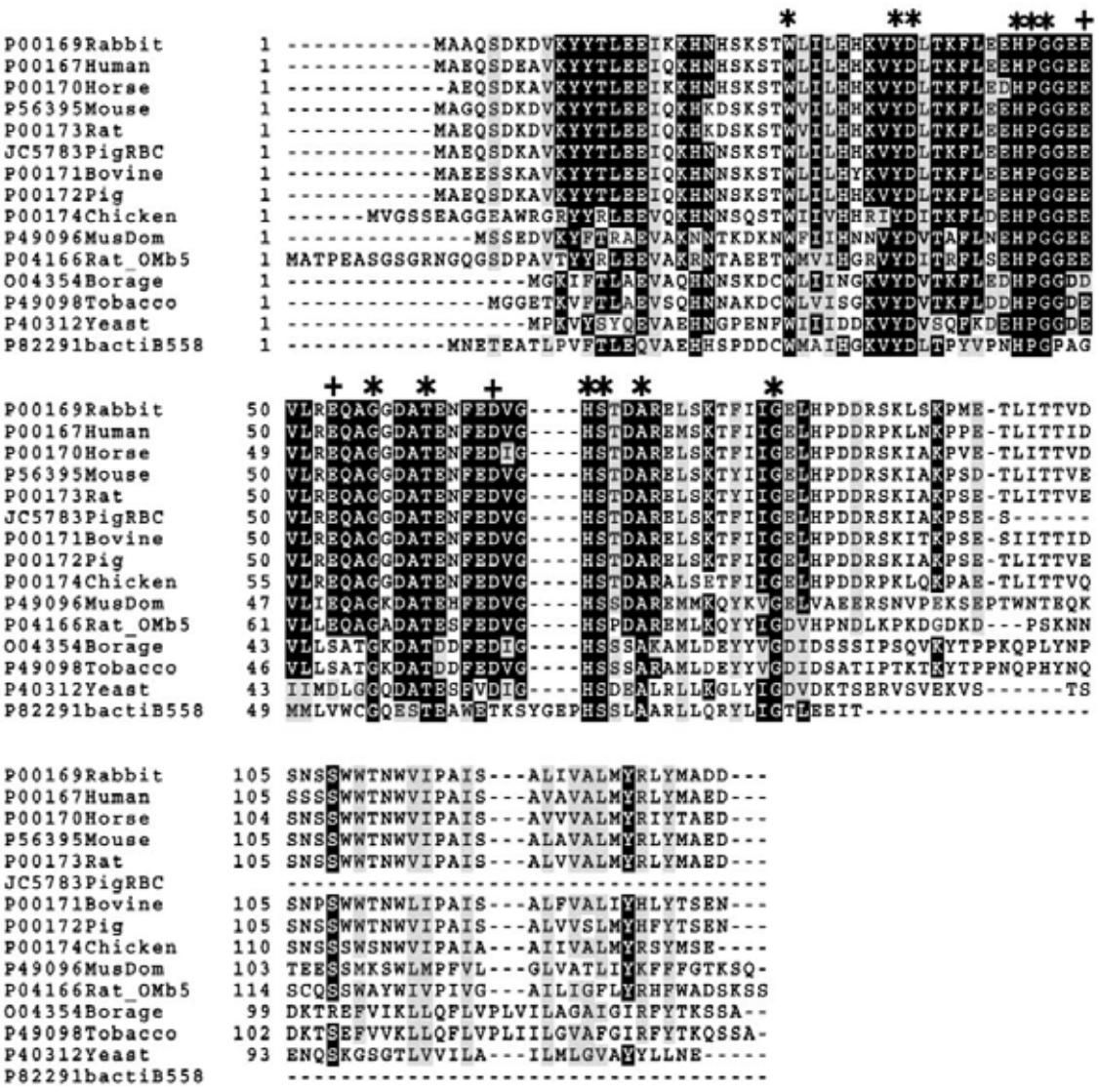

Figure 7-1: Alignment of cytochromes b5 from different phyla. Accession numbers are provided for the various forms of cytochrome b5. Forms include bacteria (bacti), tobacco plant, housefly (MusDom), rat mitochondria outer membrane (Rat_OMb5), and erythrocyte soluble protein (RBCsolpi). Asterisks above alignments indicate fully conserved residues. Plus signs above alignment indicate acidic residues implicated in charge-pairing interactions with redox partners. Black indicates identical residues for a position, grey indicates a conservative substitution (such as an aspartate for glutamate or lysine for arginine) [9].

7.2. EXPERIMENTAL

7.2.1. Reagents and chemicals

Unless otherwise stated all laboratory reagents were of analytical grade or better. Water from an 'Ultra Pure Milli-Q water system' (Millipore, USA) was used in all experiments. All proteins, enzymes and molecular weight markers were purchased from Roche, (Penzberg, Germany). Nucleic acid gel extraction/purification kits were purchased from Qiagen (California, USA). Unless otherwise stated, all bacterial growth media and chemicals were purchased from Fluka (SA).

7.2.2. Culture media and growth conditions

Bacterial cultures were grown routinely in Luria Bertani media supplemented with ampicillin (Sigma chemical company, South Africa) at a final concentration of 100 $\mu g.ml^{-1}$ at 37ºC under aerobic conditions.

7.2.3. Bacterial strains and plasmids

The commercial plasmid vector pUC18 was used as an intermediate cloning vector, which was transformed into the non-expression host *E. coli* JM109. An expression strain (*E. coli* BL21-DE3) and an expression plasmid (pET22b) were purchased from Novagen, USA.

7.2.4. Polymerase chain reaction

The polymerase chain reaction (PCR) was performed with a PCR Sprint (Madison, WI, USA). The reaction details and mixture compositions are outlined in Table 7-1. PCR primers were supplied by Whitehead Scientific, Biochemical Supplies, South Africa. Amplification of the human cytb5 cDNA was performed with the polymerase PfuI, by initial denaturation at 95°C (2 min), followed by 30 cycles of further denaturation at 96°C for 1 min, annealing at 55°C for 1 min and elongation at 72°C for 2 min. The reaction

mixtures were overlaid with mineral oil before PCR and were stored at –20°C after completion of the amplification reaction. Details of the primers used for PCR are presented below.

Left primer (PET22L)

Sequence: $^{5'}$**-ATATGAATTCCATGGCAGAGCAGTCGGACG-**$^{3'}$

Length: 30 Bp-pos: 455; %GC: 50; Tm: 77°C;

Composition: A:9 C:6 G:9 T:6

5' extension: *ATATGAATTC*

Right Primer (PET22R)

Sequence: $^{5'}$**-GCGCAAGCTTGTCCTCTGCCATGTATAGGCGA-**$^{3'}$

Length: 32 Bp-pos: 857; %GC: 56; Tm: 75°C;

Composition: A:6 C:9 G:9 T:8

5' extension: *GCGCAAGCTT*

Table 7-1: PCR protocol for insertion of EcoRI and HindIII into the termini of the human cytcochrome b5 gene

Reagents	Volume (µl)	Final Concentration
dH_2O	35.6	
10 x PCR Buffer	5.0	
dNTPs	5.0	0.2 mM
PET22L (Left Primer)	1.5	600 nM
PET22R (Right Primer)	1.5	600 nM
DNA Template	1.0	
Pfu DNA Polymerase	0.4	1.5 U
Total	50	

7.2.5. Preparation of the insert DNA

Human cytochrome b5 cDNA from an intermediate pUC18 vector was used as a template for insert preparation. The insert was modified by PCR to incorporate restriction enzyme sites on both the NH_2 and COOH termini of cytb5 that were compatible with restriction sites (EcoRI and HindIII) in the multiple cloning sites of the expression vector pET22b (Figure 7-2).

The agarose gel purified PCR product was digested with EcoRI and HindIII (according to the manufacturer's instructions). Restriction digested PCR products were first prepared for ligation into an intermediate vector pUC18 before subcloning into the periplasmic expression vector pET22b. The multiple cloning sites of these vectors have EcoRI and HindIII restriction sites (Figure 7-2) that are compatible with the restriction enzyme sites engineered into the amplified cytb5 gene.

7.2.6. Preparation of vector DNA for ligation

The incubation conditions and buffers used for vector preparation were dependent on the manufacturer's recommendations. The cloning vectors were linearised by digestion with HindIII and EcoRI and the termini of each DNA strand was dephosphorylated using calf intestinal phosphatase (Promega, USA).

The expression vector pET22b was digested with EcoRI and HindIII to generate cohesive termini. The digested plasmid was gel purified, freeze-dried and stored in sterile Milli-Q water. Restriction digested pET22b[HindIII/EcoRI] was stored at –80°C and only thawed for use in ligation reactions.

7.2.7. Ligation

The non-complimentary protruding termini of the linearised vectors (pUC18 and pET22b), shown in Figure 7-2, were ligated according to standard procedures described in Sambrook and Maniatis [12]. A 20 μl ligation reaction was performed at 14°C for 3 to 4

h, with ~ 100 ng dephosphorylated linear vector DNA and ~60 ng digested insert gene. Approximately 2U T4 DNA ligase per μg DNA was used, with 20 mM ATP (Roche). Details of the reaction mixture for the cloning vector (pUC18) and the expression vector (pET22b) are presented in Table 7-2.

Table 7-2: Ligation protocol for insertion of HindIII/EcoRI digested PCR product into dephosphorylated restriction enzyme linearised plasmid vectors using T4 DNA ligase. Typically, stock solutions of 14.65 $ng.\mu l^{-1}$ of plasmid DNA and 12.8 $ng.\mu l^{-1}$ of PCR product were used during ligation

Ligation Reaction	Volume (μl)	Negative Control	Volume (μl)
Milli-Q dH_2O	3.7	Milli-Q dH_2O	5.7
10 X Buffer	2.0	10 X Buffer	2.0
BSA	0.3	BSA	0.3
Linear plasmid vector	8.0	Linear plasmid vector	8.0
Insert DNA	2.0	Insert DNA	0
20 mM ATP	2.0	20 mM ATP	2.0
T4 DNA Ligase	2.0	T4 DNA Ligase	2.0
Total	20.0	Total	20.0

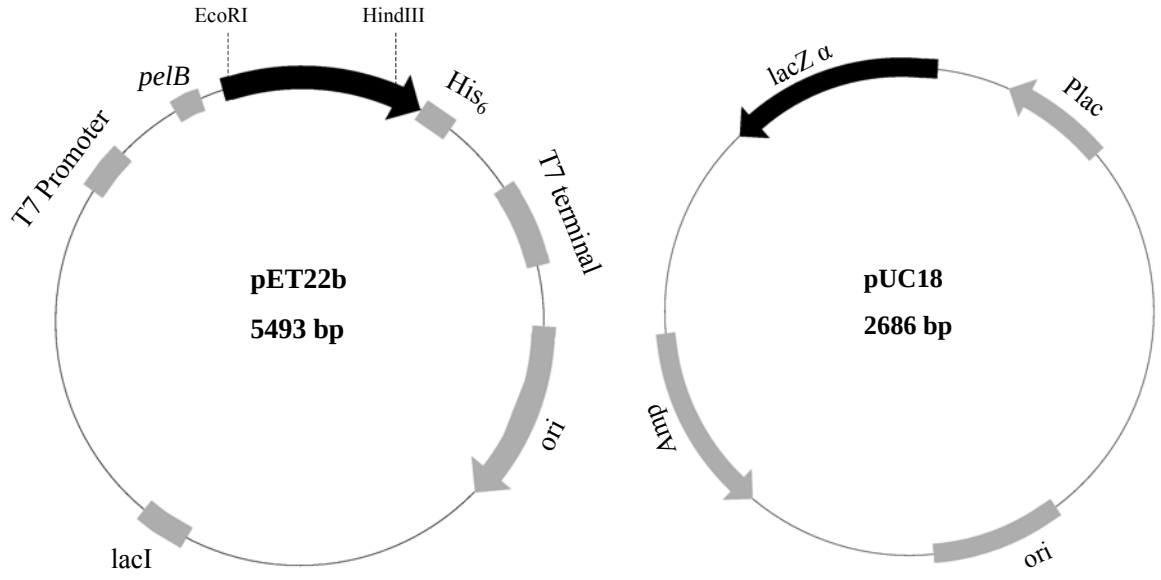

Figure 7-2: Diagrams of the cloning vectors pET22b and pUC18.

7.2.8. Transformation of competent cells

Preparation of competent cells

A single colony of JM109 and BL21(DE3) cells was inoculated into separate 50 ml sterile tubes containing 10 ml of LB-ampicillin (100 $\mu g.ml^{-1}$) and grown for 7 to 8 h at 37°C, before transferring 1 ml of this reaction mixture into 100 ml pre-warmed LB broth containing 100 $\mu g.ml^{-1}$ ampicillin (Amp) until an OD_{600} of 0.5 was reached (~ 100 min). The culture was then cooled on ice for 5 min, transferred to a sterile round bottom centrifuge tube for cell harvesting at 4000*g* for 5 min at 4°C. The supernatant was discarded carefully while the cells were kept on ice. The cells were then re-suspended in 30 ml ice-cold filter sterile TFB1 buffer (0.1 M RbCl, 50 mM $MnCl_2$, 30 mM potassium acetate, 10 mM $CaCl_2$, 15 % glycerol; pH 5.8) followed by 90 min incubation on ice. Cells were collected by centrifugation at 4000*g* for 5 min at 4°C and the supernatant was carefully discarded while the cells were maintained on ice. The cells were then carefully resuspended in ice-cold sterile TFB2 buffer (10 mM MOPS, 10 mM $RbCl_2$, 75 mM $CaCl_2$, 15 % glycerol, adjusted to pH 6.8 with KOH). Aliquots (200 µl) of competent cells were prepared in sterile 1.5 ml microcentrifuge tubes, frozen in liquid N_2 and immediately stored at -80°C.

Transformation

An aliquot of the ligation mix (5 µl) was transferred to a cold sterile microcentrifuge tube and kept on ice, while aliquots of frozen competent cells were thawed on ice. The thawed competent cells were gently resuspended and 100 µl of this cell suspension was transferred to the tube containing the ligation mix. This solution was mixed carefully and incubated on ice for 20 min, before transferring to a 42°C heating block for 90 s. Finally 500 µl of warm Psi broth was transferred to the heat shocked cells followed by shaking incubation at 37°C for 80 min at 180 RPM.

7.2.9. Selection of recombinants

Transformants (50 µl) were added to the centre of LB-ampicillin-IPTG-X-gal plates. The cells were spread radially using an ethanol flamed L-shaped glass spreader and the plates

were then allowed to stand at 25°C for 15 to 20 min. Plated transformants were then incubated overnight at 37°C. Typical negative clones were characterised by blue colonies due to the IPTG induced expression of β-galactosidase which converted the chromogenic X-gal substrate, while positive clones contained an insertion or ligated gene that disrupted the gene coding for β-galactosidase and appeared white. PCR was used to verify the presence of the inserted cytb5 gene in the positive (white) transformants.

7.2.10. Protein expression

Inoculum cultures (10 ml) of *E.coli* BL21(DE3) transformed with pET22b[cytb5(his_6)] were grown at 25°C for 8 h at 150 RPM in TB medium (tryptone 1.2 g, yeast extract 2.4 g, glycerol 0.5 g, 0.017 M KH_2PO_4, 0.072 M K_2HO_4) and carbenicillin (50 μg). A solution of trace elements of the following composition was added, 3 ml to 1 litre of medium ($g.l^{-1}$): $FeCl_3.6H_2O$ (27); $ZnCl_2.4H_2O$ (2); $CoCl_2.6H_2O$ (2); $Na_2MoO_4.2H_2O$ (2); $CaCl_2.2H_2O$ (1); $CuCl_2$ (1); H_3BO_3 (0.5); HCl conc. (100ml) [13]. The cultures were grown at 25°C for 6 h until an OD at 600 nm = 1.2 was reached, at which point 0.1 mM IPTG was added to the growth media to induce the synthesis of the T7 RNA polymerase (10 to 15 h).

7.2.11. Protein isolation and purification

The cells from the cultures expressing cytb5 were harvested by centrifugation at 4000*g* for 10 min and the pelleted cells were weighed and suspended in 4-5 vol (w/v) of PBS (12 mM phosphate buffer (pH 7.4) containing 137 mM NaCl and 3 mM KCl). The cells were pelleted by centrifugation at 4000*g* and the washed cells suspended in two volumes of buffer A (75 mM Tris-Cl, pH 8.0, 0.1 mM EDTA and 1 mM PMSF) [6]. The cells were disrupted by sonication using a Heat System Ultrasonic Inc. Sonicator™ for a total of 8 min per 100 ml of suspended cells: 30 s on, 30 s off, 30 % power. The sonicate was heated to 50°C, [14] maintained at this temperature for 15 min, cooled and the intact cells were removed by centrifugation at 12 000*g* for 10 min followed by resuspension in the original volume of buffer A, sonicated again as described and the combined supernatant centrifuged for 60 min at 100 000*g* to pellet the membranes [6]. Ultracentrifugation was

performed with a Beckman L5-75 ultracentrifuge. The supernatant fluid was decanted and saved for SDS-PAGE analysis and further purification. The green/pink gelatinous pellets were suspended with a dounce homogeniser in 1 ml of buffer B (20 mM Tris-Cl, pH 8.0; 2mM β-mercaptoethanol and 20% glycerol) for each gram of wet weight of harvested cells. The resuspended membrane fraction was stored at -80°C and the ultracentrifuged supernatant was stored at 4°C [6].

7.2.12. Analysis

DNA sequence analysis

Automated nucleotide sequence information was determined using a 3100 Genetic Analyzer (Applied Biosystems, Foster City, CA) and a BigdyeTM Version 2 Determinator sequencing kit 373 A ABI, Applied Biosystems). The sequences of the primers used for sequencing of the relevant plasmid are indicated in Table 7-3.

Table 7-3: Primers used for DNA sequencing

Template DNA	Primer specificity	Primer Sequence
pET22b (sense)	T7 promoter region	TAA TAC GAC TCA CTA TAG GG
pET22b (antisense)	T7 terminator region	ATT AAC CCT CAC TAA AGG GA
pUC18 (sense)	M13-40 region forward	GTT TTC CCA GTC ACG AC
pUC18 (antisense)	M13 region reverse	CAG GAA ACA GCT ATG AC

Protein analysis

Analysis of expressed proteins was performed with SDS-PAGE and Western blotting using horse-radish peroxidase (HRP) coupled to Ni-chelating probes and goat anti-rabbit antibodies respectively. Typically 14 and 10 % acylamide gels were prepared for SDS-PAGE and cast in a Biorad Mini-Protein® Cell for gel electrophoresis. An INDIA™ HisProbe-HRP (Pierce) was used as a nickel-chelating probe for histidine residues and HRP-conjugated goat anti-rabbit polyclonal antibodies were purchased from Sigma.

7.3. RESULTS AND DISCUSSION

7.3.1. Preparation of the insert gene

A 424 base pair (bp) fragment was amplified from a recombinant plasmid template containing the cytb5 cDNA. Using PCR, the restriction sites EcoRI and HindIII were incorporated into the 5' and 3' termini of the cytb5 gene. The amplified PCR product, obtained from 10 x (50 µl) amplification reactions, was subjected to analytical gel electrophoresis on a 0.8 % agarose gel in TAE buffer. A typical 424 bp PCR product is illustrated in Figure 7-3A. A preparatory gel (Figure 7-3B) was run for large-scale isolation of the cytb5 PCR product. The cytb5 PCR product was isolated and purified using a Qiagen gel extraction and purification kit. Approximately 10 to 20 ng.µl^{-1} of DNA was obtained per isolation and the purity was checked by UV analysis with a Beckman spectrophotometer. The PCR product was then digested with EcoRI and HindIII and the enzymes were cleaned with a Qiagen PCR clean up kit.

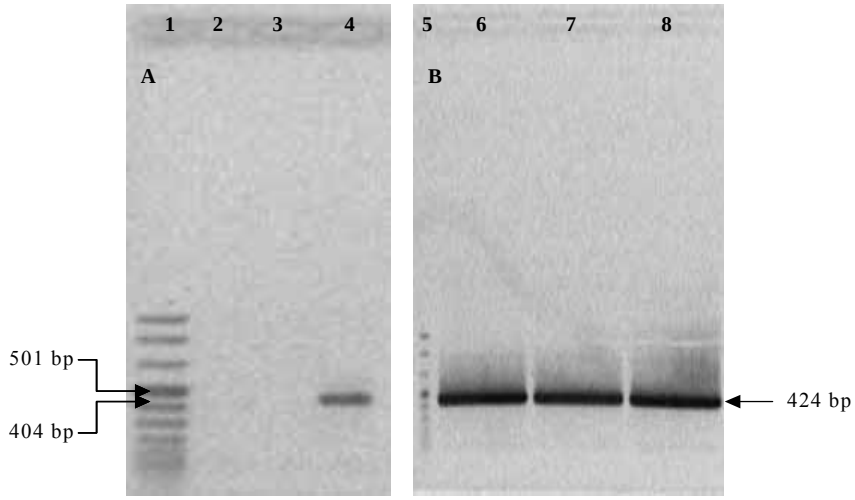

Figure 7-3: 0.7% (m/v) Agarose gels (A and B) in TAE buffer showing the amplification of the cytochrome b5 gene with EcoRI and HindIII termini. Lane 1, Roche DNA marker VIII; Lane 4, PCR amplified cytb5 gene (20 µl); Lane 5, Roche DNA Marker VIII; Lanes 6-8, PCR amplified cytb5 gene (100 µl). Gel B is a typical preparatory gel for gel extraction and purification of insert DNA for ligation.

7.3.2. Cloning and sequencing of cytochrome b5

Initial cloning should be performed in a host cell that lacks the gene for T7 RNA polymerase. This gene enables high percentage monomer plasmid yields for the examination of the construct sequence as well as separation of cloning from expression. This is generally a practical route to follow, as it can be invaluable in trouble-shooting that is inherent to the system dependent cloning procedures that are conventionally followed [15].

Cloning vectors contain three essential elements, an antibiotic resistance marker, an origin of replication (for screening *E. coli* transformants) and a polylinker region containing multiple restriction enzymes sites into which foreign DNA may be ligated. For efficient subcloning of the cytb5 gene, pUC18 was used as a cloning vector that had restriction enzyme sites compatible with many commercial expression vectors such as pET22b. The advantage of the polylinker site is that it affords versatility in the choice of restriction enzymes such that directional cloning is possible. In this study two different restriction enzymes (EcoRI and HindIII) were used to generate digested DNA products with non-compatible protruding 5' and 3' extensions such that the insert PCR product could only ligate into the vector in one direction.

Molar ratios of plasmid vector to insert DNA ranged from 1:1 to 1:2. Further increases in this ratio may reduce the yield of the undesired parent vector, but overall efficiency is not improved since the yield of products with multiple inserts also increases [15]. Additionally, the linearised vectors (pUC18 and pET22b) were dephosphorylated with calf intestinal phosphatase to reduce recircularisation, thus improving the transformation efficiency.

An important cofactor used in the ligation mix was 20 mM ATP, after it was found that ligation efficency of the T4 DNA ligase was influenced by the ATP viability in the ligation buffer. BSA was used in all enzymatic reactions as a stabiliser. A one-step screening procedure was followed based on marker inactivation using a portion of the *E. coli lacZ* gene in pUC18, which is inducible by IPTG. The ligated pUC18 vector was transformed into the bacterial strain *E. coli* JM109, which contained a second defective

lacZ gene. The two gene products complement each other by secreting an active β-galactosidase that metabolises the chromogenic substrate X-gal producing blue colonies. Inserted DNA fragments such as cytb5 into *lacZ* causes the inactivation of the gene, and transformants appear white.

The EcoRI/HindIII digested cytochrome b5 gene (~400 bp) was successfully ligated into the linear pUC18 (2499 bp). Restriction enzyme digestion of the transformed plasmids is shown in Figure 7-4A. Double digestion of a 'white' transformant containing the insert gene with HindIII and EcoRI resulted in bands at ~2700 bp and ~420 bp (lanes 3 and 5 in Figure 7-4A). The linear pUC18 plasmid in lane 4 was a control, verifying the size of the larger band as the 2686 bp pUC18 intermediate cloning vector. The absence of other significant bands, and the correlation of the sizes of the digested products, indicated that the ligation reaction was successful. A PCR reaction was also performed, using a positive transformant colony as a DNA template and the original PCR primers (Table 8-1) to verify the presence of the cytb5$(his)_6$ insert (Figure 7-4B).

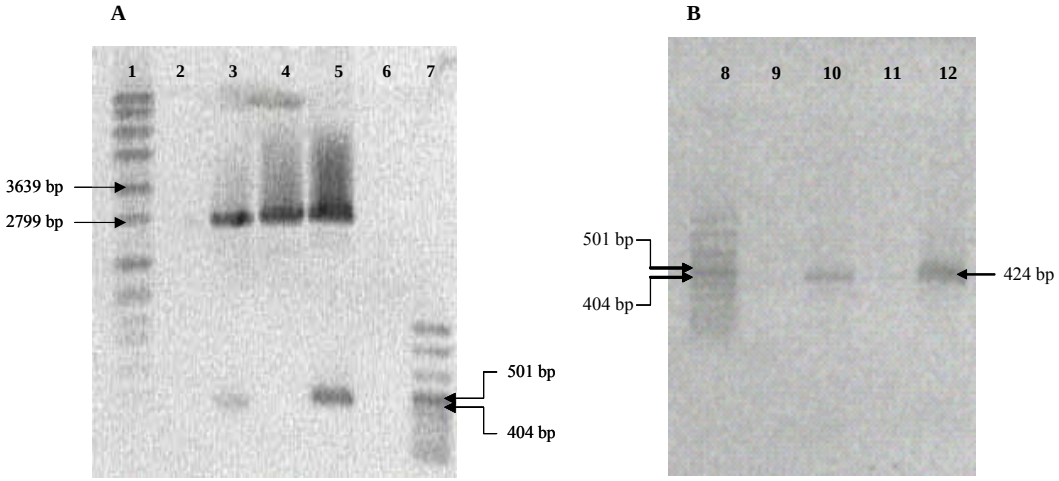

Figure 7-4: Gel A is a restriction enzyme digestion analysis of plasmids obtained from blue white transformed colonies. Lane 1, Roche DNA marker VII; Lane3, pUC18PETB (from a white colony) digested with EcoR1 and HindIII; Lane 4, pUC18 negative control (blue colony) without the insert gene; Lane 5, pUC18PETC (white colony) digested with EcoR1 and HindIII; Lane 7, DNA marker VIII. The DNA fragments and plasmids were analysed on a 0.7% agarose gel in TAE buffer, followed by ethidium bromide staining. Gel B shows the PCR confirmation of the insert gene cytb5$(his)_6$. Lane 8, Roche DNA Marker VIII; Lanes 10 and 12, white colonies containing the transformed recombinant plasmid; Lanes 9 and 11, blue colonies (negative control lacking the insert gene during ligation).

The linearised recombinant plasmid pET22b[cytb5(his)$_6$] is described in Figure 7-5A while Figure 7-5B depicts the enzymatic double digestion of pET22b clones containing the insert cytb5 gene. Double digestion with HindIII and EcoRI yielded the inserted cytb5(his)$_6$ gene (lanes 8 and 11, Figure 7-5B). DNA sequence analysis of the pUC18 and pET22b clones confirmed the success of the cloning and verified that the cytb5 gene was inserted in the correct reading frame for translation of histidine tagged cytb5 holoenzyme (Figure 7-6).

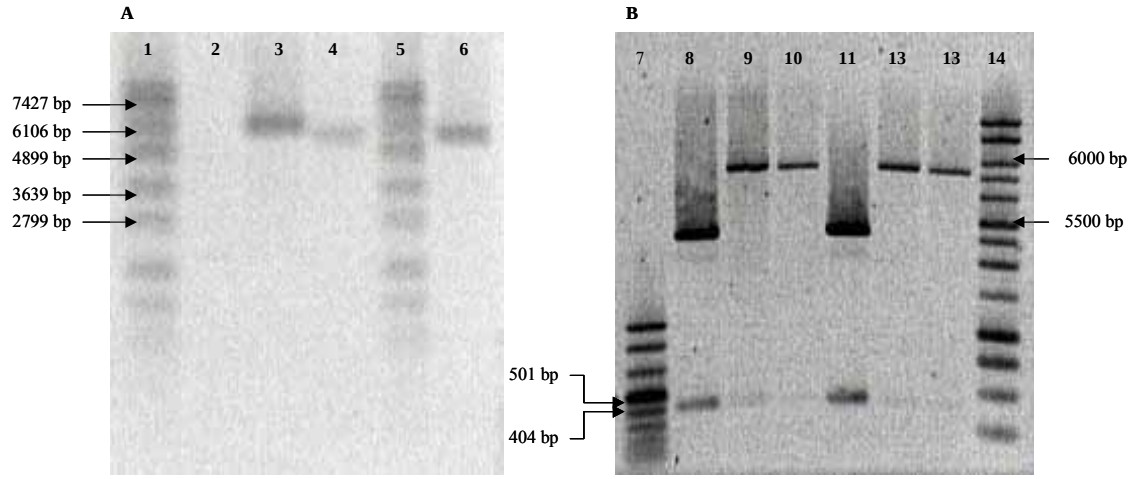

Figure 7-5: 0.7% Agarose gels (A and B) in TAE buffer. Restriction enzyme digestion analysis of plasmids obtained from cells transformed onto antibiotic selective agar plates. Lanes 1 and 5, DNA marker VII; Lane 3, positive transformant (pET22b ligated with cytb5) linearised with EcoRI; Lanes 4 and 6, transformant (negative control lacking the insert gene during ligation) linearised with EcoRI; Lane 7, DNA marker VIII; Lanes 8 and 11, positive transformant digested with HindIII and EcoRI; Lanes 9 and 10, negative control digested with HindIII and EcoRI; Lanes 12 and 13, linearised native pET22b; Lane 14, 1 kb Promega DNA marker.

The correct reading frame and base pair sequence of the inserted cytb5(his)$_6$ gene was verified using DNA sequencing generated with a sense primer from the T7 promoter region and the antisense primer specific for the T7 terminator region.

```
137   atc gga att aat tcg gat ccg aat tcc ATG GCA GAG CAG TCG GAC   181
46    Ile Gly Ile Asn Ser Asp Pro Asn Ser Met Ala Glu Gln Ser Asp   60

182   GAG GCC GTG AAG TAC TAC ACC CTA GAG GAG ATT CAG AAG CAC AAC   226
61    Glu Ala Val Lys Tyr Tyr Thr Leu Glu Glu Ile Gln Lys His Asn   75

227   CAC AGC AAG AGC ACC TGG CTG ATC CTG CAC CAC AAG GTG TAC GAT   271
76    His Ser Lys Ser Thr Trp Leu Ile Leu His His Lys Val Tyr Asp   90

272   TTG ACC AAA TTT CTG GAA GAG CAT CCT GGT GGG GAA GAA GTT TTA   316
91    Leu Thr Lys Phe Leu Glu Glu His Pro Gly Gly Glu Glu Val Leu   105

317   AGG GAA CAA GCT GGA GGT GAC GCT ACT GAG AAC TTT GAG GAT GTC   361
106   Arg Glu Gln Ala Gly Gly Asp Ala Thr Glu Asn Phe Glu Asp Val   120

362   GGG CAC TCT ACA GAT GCC AGG GAA ATG TCC AAA ACA TTC ATC ATT   406
121   Gly His Ser Thr Asp Ala Arg Glu Met Ser Lys Thr Phe Ile Ile   135

407   GGG GAG CTC CAT CCA GAT GAC AGA CCA AAG TTA AAC AAG CCT CCG   451
136   Gly Glu Leu His Pro Asp Asp Arg Pro Lys Leu Asn Lys Pro Pro   150

452   GAA ACT CTT ATC ACT ACT ATT GAT TCT AGT TCC AGT TGG TGG ACC   496
151   Glu Thr Leu Ile Thr Thr Ile Asp Ser Ser Ser Ser Trp Trp Thr   165

497   AAC TGG GTG ATC CCT GCC ATC TCT GCA GTG GCC GTC GCC TTG ATG   541
166   Asn Trp Val Ile Pro Ala Ile Ser Ala Val Ala Val Ala Leu Met   180

542   TAT CGC CTA TAC ATG GCA GAG GAC AAG CTT GCG GCC GCA CTC GAG   586
181   Tyr Arg Leu Tyr Met Ala Glu Asp Lys Leu Ala Ala Ala Leu Glu   195

587   CAC CAC CAC CAC CAC CAC TGA gat ccg gct gct aac aaa gcc cga   631
196   His His His His His His End Asp Pro Ala Ala Asn Lys Ala Arg   210
```

Figure 7-6: Sequence analysis of the sense strand (3' to 5'), of the cloned pET22b[cytb5] plasmid to confirm the DNA sequence of the inserted gene and verify the reading frame of the inserted cytb5 gene. The nucleotides indicated by uppercase letters code for the expressed recombinant cytb5$(his)_6$ protein while the lowercase nucleotides are native to the parent pET22b plasmid vector. Restriction enzyme sites for EcoRI and HindIII are indicated in bold.

7.3.3. Bacterial expression of cytochrome b5

Expression of recombinant proteins can be approached in general by starting with a plasmid that encodes the desired protein, transforming the plasmid into the required host cells, inducing expression, and ending with cell lysis and SDS-PAGE analysis to verify the presence of the expressed protein. Successful expression of appreciable levels of recombinant protein is dependent on the choice of host strain, vectors, growth conditions and purification buffers. However, many polypeptide gene products that are expressed in bacteria (*E. coli*) accumulate as insoluble aggregates that lack functional activity. Other problems may include cell toxicity, protein instability, incomplete folding, improper processing such as post-translational modification and inefficient transcription [16].

To facilitate the expression of correctly folded non-truncated human cytochrome b5 in *E. coli* it was necessary to compromise protein quantity for protein stability. Thus a pET22b plasmid vector containing a *pelB* signal sequence that directs histidine tagged recombinant proteins to the periplasm was selected as an expression vector. Expressed periplasmic proteins were considered more stable but in general, yields were found to be significantly lower than recombinant proteins expressed in the cytoplasm [12].

SDS-PAGE evaluation of the IPTG induced T7 expression procedure is illustrated in Figure 7-7. The protein molecular weight marker in lane 8 was used to estimate the size of the proteins in the respective bands. There was no observable evidence of an intact cytb5 holoenzyme or a distinct band at 16 kDa. Analysis of proteins in the induced soluble and insoluble fractions (Lanes 1 and 5) did not reveal the presence of a cytb5 monomer. Since the soluble and insoluble fractions can be prone to protease degradation, expressed proteins can also be transported to the periplasm. However, analysis of the periplasmic fractions also failed to show clear evidence of the expected soluble 16.7 kDa cytb5 holoenzyme.

An analysis of all the induced fractions in Figure 7-7 (lanes 1,5,7) reveals the presence of a prominent band at ~97 kDa. This phenomenon was repeatedly observed even when growth expression conditions such as growth temperature and IPTG concentration were varied. These variations include shifting the induction temperature from 37°C to 22°C,

lowering the IPTG concentration and the addition of growth additives such as hemin chloride and ferric citrate. Holmans *et al*., [6] suggested that reduced temperature (25°C) and extended expression time (15 – 20 h) could allow for adequate cytb5 biosynthesis [6]. However, the expression of soluble intact, correctly folded cytb5 holoenzyme was not detected using conventional SDS-PAGE analysis with coomasie blue staining. This was consistent with reports by Fahnert *et al*., [11], who concluded that the *in vivo* folding of many heterologous eukaryotic proteins is a major bottleneck of high level production in bacterial hosts. This review also noted that simple optimisation protocols are currently unavailable and that this is a field requiring more study.

In a conflicting report by Miroux [17], who investigated the over-expression of seven membrane proteins in *E. coli* BL21(DE3), cell toxicity and death after induction was shown. These authors then suggested the use of *E. coli* mutants that survived and subsequently expressed the proteins as inclusion bodies.

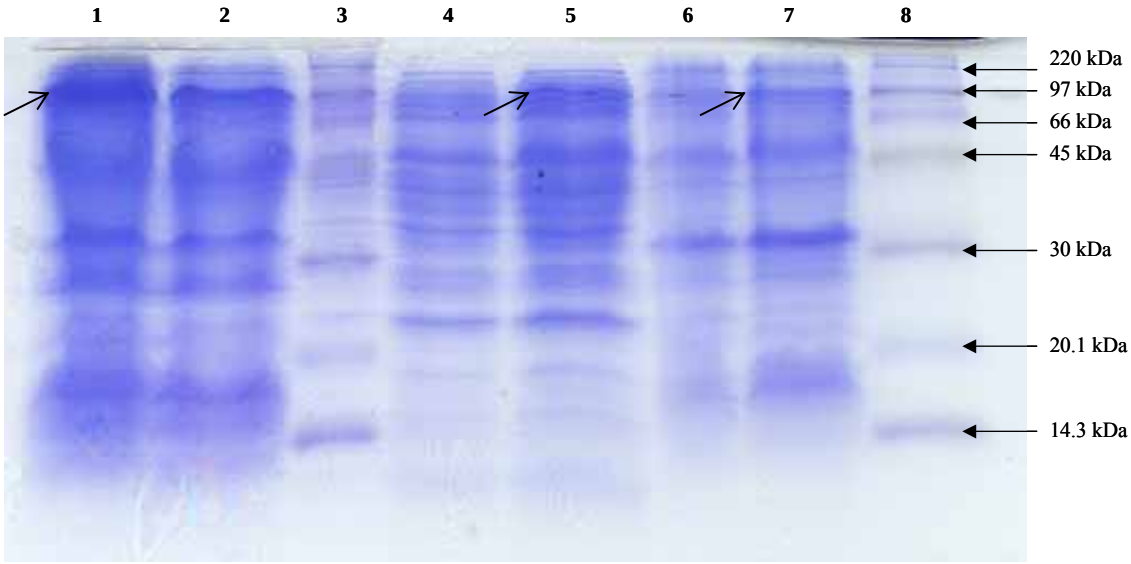

Figure 7-7: Coomassie stained SDS-PAGE gel; Lane 1, Soluble fraction (induced cells); Lane 2, soluble fraction (uninduced cells); Lanes 3 and 8, Roche molecular weight protein rainbow-marker; Lane 4, Insoluble fraction (uninduced cells); Lane 5, insoluble fraction (induced cells); Lane 6, periplasmic fraction (uninduced cells); Lane 7, periplasmic fraction (induced cells). Arrows on the gel indicate the positions of the cytb5 aggregates.

A western blot using a Ni chelating probe conjugated to horse radish peroxidase, which is specific to both surface histidine residues and metal moieties of metallo-proteins was used to check for the presence of low levels of cytb5$(his)_6$. Figure 7-8 is a typical blot obtained. The non-specific appearance of signals due to proteins in both the induced and uninduced cultures suggests that this particular probe is not ideal for this study. While the Ni probe is specific for surface histidine residues on proteins, it is also specific for metalloproteins as observed by the clear, reproducible band at 30 kDa (carboxypeptidase marker in Lanes 1 and 9).

The advantages of this probe were also curtailed largely by the trace element and ferric hemin chloride solutions used as nutrient additives, which caused many false positive signals by binding to the *E. coli* proteins and subsequently, being detected by the highly sensitive metal specific probe. Additionally, when amphiphilic proteins form aggregates or inclusion bodies, the resultant superstructure of the complex, may block or shield metal ion interaction with the terminal surface histidine tag. Zhang *et al*., [18], tried to overcome this problem by inserting hex histidine tags, at both the amino and carboxyl termini of the recombinant human aromatase protein.

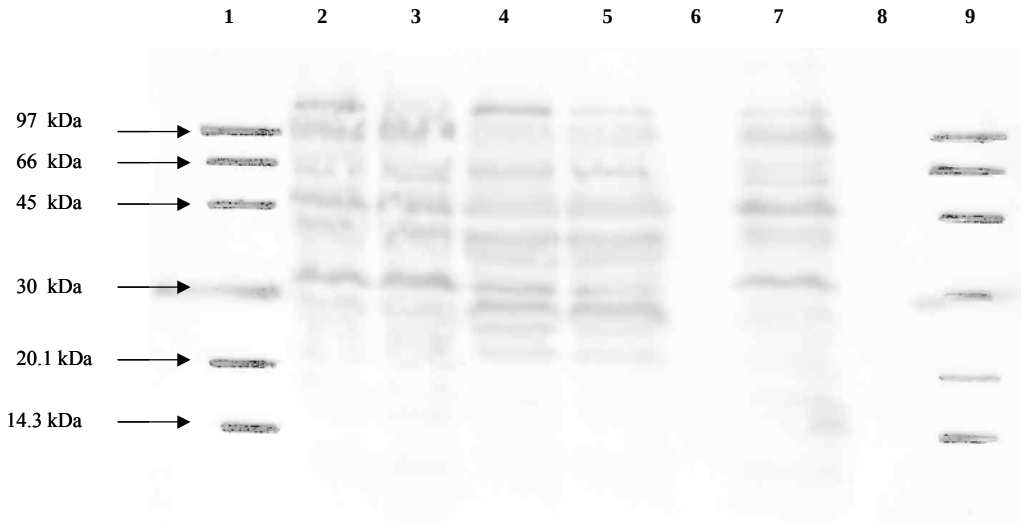

Figure 7-8: Western blot performed with a Ni chelating probe conjugated to horse radish peroxidase. Lane 1, protein marker; Lane 2, induced soluble fraction; Lane 3, uninduced soluble fraction; Lane 4, induced insoluble fraction; Lane 5, uninduced insoluble fraction; Lane 6, uninduced periplasmic fraction; Lane 7, induced periplasmic fraction; Lane 9, protein marker.

A different approach was attempted to verify the presence of recombinant cytb5 using polyclonal antibodies raised against sheep liver cytb5 (anti-cytb5) and a secondary Ab raised against anti-sheep cytb5 in rabbits (goat anti-sheep antibodies). Sheep liver cytb5 was used as a positive control in lane 8. A western blot depicting this experiment is shown in Figure 7-9. A large amount of non-specific bands however were observed in both the induced samples (lanes 3 and 7) and the uninduced samples (lanes 2 and 6).

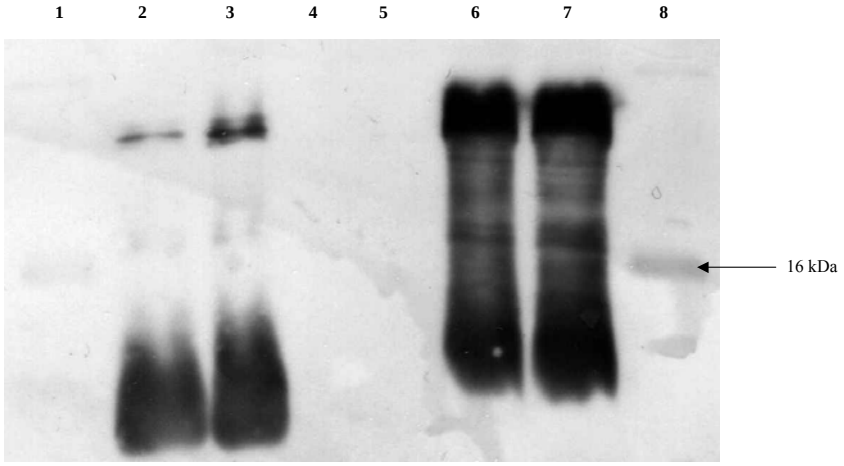

Figure 7-9: Western blot performed with primary polyclonal Ab raised against ovine cytb5 in rabbits and a secondary anti-rabbit polyclonal Ab raised in goats conjugated to horse radish peroxidase. Lane 2, uninduced insoluble fraction, Lane 3, induced insoluble fraction; Lane 6, uninduced soluble fraction; Lane 7, induced soluble fraction, Lane 8, soluble ovine cytb5.

The western blot analysis detailed in Figure 7-9, was inconclusive for the following reasons:

- the large number of non-specific signals routinely detected in both induced and uninduced samples;
- lack of clear evidence showing antibody binding to monomeric cytb5 or possible aggregates;
- possible non-specificity of the rabbit anti-sheep liver cytb5 antibodies for the recombinant human cytb5.

7.4. CONCLUSIONS

Using PCR, the cDNA of human cytb5 was amplified along with the addition of restriction enzyme sites HindIII and EcoRI, which were incorporated into the 3' and 5' termini of the gene respectively. This gene was then subcloned into the expression vector pET22b, which contains a carboxyl terminus hex histidine sequence under the control of the T7 promoter. This recombinant pET22b[cytb5$(his)_6$] plasmid was transformed into an *E. coli* BL21(DE3) expression strain, which allows for high-level intracellular expression of proteins. Recombinant proteins are transported to the periplasm via *E. coli* molecular chaperones under the control of the *pELB* signal sequence [19]. However, expression of intact cytb5 holoenzyme was not detected using this expression system. SDS-PAGE analysis suggests that the protein is sequestered into aggregates after translation and there is evidence of the formation of hexamers corresponding to ~97 kDa. Although yields are generally higher in bacterial systems, the consequently powerful action of the frequently used T7 and T7 lac promoters are known to cause aggregation of membrane proteins [20,21].

Confirmation of the presence of histidine tagged cytb5 or soluble cytb5 using a metal chelating probe and polyclonal antibodies raised against sheep liver cytb5 were inconclusive. The problems associated with bacterial expression systems and integral membrane metallo-proteins have been widely reported and alternate expression hosts/mutants have also been suggested, depending on the nature of the target protein. Expression of histidine tagged cytochrome b5 holoenzymes might be more successful using a yeast system such as *Pichia pastoris*. This expression system is becoming increasingly popular for the production of amphipathic mammalian proteins. Yeasts are also eukaryotic expression systems that produce heme and possess the machinery for post-translational modifications that allow for protein folding around the ferric heme group. Alternative expression systems include the baculoviruses, where higher yields may be sacrificed for proper enzyme folding with no reconstitution and no aggregation [20].

The inability to produce high levels of histidine tagged cytb5 holoenzyme, with *E. coli* BL21(DE3), necessitated the use instead of histidine tagged bacterial pantothenate kinase for the testing of a potential IMAM system using a new bio-ligand. The synthesis, surface characterisation and bio-specific binding of these ligands are described in chapter 8.

7.5. REFERENCES

1. V. Smith, J.E. Walker, Protein Expression Purificat. **29** (2003) 209.
2. G. Georgiou, P. Valax, Methods in Enzymology **309** (1999) 48.
3. R.R. Reed, P.F. Hollenberg, J. Inorg. Biochemistry **97** (2003) 265.
4. M.A. Khaderbhai, R. Morgan, N.N. Kaderbhai, Arch. Biochem. Biophys. **412** (2003) 259.
5. B.J. Curry, S.D. Roman, C.A. Wallace, R. Scott, E. Miriami, R.J. Aitken, Genomics **83** (2004) 425.
6. P.L. Holmans, M.S. Shet, C.A. Martin-Wixtrom, C.W. Fisher, R.W. Estabrook, Arch. Biochem. Biophys. **312** (1994) 554.
7. S.B. Mulrooney, L. Waskell, Protein Expression Purification **19** (2000) 173.
8. W. Boireau, J.C. Zech, P.E. Puig, D. Pompon, Biosensors Bioelectronics **20** (2005) 1631.
9. J.B. Schenkman, I. Jansson, Pharmacol. Therapeutics. **97** (2003) 139.
10. G. Vergeres, L. Waskell, Biochemie **77** (1995) 604.
11. B. Fahnert, H. Lilie, P. Naubauer, Advances in Biochem. Engineering Biotechnol. **89** (2004) 93.
12. J. Sambrook, E.F. Fritsch, T. Maiatis, Molecular cloning. A laboratory manual. Cold spring Harbour Laboratory Press, New York.
13. S. Bauer, J. Shiloach, Biotechnol. Bioeng. **16** (1974) 933.
14. A.S. Ladokhin, L. Wang, A.W. Steggies, P.W. Holloway, Biochemistry. **30** (1991) 10200.
15. A.J. Harwood, Basic DNA and RNA protocols. Methods in Molecular Biology. **58** (1996) Humana Press, Totowa, New Jersey, p.219.
16. D.L. Kaufman, G.A. Evans, BioTechniques **9** (1990) 306.
17. B. Miroux, J.E. Walker, J. Mol. Biol. **260** (1996) 289.
18. F. Zhang, D. Zhou, Y-C. Kao, J. Ye, S. Chen, Biochemical Phamacol. **64** (2002) 1317.
19. M.K. Akhtar, N.N. Khaderbhai, D.J. Hopper, S.L. Kelly, M.A. Kaderbhai, B. Biol. Chem. **278** (2003) 45555.
20. R.E. Whitwam, I.G. Gozarian, M. Tien, Biochem. Biophys. Res. Comun. **216** (1995) 1013.
21. G-Q, Chen, E. Gouaux, Proc. Natl. Acad. Sci. USA. **94** (1997) 13431.

CHAPTER 8: A PLURONIC COUPLED METAL-CHELATING LIGAND FOR MEMBRANE AFFINITY CHROMATOGRAPHY

This chapter has been accepted as is for publication in Journal of Membrane Science. S. Govender performed all the experiments and data analysis described in this manuscript. The aim of this study was to couple a novel metal-chelating Pluronic to PVDF membranes, for the bio-specific immobilisation and elution of histidine tagged proteins and to quantify the ligand binding capacity of this new immobilised metal affinity membrane.

S. Govender [1,2,4], W.J. Przybylowicz [2*], L. van Kralingen[3], M.W. Bredenkamp [3], E.P. Jacobs [3,4], P. Swart [1**]

[1]Department of Biochemistry, [3]Department of Chemistry and Polymer Science, University of Stellenbosch, Private Bag X1, Matieland, 7602, South Africa, [2]Materials Research Group, iThemba LABS, Somerset West, 7129, South Africa, [4]UNESCO Associated Centre for Macromolecules and Materials, University of Stellenbosch, Private Bag X1, Matieland, 7602, South Africa

** To whom all correspondence should be addressed
Pieter Swart
Department of Biochemistry, University of Stellenbosch, Private Bag X1, Matieland, 7602, South Africa
Email: pswart@sun.ac.za
Tel: +2721 808 5865
Fax: +2721 808 5863

*On leave from the Faculty of Physics and Applied Informatics, AGH University of Science and Technology, Cracow, Poland

Abstract

A technique for bio-specific affinity chromatography using synthetic nonporous membranes and a new metal chelating Pluronic surfactant is described. Synthetic polymeric poly(vinyldiene fluoride) membranes were fabricated for use as solid, hydrophobic adsorption membrane matrices. An ethylene diamine tetraacetic acid dianhydride was coupled to the terminal hydroxyl end groups of Pluronic® F108 via a two-step reaction at 40°C, to create a new metal affinity ligand, Pluronic-*N*,*N*-dicarboxymethyl-3,6-diazaoctanedioate (Pluronic-DMDDO). The hydrophobic poly(propylene oxide) moiety of Pluronic allowed non-covalent adsorption of the ligand to the hydrophobic membrane matrix. The protein repellent-properties of the hydrophilic poly(ethylene oxide) brush layer of Pluronic, served to preserve the bio-specific activity of the ligand and to increase ligand accessibility. Proton induced X-ray emission (PIXE) analysis was used to determine the metal binding capacity, stability and surface homogeneity of this immobilised metal affinity membrane system and to generate surface homogeneity maps of the chelated metal ions. The chelate capacity of Pluronic-DMDDO was determined under non-competitive conditions and was of the order (Zn^{2+} > Ni^{2+} > Cu^{2+}). An amino terminal hex-histidine tagged recombinant *Escherichic coli* pantothenate kinase was used as a test protein. Histidine tagged pantothenate kinase bound strongly to Pluronic-DMDDO treated membranes specifically in the presence of Ni^{2+}. Eluted immobilised histidine tagged proteins retained their biochemical activity and the membranes were capable of being regenerated and re-used.

Key Words:

Membrane affinity chromatography, Pluronic® F108, metal chelating ligand, PIXE

8.1. INTRODUCTION

Affinity chromatography is becoming the method of choice for rapid and high purity down-stream bio-processing in pharmaceutical and medical applications. For the isolation and purification of therapeutically relevant bio-molecules such as interferons, vaccines, antibodies, hormones, polynucleotides and peptides, etc; high quality ligands are required [1-3]. Immobilised metal affinity chromatography (IMAC) shows great potential for ligand purification using immobilised divalent metal ions [4]. This is due largely to IMAC being a low cost, well-characterised re-usable technology with higher adsorption capacity than conventional affinity matrices [5,6].

Lately, after the emergence of membranes in filtration processes, synthetic polymeric membranes have become promising candidates as affinity matrices [5,6]. An ideal membrane affinity matrix offers the following advantages: a large surface area to volume ratio, high chemical, thermal and mechanical stability, bio-compatibility, a wide variety of surface functional groups, controlled pore size for filtration, scaleability and non-toxicity [3,7]. Many commercially available membranes are either hydrophobic (hence susceptible to non-specific protein adsorption) or have covalently grafted surface functional groups that are difficult to activate or regenerate. These inherent features of some affinity membranes could hamper the development of membrane-based IMAC applications. A possible solution to preventing non-specific binding and to simultaneously present functional groups for covalent modification with ligands is to functionalise the membrane surface with an amphiphilic surfactant like Pluronic F108 [8].

Pluronic surfactants are commercially available poly(ethylene oxide)$_x$-poly(propylene oxide)$_y$-poly(ethylene oxide)$_x$ (PEO_x-PPO_y-PEO_x) triblock copolymers, which are water soluble, non-ionic, micelle forming surface acting detergents that can self assemble into monolayers at hydrophobic interfaces [9]. These low-cost, non-toxic surfactants are widely used in bio-medical, pharmaceutical and biotechnological applications [10]. Pluronic pre-treatment of membranes in filtration applications has already been shown to reduce protein and cell adhesion and enhance permeate flux [11,12]. Since Pluronic interacts at the solid interface with membranes via non-covalent intermolecular interactions, it is also a potential re-usable affinity linker for IMAC systems. Membrane affinity separation techniques utilising Pluronic surfactants have several advantages over

conventional methods that are dependent on surface grafted ligands [8,13]. These surfactant-based separations generally have low-energy requirements and are approved by the environmental protection agency and the food and drug administration, thus facilitating their acceptability in biotechnological and medical applications [10].

As with conventional chromatographic matrices such as agarose and silica, metal affinity membranes require the surface immobilisation of a ligand. The most commonly used chelators for IMAC include the tridentate IDA, tetradentate NTA and the pentadenate TED [14]. The choice of chelator is dependent on the chemistry of the matrix reactive groups, ligate and its attendant cost. Based on a recent review by Suen *et al*., [6] the tridenate IDA is the most commonly used chelator, because of its lower price and convenient availability. Once an appropriate membrane matrix and chelator are selected, other important parameters for investigation include the chemistry of surface functional groups, chelate capacity, metal ion sorption capacity, immobilisation method and the effects of the buffer regime on ligate stability and purification.

This work is directed towards the fabrication of planar, nonporous PVDF membranes for the reversible immobilisation of a new metal chelating Pluronic. This novel chelating ligand was synthesised by covalent coupling of an EDTA type ligand (ethylene diamine tetraacetic acid dianhydride) to Pluronic F108 via a two-step reaction to yield the chelating ligand Pluonic-DMDDO. The nuclear microprobe technique, PIXE was adapted to directly study the interfacial chelating capacity of divalent metal ions (Ni^{2+}, Cu^{2+} and Zn^{2+}) on the membrane surface. The chelate density, metal stability and metal sorption capacity were directly quantified using solid-state PIXE analysis. Using non-denaturing buffers and protein analysis we were able to demonstrate the biospecific immobilisation of an amino-terminal histidine-tagged recombinant pantothenate kinase [his_6(PK)].

8.2. EXPERIMENTAL

8.2.1. Reagents and Chemicals

Pluronic® F108 was obtained from BASF (Germany). Unless otherwise stated all chemicals were purchased from Merck, Chemical company, South Africa. All enzymes and enzyme solutions were purchased from Roche (Penzberg, Germany).

8.2.2. Inductively Coupled Plasma

Inductively coupled plasma (ICP) analysis was performed on a Liberty Series II radial emission ICP-atomic emission spectrometer. High purity grade reagents were used in this work. The water used was prepared by further purification of de-ionised water with a Milli-Q water purification system (Millipore, USA). Samples were dissolved in 10 ml Milli-Q water.

8.2.3. Proton Induced X-Ray Emission

Proton induced X-ray emission (PIXE) was used to quantify the number of metal atoms on the surface of chelated membranes. Measurements were performed using a nuclear microprobe at Materials Research Group, iThemba LABS, South Africa [15]. A 3.0 MeV H^+ beam was focused to a 5 μm x 5 μm spot and scanned on the membrane surface. Scans of 1.5 mm x 1.5 mm were used close to the centre of the membrane surface where the highest surface homogeneity was observed [16]. PIXE spectra were recorded with a Si(Li) detector positioned at 135° to the beam direction, ca. 25 mm from the specimen, shielded from backscattered protons by an external 155 μm Kapton absorber. Proton backscattering spectra were simultaneously recorded with an annular Si surface barrier detector, 100 μm thick, positioned at an average angle of 176°. Data were collected using XSYS data acquisition system in list mode. GUPIX software was used for the evaluation of the concentration of metals on the membrane surface from the PIXE spectra. PIXE elemental maps were obtained with GeoPIXE-II software and generated using the *dynamic*

analysis method [17]. Proton backscattering spectra were used for qualitative evaluation of the depth distribution of metal atoms.

8.2.4. Nuclear Magnetic Resonance Spectroscopy

NMR analysis was done using a Varian VXR 600 NMR spectrometer. 60 to 80 mg Pluronic-DMDO was dissolved in deuterated chloroform ($CDCl_3$) with tetramethylsilane as internal standard for ^{13}C analysis.

8.2.5. Spectrophotometric analysis

Protein concentration was measured using a bicinchoninic acid protein assay kit from Pierce chemical company, with bovine serum albumin as standard. Pluronic® F108 and its derivatives were extracted and quantified according to the biphasic desorption system and colorimetric assay described in [16].

8.2.6. Membrane fabrication

Planar nonporous immersion precipitation membranes were cast from a solution containing 27 % [m/m] PVDF and 73 % (m/m) *N*,*N*-Dimethylacetamide (DMAc). The PVDF solution required sonication in an ultrasonic water bath for 30 min and further heat treatment at 55˚C for 48 h to dissolve. The solutions were subsequently degassed before being used to cast the 200 μm planar membranes. These membranes were cut into 1 cm^2 sections and were stored in 0.04 M aqueous sodium azide to prevent microbial growth. In preparation for adsorption studies, membranes were washed overnight in sterile, deionised water, followed by three further washes with deionised water. Prior to non-covalent surface modification, the membranes were sonicated three times in sterile deionised water in an ultrasonic bath for 5 min followed by drying in a laminar flow cupboard.

8.2.7. Synthesis of a chelating ligand modified Pluronic F108

The terminal hydroxy groups of Pluronic were modified in a two-step reaction to yield the tetradentate DMDDO type ligand at the hydroxyl terminals of Pluronic (Figure 8-1). This reaction was carried out by dissolving a 10-fold excess of the EDTA dianhydride (256 mg) and 156 mg imidazole (Sigma-Aldrich, Chemical Co.) in dry DMF (10 ml) after which Pluronic F108 (1.5 g) was added and reacted for 8 h at 40°C. Methanol (3 to 5 ml) was subsequently added and reacted for another 8 h after which the DMF was removed *in vacuo*. Longer reaction times were employed due to the size of Pluronic F108. The residue was treated with toluene to selectively dissolve ligand-modified Pluronic from the DMDDO by-product. The final product was characterised mainly by NMR with the aid of model ligands based on mono and diethylene glycol.

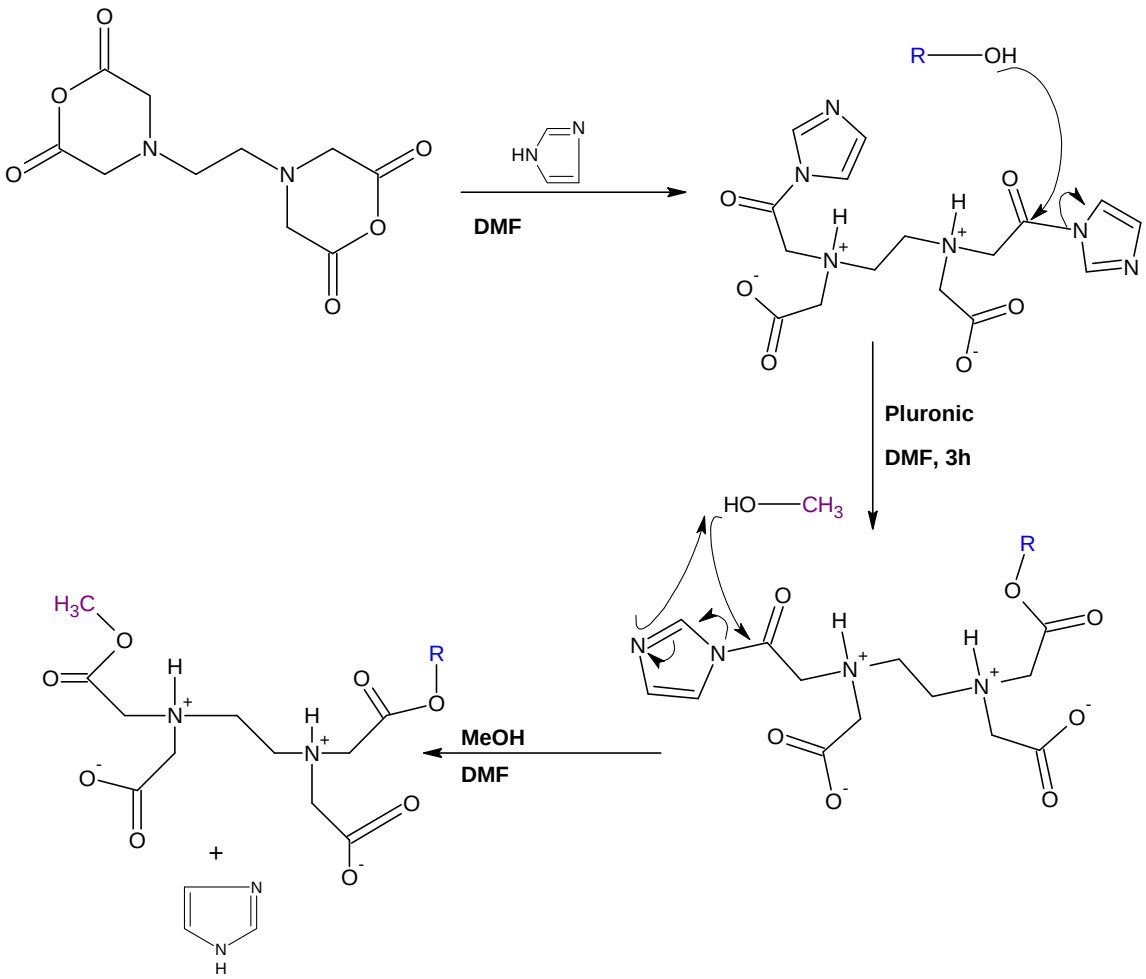

Figure 8-1: Reaction scheme for the synthesis of Pluronic – *N*,*N*-dicarboxymethyl-3,6-diazaoctanedioate.

8.2.8. Chelation using ligand modified membranes

PVDF membranes were coated in a solution of Pluronic-DMDDO for 8 h at 25°C. For batch chelation with divalent metal ions, 1 cm^2 pieces of planar nonporous membranes (non-covalently modified with Pluronic-DMDDO) were incubated in 10 ml of 0.05 M solutions of $NiCl_2.6H_2O$ (Aldrich), $Cu(NO_3)_2.xH_2O$ (Sigma) and $Zn(NO_3)_2.6H_2O$ (Aldrich) in 0.007 M NaOH. The incubation was carried out at room temperature for 60 min. Membranes were then removed, washed in 10 ml dH_2O, air-dried and stored under inert atmosphere for further analysis. Metal ions in the bulk equilibrium solution were quantified by ICP analysis.

8.2.9. Pantothenate kinase assay

Recombinant *Escherichia coli* pantothenate kinase (a kind gift by Dr. E. Strauss, Department of Chemistry and Polymer Science, University of Stellenbosch), was purified on an Amersham AKTA Prime (Amersham Biosciences) using a Ni-NTA column (Sigma) and was eluted with an imidazole gradient. Pantothenate kinase (PK) activity was based on the measurement of the decrease in the absorbance at 340 nm [18]. An extinction coefficient of 6220 $M^{-1}.cm^{-1}$ was used for the calculation of NADH concentrations. Reactions were monitored at 25°C in a CARY 110 UV-Vis spectrophotometer. PK activity was determined using a continuous spectrophotometric assay that coupled the production of ADP to the consumption of NADH. Each 500 µl reaction mixture contained 1.5 mM ATP (Sigma), Tris-Cl, pH 7.6 (50 mM), $MgCl_2$ (10 mM), KCl (20 mM), β-NADH (0.3 mM), 0.5 mM phosphoenol pyruvate (Sigma) pyruvate kinase (5 units), lactic dehydrogenase (5 units), 5 µg pantothenate kinase, and 0.5 mM sodium pantothenate (Sigma). The reaction was initiated by the addition of the pantothenic acid substrate [18] and is detailed in Figure 8-2.

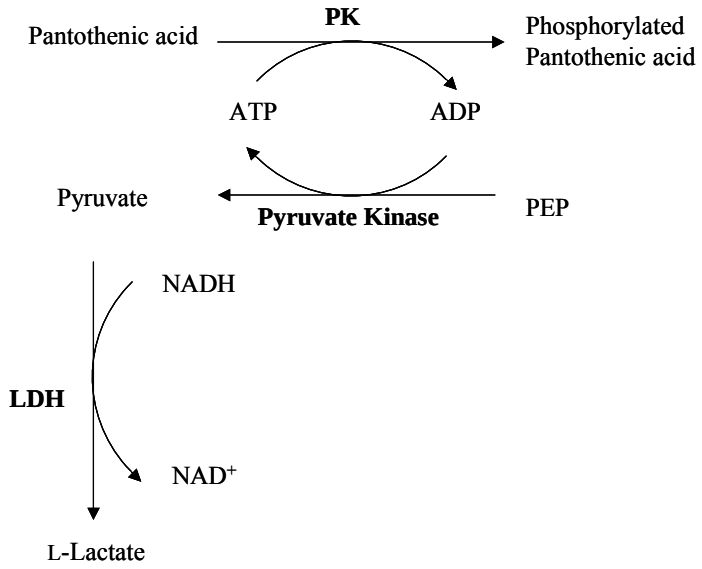

Figure 8-2: Schematic representation of the interactions of histidine tagged pantothenate kinase (PK), Pyruvate kinase and lactate dehydrogenase (LDH) in the spectrophotometric assay based on NADH consumption at 340 nm. The reaction was initiated with pantothenic acid while phosphoenolpyruvate (PEP) and ATP were used as cofactors.

8.2.10. Bio-specific separation

Ni^{2+} chelated ligand coupled PVDF membranes were washed 3 times in 10 ml dH_2O, air-dried and then immersed into a loading buffer of (0.3 M NaCl, 0.01 M imidazole, 0.05 M NaH_2PO_4, pH 8.0) and a his_6(PK) solution at a bulk initial protein concentration of 0.2 $mg.ml^{-1}$. A non-derivatised Pluronic coated PVDF membrane was used as a negative control. After 120 min incubation with gentle shaking at 4°C, the enzyme assays were performed on the bulk equilibrium enzyme solution and the protein concentration was measured. Unbound protein was removed by washing the membrane in 5 ml of washing buffer (0.3 M NaCl, 0.05 M NaH_2PO_4, pH 8.0). Affinity immobilised his_6(PK) was eluted with an elution buffer (0.3 M NaCl, 0.25 M imidazole, 0.05 M NaH_2PO_4, pH 8.0). The contact time of the membrane in each buffer was 120 min at 4°C with gentle shaking and the enzyme assays were performed on the bulk equilibrium enzyme solution and the protein concentration was determined with a Pierce™ colorimetric spectrophotometric assay.

8.3. RESULTS AND DISCUSSION

8.3.1. Synthesis of Pluronic-DMDDO

The widely used nitrilotriacetate (NTA) IMAC system involves covalent coupling to Sepharose® CL-6B and is chelated to Ni^{2+} by perfusing a NTA-Sepharose® column with a metal ion solution until equilibrium is reached between the metal chelated to the stationary phase and the metal ion in solution. Preparation of these columns is typically very cumbersome, agarose is mildewy and ultimately adds to the high costs of biological downstream processing [3,6,19,20]. According to Suen *et al*., [6], the most commonly used chelator is imidodiacetic acid (IDA), because of its low cost and convenience. The synthetic route and yields greatly influence cost [6,19] so direct chemical attachment of a chelator is thus favoured because multiple steps lead to higher labour associated costs and eventual loss of compound. This is of greater significance when working with relatively large polymers like Pluronic® F108.

The attachment of the widely used and relatively inexpensive EDTA chelator to Pluronic is an example of direct chemical coupling. EDTA is hexadentate, capable of filling the octahedral coordination system and can thus complex a number of metal cations. The coupling chemistry was based on using one of the acids of EDTA dianhydride, the reactive precursor derivative of EDTA to bind to Pluronic by esterification (thus removing it from coordination) and another acid by esterification with methanol (Figure 8-1). Imidazole was used to activate and solubilise the EDTA-dianhydride. This yielded a tetradentate ligand with coordination sites on the octahedral system open for ligand attachment and a nonpolar centre block available for hydrophobic surface interaction. The ligand Pluronic-DMDDO was characterised using ^{13}C NMR spectroscopy and is soluble in water or organic solvents and can be stored indefinitely, either in solution or as a desiccate.

8.3.2. The ligand functionalised membrane

The PVDF polymer is of increasing scientific and industrial significance because of its outstanding electrical properties (piezoelectricity), chemical resistance, durability and its biocompatibility in soft tissue applications [21,22]. The fabricated PVDF membranes are stable and can be stored indefinitely under ambient conditions or in a NaN_3 solution to prevent possible microbial growth. PVDF exists in at least three main crystalline forms, designated as α (form II), β (form I) and γ (form III), and also in a minor phase, designated as δ [21]. PVDF membranes were fabricated as hydrophobic affinity matrices and were characterised using photo-acoustic FT-IR (Figure 8-3).

The α phase of PVDF has a unique IR absorption band at 763 cm^{-1} (Figure 8-3), which was baseline separated from the other peaks. Other relevant peaks in Figure 8-3 that correlate to the α phase are the vibration bands at 532 (CF_2 bending), 763, 613 (CF_2 bending and skeletal bending), 792 (CH_2 rocking). The vibration band at 840 cm^{-1} can be assigned to the β form.

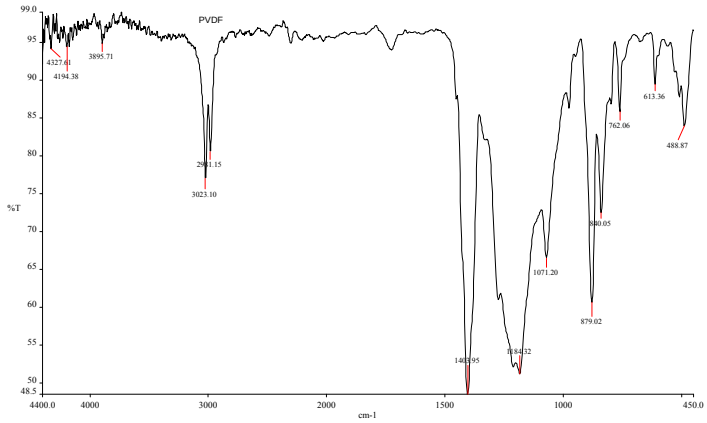

Figure 8-3: Photoacoustic FT-IR spectra of a native nonporous planar PVDF membrane.

The immobilisation of a ligand to an affinity matrix usually occurs via covalent coupling but this was found to reduce its freedom to interact with the ligate [14]. The PEO chain of Pluronic counteracts this by functioning as a large spacer arm between the matrix and the metal chelating ligand. The PEO chain does not impart any adverse properties to the adsorbent and because it is hydrophilic, it does not serve as an adsorption centre for

proteins, thus it is more likely to inhibit non-specific protein adsorption. A schematic illustration of the coupling of a Ni chelated Pluronic-DMDDO membrane for histidine tagged protein immobilisation is depicted in Figure 8-4.

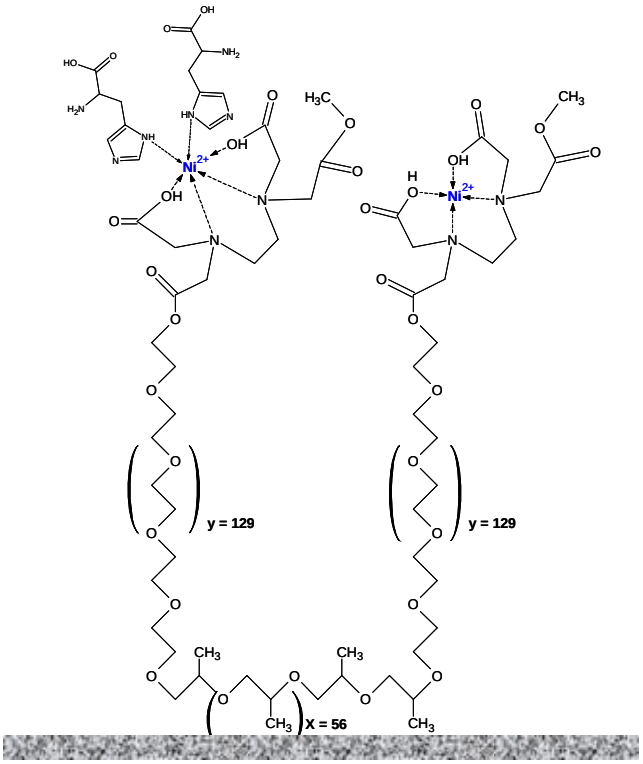

Figure 8-4: Schematic illustration of affinity immobilisation of histidine tagged proteins using membrane coupled Pluronic-DMDDO-Ni^{2+}.

Saturation curves for the adsorption of Pluronic F108 and Pluronic-DMDDO are shown in Figure 8-5. The similarities in the saturation curves in Figure 8-5 indicate that EDTA dianhydride coupling to the hydroxyl terminus of Pluronic F108 did not affect its adsorption affinity for hydrophobic surfaces via the unmodified PPO moiety. The adsorption of Pluronic DMDDO (Figure 8-5) showed a typical Langmuir type adsorption profile at 25°C with a plateau at ~ 5 $mg.ml^{-1}$. Ligand coupled Pluronic coating solutions were maintained at 5 $mg.ml^{-1}$ for all experiments in this study as surface tension analysis revealed that Pluronic F108 and its associated derivatives tended to self assemble into micelles at 7 $mg.ml^{-1}$ [16].

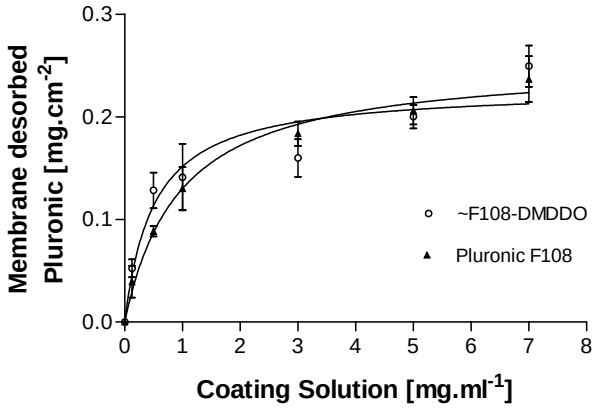

Figure 8-5: Saturation curves for Pluroninc F108 and Pluronic~DMDDO adsorbed on 1 cm^2 planar nonporous PVDF membranes at 25°C.

8.3.3. Chelation and ligand capacity

Micro-PIXE analysis was used to confirm the specific chelation of Ni^{2+}, Cu^{2+} and Zn^{2+} ions to membrane coupled Pluronic-DMDDO. Proton backscattering spectra confirmed that these ions were located exclusively on the membrane surface. A summary of the quantitative investigation of metal ion chelation using the PVDF affinity matrix is listed in Table 8-1.

Metal ions can adsorb passively and non-specifically to both untreated membrane surfaces and to Pluronic modified membranes (Table 8-1), but at much lower levels than with ligand modified membranes. The specific sorption capacity of the ligands for Zn^{2+}, Ni^{2+} and Cu^{2+} were 0.52 $\mu mol.cm^{-2}$, 0.47 $\mu mol.cm^{-2}$ and 0.32 $\mu mol.cm^{-2}$ respectively. Typical PIXE spectra are depicted in Figure 8-6, where distinct metal (Ni, Zn and Cu) K_α and K_β peaks are observed with no significant levels of other elemental species other than a minor chlorine peak on the Ni chelated membrane.

Table 8-1: Summary of PIXE analysis of ligand modified (PVDF~F108-DMDO), Pluronic coated (PVDF~F108) and native PVDF membranes

	PVDF~F108-DMDDO		PVDF~F108		PVDF	
	$\mu g.cm^{-2}$	% Stat Error	$\mu g.cm^{-2}$	% Stat Error	$\mu g.cm^{-2}$	% Stat Error
Ni^{2+}	27.99	0.16	0.651	2.73	0.777	3.18
Zn^{2+}	34.22	0.18	0.106	3.67	0.232	2.95
Cu^{2+}	20.74	0.21	0.301	4.47	0.337.6	4.16

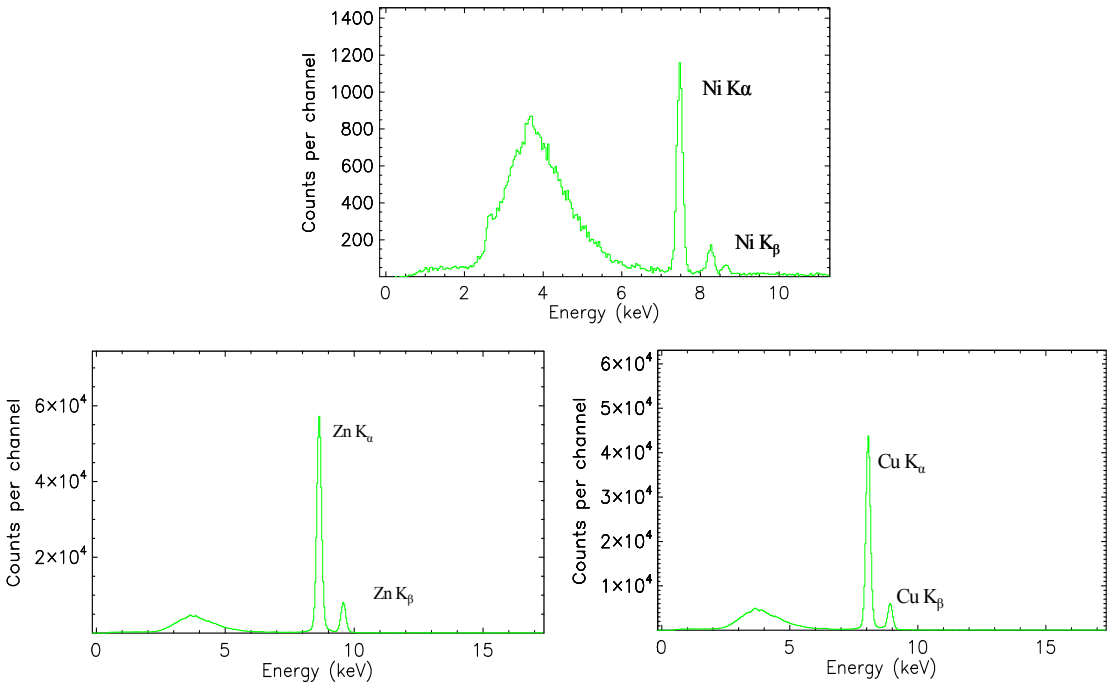

Figure 8-6: PIXE spectra showing specific divalent cation binding on PVDF~F108-DMDDO

PIXE elemental maps showing homogeneity of the distribution of elements on the membrane surface (Figure 8-7), were generated for each metal chelated affinity

membrane. The colour intensity gives an indication of the distribution of the respective metal ions on the membrane surface. A uniform surface is indicative of a homogenous distribution or sorption of metal ions on the surface. Provided we assume monolayer coverage and an even distribution of the DMDDO coupled to Pluronic, the homogeneity maps depicted in Figure 8-7 suggests that uniformity in metal distribution or surface homogeneity was of the order $Cu^{2+} > Zn^{2+} > Ni^{2+}$.

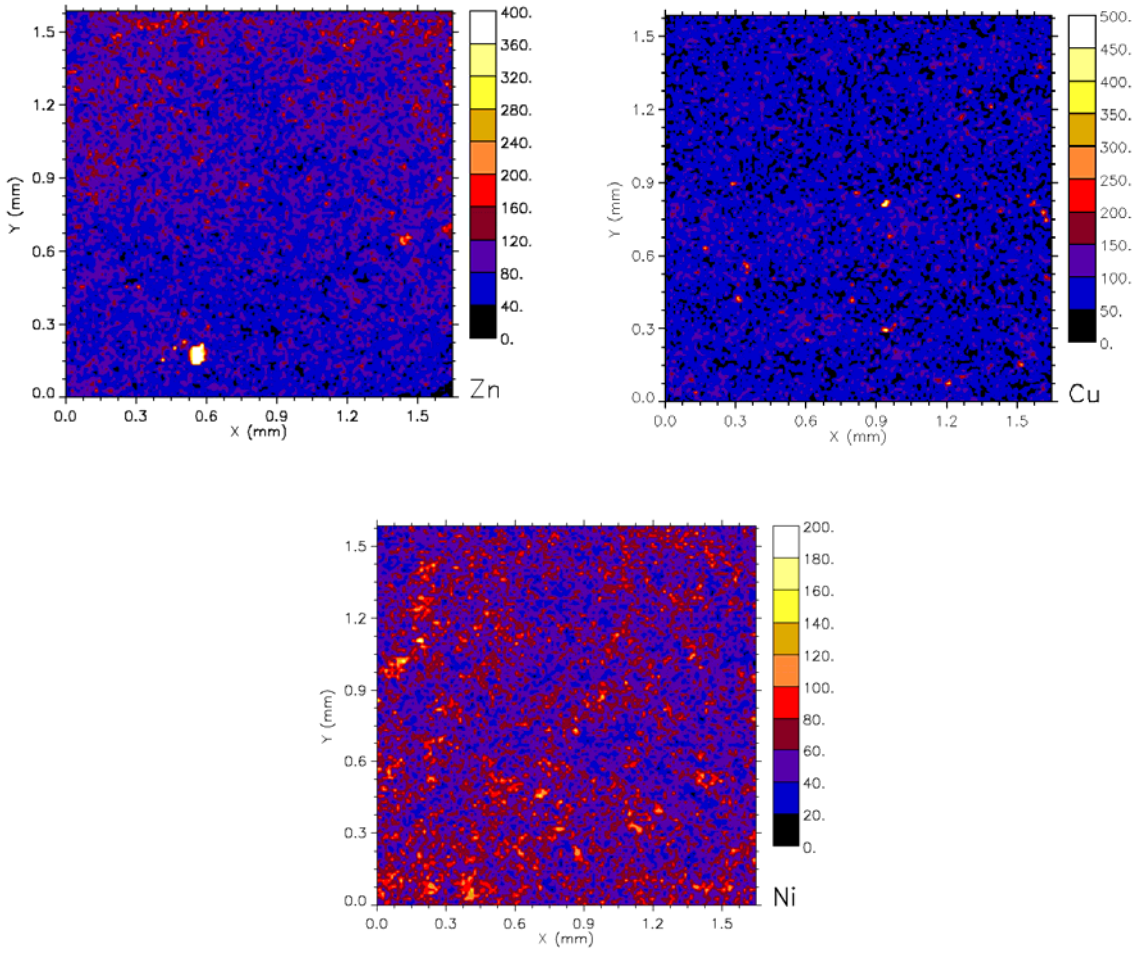

Figure 8-7: PIXE elemental maps showing the distribution of Ni, Cu and Zn localisation of planar PVDF membranes, surface modified with Pluronic-DMDDO.

The Ni^{2+} inhomogeneity could be explained by the presence of the chlorine peak in the PIXE spectrum (Figure 8-6), suggesting the formation of chloride salts on the surface, which could be caused by high salt and pH induced precipitation during Ni chelation using the Ni(II) salt $NiCl_2.6H_2O$.

8.3.4. Chelate stability and repeated use

An important characteristic of chelating ligands is their ability to be regenerated and reused [9] with minimal leaching of metal ions. The stability of the repeated application of the chelating copolymer can be estimated from results obtained in several sorption/desorption cycles [23]. Previous studies related to the stability and regeneration of membrane associated metal chelating ligands make use of either the relatively non-specific monochlorotriazinyl dye cibacron blue F3GA [24] in conjunction with strong acids (2 M HCl) or conventional ligands like IDA [7].

The pH plays a complex role in the chelation, retention and elution processes because of its affects on the nucleophilic behaviour of the buffer components [2]. Metal coordination can therefore be controlled by varying the pH [1,2]. The carboxymethyl groups on the Pluronic-DMDDO chelator need to be deprotonated for metal ion chelation. This is usually achieved at pH 4 or higher. Metal ion displacement, however, is relatively simple to implement with 0.1 M EDTA [24,25]. Treatment of chelated membranes in the elution buffer set at a pH range from 2.5 to 8.5 suggested that the stability of the Ni^{2+} chelate was very high above pH 5.5, with Ni2+ most stable at physiological pH (7.5). However, metal leaching (5 – 10%) was observed below pH 5 (Table 8-2). Reliable ICP analysis of Cu and Zn was hampered by the formation of precipitates in solution.

Table 8-2: ICP data for pH dependent desorption of Ni from chelated membranes

pH of Elution buffer	$[Ni^{2+}]$ desorbed from membrane coupled ligand
pH 2.5	2.59 $\mu g.cm^{-2}$
pH 3.5	1.74 $\mu g.cm^{-2}$
pH 4.5	1.66 $\mu g.cm^{-2}$
pH 5.5	0.04 $\mu g.cm^{-2}$
pH 6.5	0.02 $\mu g.cm^{-2}$
pH 7.5	< 0.02 $\mu g.cm^{-2}$
pH 8.5	< 0.02 $\mu g.cm^{-2}$

The sorption rate and capacity of the chelating polymers towards metal ions depend on several parameters such as shear stress (or flow rate), structural properties of the sorbent, metal ion properties (hydrated ionic radius), metal ion concentration, pH, chelate formation rate, and the presence of competitive ions for the active sites [23]. However, the published results regarding metal sorption on chelating polymers have been obtained under different experimental conditions so it is difficult to make reliable comparisons.

The high salt concentration used in the loading, washing and elution buffers can give high recovery but repeated use may cause severe metal ion leakages. From Figure 8-8 it can be seen that Ni^{2+} leakage did occur after cycles 4 and 5.

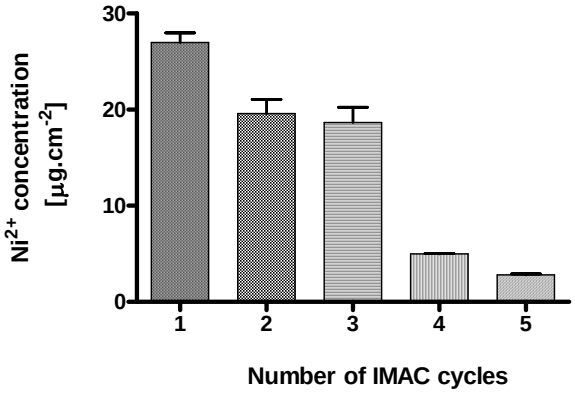

Figure 8-8: Stability of surface chelated Ni^{2+} after repeated membrane incubation in loading, elution and washing buffers. Initially 10 membranes were chelated under identical conditions and after every typical IMAC cycle of incubation in loading, washing and elution buffers, 2 membranes were subsequently removed for PIXE analysis.

Reduction in salt concentration from 0.3 M NaCl to approximately 0.1 to 0.2 M may diminish the metal ion leakage from the affinity membrane but affinity immobilised histidine tagged proteins or any surface amino acid coupled protein may present difficulties during the elution procedure. Although an appropriate salt concentration should be carefully selected [26], other alternatives include the use of a post-trap for leaching metal ions [27] or regeneration of the membrane coupled ligand with a metal ion solution [6].

8.3.5. Bio-specific protein immobilisation

Evaluation of PVDF~Pluronic-DMDDO as an affinity ligand for immobilised metal affinity protein immobilisation was performed with an amino-terminal histidine tagged *E. coli* pantothenate kinase. His_6(PK) was used as a test protein because of the high levels that could be expressed and purified, and because it was stable and its biological activity could be conveniently and accurately determined spectrophotometrically [18]. His_6(PK) activity was determined by monitoring the decrease in NADH concentration over time at 340nm.

A 2 ml solution of 0.2 $mg.ml^{-1}$ His_6(PK) was incubated with ligand modified Pluronic, unmodified Pluronic and native PVDF membranes. Curves representing PK activity as a function of NADH concentration are depicted in Figure 8-9, while the protein and NADH concentrations are listed in Table 8-3. Curve A in Figure 8-9 is an example of a typical activity profile of the enzyme in solution, without the addition of ligand functionalised membranes. Curve B in Figure 8-9 shows a similar activity profile due to a 0.17 $mg.ml^{-1}$ solution of PK, which suggests that low levels of PK adsorbed non-specifically to PVDF~Pluronic at a concentration of 0.066 $mg.cm^{-2}$. Incubation of this membrane in a wash buffer resulted in the displacement of 0.06 mg protein.

Ligand modified PVDF membranes however, produced a flatter activity curve, characterised by a low NADH conversion rate and depletion of His_6(PK) from the bulk solution. Affinity adsorption using a single PVDF~Pluronic-DMDDO membrane, specifically immobilised 0.17 mg $PK.cm^{-2}$ of membrane. Treatment of a 0.2 $mg.ml^{-1}$ solution of PK with three ligand modified membranes (3 x 1 cm^2) yielded virtually no PK activity and removed 0.24 mg of His_6(PK). Treatment of these PVDF~DMDDO-Ni bound His6(PK) membranes in the wash buffer showed no significant desorption of the protein.

To reduce non-specific binding of pantothenate kinase, high ionic strength buffers were used for all the steps from loading and washing to elution. Another advantage relevant to membrane affinity separation is that any weakly bound biospecies containing certain surface exposed amino acids can be washed off the affinity membrane [6]. Elution was attempted under non-denaturing conditions using strong displacing agents such as

imidazole and a high salt concentration. A single incubation step of the IMAM in the imidazole containing elution buffer resulted in 78% displacement of immobilised protein His_6(PK). Other methods of elution of histidine tagged proteins could involve using a milder strategy such as a lower pH buffer (a pH lower than the pKa for the electron donating histidine) or with a stronger metal chelating agent.

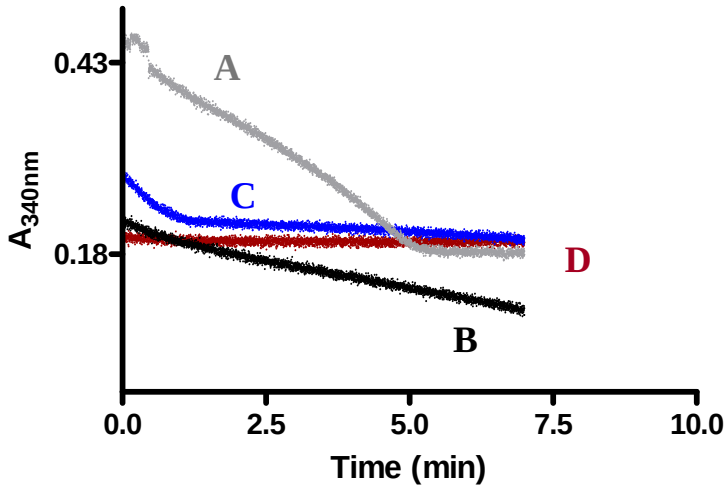

Figure 8-9: Pantothenate Kinase [his_6(PK)] activity, a) Typical PK assay under standard conditions, his_6(PK) incubated with b) 1 cm^2 Pluronic coated PVDF membrane, c) 1 cm^2 Ni chelated ligand modified Pluronic-PVDF, d) three (3x 1 cm^2) Ni chelated ligand modified Pluronic-PVDF membranes. The change in absorbance over time for each assay is depicted as $\Delta A/\Delta t$, while the enzyme concentrations were calculated from the bulk equilibrium protein remaining after removal of membranes from the incubation vessel. The initial enzyme concentration prior to the addition of membranes was ~0.2 mg/ml.

The NADH concentrations were calculated from Beer Lamberts Law: $A = E.c.l$, where A is the absorbance and c the NADH concentration. The molar extinction coefficient (E) for NADH is 6220 $M^{-1}.cm^{-1}$ and a 1 cm path length (l) cuvette was used. The change in NADH concentration was calculated from the absorbance time point extremities (Table 8-3). The Ni-chelated membranes in C and D, show a much lower % reduction of NADH which suggests that there is much less PK remaining in solution, due to the specific removal of PK by the chelated membranes.

Table 8-3: Rate of change of absorbance and NADH concentration due to His_6(PK) activity. The concentration of pantothenate kinase refers to the bulk equilibrium amount remaining in solution after contacting with chelating membranes in a 2 $mg.ml^{-1}$ solution of His_6(PK)

	Pantothenate Kinase	ΔA/Δt	ΔNADH	Percentage Reduction
A] Control	0.20 $mg.ml^{-1}$	0.04	4.26 x 10^{-5} M	59.58 %
B] PVDF~F108-DMDDO	0.17 $mg.ml^{-1}$	0.025	1.86 x 10^{-5} M	51.24 %
C] PVDF~F108-DMDDO-Ni^{2+}	0.11 $mg.ml^{-1}$	0.012	1.35 x 10^{-5} M	29.54 %
D] PVDF~F108-DMDDO-Ni^{2+} (3x)	0.078 $mg.ml^{-1}$	0.005	8.0 x 10^{-7} M	2.42 %

8.4. CONCLUSIONS

When used as an affinity linker, the amphiphilic surfactant Pluronic F108 provides a method to: 1) hydrophilise a hydrophobic affinity membrane matrix, 2) serve as a 129 carbon affinity spacer molecule and 3) allows for the covalent modification of the terminal hydroxyl groups of the PEO chain for the direct coupling of an EDTA-type ligand (DMDDO). The synthesised nonporous affinity matrices and ligand were stable and well characterised using direct solid-state PIXE analysis. Non-covalent coupling of the chelating ligand to PVDF membranes followed Langmuir type adsorption with maximum monolayer coverage at 5 $mg.ml^{-1}$.

The sorption capacity of the ligands for Zn^{2+}, Ni^{2+} and Cu^{2+} were 0.52 $\mu mol.cm^{-2}$, 0.47 $\mu mol.cm^{-2}$ and 0.32 $\mu mol.cm^{-2}$ respectively. Accurate quantification and chelating homogeneity maps were obtained using the highly sensitive and direct PIXE technique. The Ni^{2+} chelating properties of the PVDF~F108-DMDDO membranes were consistent for up to three typical IMAC cycles of binding, washing and elution. However, a five-fold decrease in chelated Ni^{2+} was observed after four cycles. Since Pluronic displacement was found to be negligible during incubation in mild physiological buffers [16], it is likely that Ni^{2+} ions leached off the ligand modified membranes. This IMAM system was also able to specifically immobilise up to 0.17 $mg.cm^{-2}$ his_6(PK). A his_6(PK) elution efficiency of 78% was achieved with a single treatment of the histidine tagged protein immobilised PVDF~DMDDO-Ni membrane in a non-denaturing elution buffer. The activity of the enzyme in both the bulk equilibrium solution and in the eluted form, were unaffected by the chelating membrane, as demonstrated spectrophotometrically, by monitoring NADH consumption.

Acknowledgements

The Water Research Commission and the National Research Foundation provided financial support for this study. Histidine tagged *E. coli* pantothenate kinase was provided by Dr. E. Strauss and Ms. L.A. Brand at the Department of Organic Chemistry, Stellenbosch University.

8.5. REFERENCES

1. J. Porath, Trends In Analytical Chemistry **7**(7) (1988) 254.
2. U. Bora, K. Kannan, P. Nahar, J. Mem. Sci. **250**(1-2) (2005) 215.
3. D.K. Roper, E.N. Lightfoot, J. Chromat. A. **702** (1995) 3.
4. J. Porath, J. Carlsson, I. Olsson, G. Belfrage, Nature **258** (1975) 598.
5. W. Hao, Z. Chen, J. Wang, X. Liu, Analytical Letters **37** (2004) 1319.
6. S-Y. Suen, Y-C. Liu, C-S. Chang, J. Chromat. B. **797** (2003) 305.
7. Y-C. Liu, (2003). J. Chromat. B. **794** (2003) 67.
8. J-T. Li, J. Carlsson, J-N. Lin, K.D. Caldwell, Biocon. Chem. **7** (1996) 592.
9. S.C. McLean, H. Lioe, L. Meagher, M.L. Gee, Langmuir **21**(6) (2005) 2199.
10. S. Stolnik, B. Daudali, B. Arien, J. Whetsone, C.R. Heald, M.C. Garnett, S.S. Davis, S.S., L. Illum, Biochimica Biophysica Acta **1514** (2001) 261.
11. H.K. Shon, S. Vigneswaran, I.S. Kim, H.H. Ngo, J. Mem. Sci. **234** (2004) 111.
12. X.J. Yang, A.G. Fane, C. Pin, Chemical Eng. Journal. **88** (2002) 45.
13. C-H. Ho, L. Limberis, K.D. Caldwell, R.J. Stewart, Langmuir **14** (1998) 3889.
14. J. Porath, J. Chromatogr. **218** (1981) 241.
15. V.M. Prozesky, W.J. Przybylowicz, C.L. Churms, C.A. Pineda, K.A. Springhorn, C.G. Ryan, T. Swart, Nucl. Instrum. Meth. B. **104 (**1995) 36.
16. S. Govender, E.P. Jacobs, M.W. Bredenkamp, P. Swart, J. Colloid Interface Sci. **282** (2005) 306.
17. C.G. Ryan, D.N. Jamieson, C.L. Churms, J.V. Pilcher, Nucl. Instr. Meth. B. **104** (1995) 157.
18. E. Strauss, T.D. Begley, J. Biol. Chem. **277**(50) (2002) 48205.
19. Q. Zheng, J. Xu, R. Fu, Q. Ye, J. Chrom. A. **921** (2001) 197.
20. E. Lightfoot, J.S. Moscariello, Biotechnol. Bioeng. **87**(3) (2004) 259.
21. M. Benz, W.B. Euler, J. Applied Polymer Sci. **89** (2003) 1093.
22. A. Salimi, A.A. Yousefi, J. Polymer Sci. **42** (2004) 3487.
23. A. Nastasovic, S. Jovanovic, D. Dordevic, A. Onija, D. Jakovlejevic, T. Novakovic, Reactive and Functional Polymers **58** (2003) 139.
24. V. Gaberc-Porekar, V. Menart, J. Biochem. Biophys. Methods. **49** (2001) 335.
25. N. Labrou, Y.D. Clonis, J. Biotechnology **36** (1994) 95.
26. C-Y. Wu, S-Y. Suen, S-C. Chen, J-H. Tzeng, J. Chromat. A. **996** (2003) 53.
27. G.S. Chaga, J. Biochem. Biophys. Methods **49** (2001) 313.

CHAPTER 9: CONCLUSIONS AND RECOMMENDATIONS

9.1. SUMMARY

The great interest in affinity membrane technology stems from the expectations generated by combining the exceptional selectivity of bioaffinity ligands with the high productivity associated with filtration membranes [1]. However, there have been very few commercial applications arising from the numerous reports that generally focus on the chemical coupling of biological ligands onto various polymeric membranes. Typically the development of affinity membranes for bioseparation technology follows distinct phases: proof of concept, characterisation, and optimisation, followed by process scale-up.

This study has focused largely on the interfacial analysis of a new bio-compatible, ligand-modified Pluronic coated membrane, and has provided key quantitative information concerning the ligand capacity of the membrane and its ability to be regenerated and re-used. Additionally, proof of concept was demonstrated using two novel bioligands (Pluronic-biotin and Pluronic-DMDDO) for the bio-specific immobilisation of avidin-peroxidase and histidine tagged pantothenate kinase respectively. Experimentally, a multi-disciplinary approach was adopted, involving polymer chemistry, materials science, and biology with the objective of formulating a solution to what is widely perceived as an engineering problem, from a biochemical perspective.

9.1.1. The membrane matrix

As traditional commercially available filtration membranes tend to be developed to encompass a wide range of applications, the resultant membrane properties depend largely on both the fabrication protocol and the choice of polymer material. In this study, we have focused on adsorptive membranes that are hydrophobic, robust, of a simple, well defined surface architecture, while of suitable chemical and mechanical strength. The three candidate membranes (fabricated from PSU, PVDF and PEI), were prepared and characterised with these properties in mind (detailed in chapter 3).

SEM and AFM analysis were useful in qualitatively imaging the membranes in their native states and after Pluronic coating and treatment in various solvents. Membrane surface roughness was found to decrease after Pluronic treatment; while the membrane integrity was conserved after incubation in these solvents. The surface chemistry of each polymeric membrane was monitored with photo-acoustic FT-IR and the surface hydrophobicity was measured using static contact angle analysis. SCA confirmed surface hydrophobicity of planar nonporous membranes to follow the order PVDF>PSU>PEI. The piezoelectric polymer PVDF was found to be the most hydrophobic membrane and the next phase of the study involved studying the adsorption of Pluronic and modified Pluronic on the membrane surface (chapter 4).

9.1.2. Surface modification with Pluronic

The adsorptive capacity of immunoaffinity membranes is known to be enhanced by the presence of a spacer molecule between the ligand and the support matrix [2]. This was initially a short aliphatic hydrocarbon chain (4 – 10 carbons), which was effective at facilitating interactions involving small ligands and target solutes. However to facilitate surface interactions between macromolecules or biological complexes such as fusion proteins, the use of a much longer spacer is best.

Pluronic® tri-block coplymers are commercially available, surface active, micelle forming amphiphilic compounds with high chemical and thermal stability. They are also approved by the FDA and EPA as direct and indirect food additives in biotechnological applications, agricultural products and as pharmaceutical ingredients [3,4]. It was thus selected as an affinity linker, because of its ability to non-covalently attach to hydrophobic membranes via its hydrophobic PPO centre block. Additionally, Pluronic F108 has two large PEO chains per molecule which shield the membrane from the non-specific adsorption of macromolecules found in the surrounding bulk liquid phase. Therefore it was necessary to study the adsorption behaviour of Pluronic and 'model' affinity ligands such as halogenated Pluronic (Pluronic-Br and Pluronic-I) on both planar and curved interfaces.

The focus of this particular study [5], described in chapter 4, was to develop an accurate, reliable, robust, reproducible protocol for both the extraction (desorption) and quantification of membrane adsorbed Pluronic at both planar and curved interfaces. Bisolvent hexane:isopropanol (3:2) extraction of Pluronic at 70ºC, was extremely effective in complete desorption of Pluronic from both planar and capillary membranes. A biphasic colorimetric spectrophotometric assay was also developed to accurately measure Pluronic from both planar and capillary membranes. This assay is based on the specific binding of NH_4FeSCN to PEO in $CHCl_3$, and can reproducibly and accurately measure Pluronic F108 at 510 nm. This assay was sensitive to Pluronic F108 (3 to 130 $\mu g.ml^{-1}$) and insensitive to dextran, biotin, human plasma and BSA. Saturation curves followed a typical Langmuir type adsorption onto PSU, PVDF and PEI membranes, while the corresponding Langmuir isotherms correlated to the current understanding (published reports) of Pluronic adsorption on membranes and can be applied to various matrices or PEG based surfactants that are compatible with the solvents described in chapter 3.

The influence of interfacial curvature on Pluronic adsorption was investigated using HF and HFF nonporous membranes. This study has shown that an increase in capillary diameter (0.9 to 1.88 mm) leads to a corresponding increase in Pluronic adsorption. Applications of Pluronic affinity ligands to capillary membranes should therefore consider the impact of interfacial curvature on lateral crowding of the adsorbed PPO/PEO blocks, which may sterically hinder the adsorption of additional PPO chains.

Pluronic adsorption onto hydrophobic membrane surfaces (PVDF and PSU) increased the hydrophilicity as noticed by convincing SCA measurements, while Pluronic adsorbed onto the relatively hydrophilic PEI via its hydrophilic PEO blocks such that the surface hydrophobicity increased, resulting in multi-layer formation. Adsorption isotherms for PEI membranes generated at 25ºC do not exhibit typical Langmuir characteristics, possibly promoting non-uniform multi-layer formation of the tri-block copolymer that could subsequently shield the potential ligand-ligate interactions with biomolecules such as proteins. Ligand modified Pluronic treatment of membranes is thus most useful for hydrophobic membranes and the interfacial analysis data favoured the use of 5 $mg.ml^{-1}$ Pluronic at 25°C on PVDF membranes as an affinity linker.

9.1.3. Surface analysis

The self-assembly of the PEO-PPO-PEO chains on the membrane surface is influenced by the CMC and coating concentration of Pluronic, incubation temperature and surface matrix hydrophobicity. Solid-state analysis could also be used to generate information on the physical and chemical state of the covalently modified Pluronic using 'model' ligands such as the halogenated derivatives. Using these PEO attached halogens as ligand mimics, XPS, PIXE and RBS were used to generate information on the coating homogeneity of Pluronic, layer thickness, and protocols for calculating the number of ligand binding sites per cm^2 of membrane surface (chapter 5).

RBS spectra estimated an adsorbed Pluronic-Br layer thickness of 157 x 10^{15} atoms.cm^{-2} which suggested PPO self-assembly with a nearest neighbour distance of 4.7 nm. Analysis of surface adsorbed Pluronic-Br correlated to 2.5 x 10^{14} Br atoms.cm^{-2}. XPS analysis was hindered by the weak CH_2-Br and CH_2-I signals, which were much smaller in comparison to the strong C and O related signals of the Pluronic molecule. Consequently Br levels were below the detection limit of XPS. Adsorbed layer thickness can also be more conveniently measured using ellipsometry and small angle neutron scattering. These techniques are well documented but are however, not routinely available in most laboratories.

9.1.4. Affinity membrane regeneration and biocompatibility

Hydrophobic membrane surfaces are non-specifically active to the adsorption of proteins and lipids, so much effort has been devoted to the development of biocompatible, protein-shielding surfaces [6-9]. Realistically, membrane fouling in affinity separation devices is practically inevitable [10,11] and an effective and acceptable regeneration protocol could increase the lifespan of affinity devices and subsequently reduce process costs in biotechnological applications. As a step towards the accomplishment of such an endeavour, we have developed a bio-specific affinity immobilisation system that has shown excellent protein repellent properties and is capable of being regenerated and re-used (chapter 6).

Using Pluronic coated, planar, nonporous membranes (PVDF, PSU and PEI) and model protein foulants (BSA and lysozyme), we have also shown that the protein repellent properties of Pluronic were influenced by the adsorption capacity of the membrane and the nature of the protein foulant. Hydrophobic PVDF had the largest adsorption capacity for Pluronic and had the best protein shielding properties, with 98% shielding of lysoyzme and 75% shielding of BSA adsorption at high protein loading concentrations (0.25 $mg.ml^{-1}$). Hydrophilic PEI membranes were however, hydrophobised by Pluronic and showed an increase in protein adsorption, compared to native PEI membranes. Therefore an understanding of the surface properties of the membrane matrix is important to the successful application of ligand-modified, Pluronic coated membranes in affinity separation.

Anionic SDS solutions (5 and 34 mM), formed the basis of a membrane regeneration strategy by displacing both surface adsorbed proteins and Pluronic after 20 h of shaking incubation at 20°C. BSA, lysoyzme and avidin-peroxidase were most effectively displaced by SDS micelles (34 mM) while Pluronic desorption was favoured below the CMC of SDS (i.e. 5 mM).

The aforementioned biocompatible, regeneration protocols were tested using the model affinity separation ligand-ligate system of biotin and avidin conjugated peroxidase. This was achieved with the successful covalent modification of Pluronic from a hydrazine intermediate to a new, biotinylated Pluronic derivative. The hydrophobic, electroactive PVDF membrane matrix showed similar saturation curves for both unmodified and biotin-modified Pluronic. The typical dose-response curves obtained with avidin-peroxidase immobilised biotinylated-membranes suggested that the colorimetric response measured is proportional to the concentration of avidin-peroxidase used in the study. Non-specific binding was only found to occur at high enzyme concentrations ($> 1\ U.ml^{-1}$) where protein saturation of the surface was anticipated.

SDS regeneration was found to have no effect on the specificity of the dose-response curves and the corresponding EC_{50} data for up to 3 cycles of regeneration. After the fourth cycle, both a gradual decrease in the signal intensity and bio-specificity of membrane immobilised biotinylated Pluronic for avidin-peroxidase was observed. However, it can be argued that the regeneration protocol still has room for optimisation, as

the agitation and incubation temperature parameters were selected emperically. Nevertheless, the results described in this study merit further investigation of this process friendly SDS-regeneration protocol.

Competitive binding assays incorporating the model protein foulants BSA and lysozyme into the target biomolecule solution suggest that bio-specific binding of avidin-peroxidase on the affinity-membrane surface is not influenced by up to 0.2 $mg.ml^{-1}$ of lysoyzme. However, large amounts of the globular protein BSA (0.2 $mg.ml^{-1}$), does affect the competitive affinity binding sites on the membrane for avidin-peroxidase. The problems associated with BSA adsorption onto both hydrophobic and hydrophilic surfaces have been well documented [10,11]. This author proposes that if non-specific adsorption of globular protein is confirmed as a serious problem during an affinity separation process, then perhaps a pre-filtration procedure (e.g. size exclusion chromatography or UF) be performed before the affinity immobilisation step.

9.1.5. Metal chelation and immobilisation of histidine tagged proteins

Immobilised metal affinity membranes are one of the most widely used affinity membrane separation techniques [12] with applications in pharmaceutics and the broader biotechnology industry. This has generated much research into the design of membrane matrices for ligand coupling and chelating ligands for the immobilisation of proteins with engineered, proximal, side chain groups. An important focus of this study was to couple a simple and inexpensive chelator (DMDDO) to the affinity linker Pluronic F108, such that biocompatible membranes could thus be created for metal ion chelation. Additionally this system has been characterised and we have also shown the specific immobilisation of a soluble, recombinant, bacterial histidine tagged pantothenate kinase.

EDTA is a commercially available hexadentate ligand and can be directly coupled to Pluronic via one of the acids of the reactive precursor, EDTA dianhydride by esterification. The resultant tetradentate ligand Pluronic-DMMDO has coordination sites available for metal ion chelation and non-covalent hydrophobic interaction with hydrophobic PVDF membranes via the unmodified, non-polar PPO centre block of Pluronic. Saturation curves at 25°C for Pluronic-DMDDO adsorption onto planar

membranes, showed a typical Langmuir type adsorption profile with a plateau at 5 $mg.ml^{-1}$, suggesting that ligand coupling to Pluronic did not influence its adsorption properties.

The sorption capacity of PVDF-Pluronic-DMDDO for Ni^{2+}, Cu^{2+} and Zn^{2+} and the attendant stability within the chelate complex was studied using ICP and micro-PIXE analysis. The specific chelation capacity of the ligand for Ni, Cu and Zn was 0.47, 0.32 and 0.52 $\mu mol.cm^{-2}$ respectively. PIXE elemental maps indicated that uniformity in metal distribution or surface homogeneity was of the order $Cu^{2+} > Zn^{2+} > Ni^{2+}$. The stability of the chelated ligand (Pluronic-DMDDO-Ni^{2+}) was investigated using an elution buffer (0.3 M NaCl, 0.25 M imidazole, 0.05 M NaH_2PO_4) set at a pH range of 2.5 – 8.5. The Ni^{2+} chelate was found to be most stable at a higer pH (> 6), as deprotonation of the carboxymethyl groups of Pluronic-DMDDO for metal chelation is favoured above pH 4.

The stability of the Ni^{2+} chelate after repeated cycles of membrane (PVDF-Pluronic-DMDDO- Ni^{2+}) incubation in loading, washing, and elution buffers decreased significantly (5 fold) after the fourth cycle. Metal ion leakage may be remedied by decreasing the salt concentration from 0.3 M to 0.15 M, but this may then reduce the elution efficiency of immobilised histidine tagged proteins. A more practical approach could involve the use of a post-trap for leaching metal ions [13], or regeneration with a Ni^{2+} salt solution as early as before the fourth operation cycle.

Proof of concept of this new IMAM technology was achieved using a soluble histidine tagged pantothenate kinase. PVDF-DMDDO-Ni^{2+} membranes specifically immobilised up to 0.17 $mg.cm^{-2}$ his_6(PK). An elution efficiency of 78% was achieved with a single treatment of the immobilised his_6(PK) membrane in a non-denaturing elution buffer. The activity of the enzyme was unaffected by the chelating membrane, as confirmed by monitoring the consumption of NADH spectrophotometrically. A cloned and expressed human cytochrome b5 described in chapter 7, could also be used (when purified as a monomer) to test the versatility of this system with an insoluble membrane protein. However, since cytb5 tends to form aggregates in solution, a denaturing buffer would also have to be used in conjunction with the PVDF-DMDDO-Ni^{2+} membrane. This technology is nevertheless well charactersied for planar nonporous membranes and qualifies for scale-up studies for incorporation into a well-characterised HF membrane system.

9.1.6. Conclusion

The preceding summary detailed the research objectives that were experimentally fulfilled. Specifically it was shown that inexpensive nonporous membranes could be surface functionalised with Pluronic bioligands for bio-specific protein immobilisation while resisting non-specific protein adsorption. Additionally, this Pluronic-modified affinity matrix was well characterised and the ligand and chelate capacity was estimated using direct solid-state analysis. The design of the metal chelating membrane also makes it possible to accurately control the density of the immobilised ligand onto a biocompatible or bio-mimetic surface such that the ratio between sensitivity and specificity for various applications can be optimised.

This thus supports the hypothesis that it is possible to design a membrane-based affinity separation system using Pluronic bioligands that has the following properties:

- a well characterised affinity matrix and ligand chemistry;
- able to shield non-specific protein adsorption;
- can specifically remove proteins from solution;
- capable of being regenerated and re-used.

9.2. FUTURE RESEARCH AND RECOMMENDATIONS

Pluronic surfactants, membrane technology and affinity ligand development are fields of study on their own and therefore present a plethora of opportunities for future applications or even improvement. Within the context of the multi-disciplinary approach of this work and the success of affinity membrane separation technology in the field of biotechnology, the following possible areas for improvement and future application are discussed.

9.2.1. The membrane matrix and module

The great advantage of polymeric membranes is their wide range of applications. Similarly, much more work can be done with the affinity membrane matrix used in this study. An area of particular interest, now that planar nonporous membranes have helped in characterisation and demonstration of proof of concept of bio-specific affinity immobilisation, is to couple the filtration properties of UF capillary membranes to the high selectivity of bio-ligand functionalised affinity membranes. This process, as expected, is limited by concentration polarisation and fouling. Hence it is crucial to quantify this process in order to predict membrane flux and performance.

Hydrodynamic characterisation of both axial and transverse flow membrane modules is not a trivial process but has nevertheless been well described in the literature. The interpretation of protein fouling on UF membranes based on a pore flow model [14] and Monte Carlo simulations for investigating possible phase transition [15] are just two examples of numerous techniques that can be employed to understand flow and fouling in HF membranes.

9.2.2. Biosensor and probe development

The field of biosensor development, involving the incorporation of a biologial element in a sensing layer that is intimately connected to a transducer has been growing tremendously in the last decade [16]. However the design of macromolecular assemblies containing both protein and nucleic acids for DNA sensors or bioelectronic devices remains a challenge. A recent report by Boireau *et al*., [17], describes a DNA chip sensor that can potentially overcome the shortcomings of the other reported devices by using a well characterised affinity ligand and a short spacer molecule while still maintaining high sensitivity and bioselectivity using modified cytb5 and modified ssDNA (Figure 9-1). The domain of cytb5 contained two opposite poles for molecular coupling: one allowing for association with a functionalised hybrid bi-layer, the other allowing the covalent link of a modified nucleic acid via a hetero bi-functional cross-linker (succinimidyl 6-[3´-(2-pyridylthio)-propionamidyl] hexanoate). It is this short cross-linker that separates this technology [17] from other reported DNA chip systems.

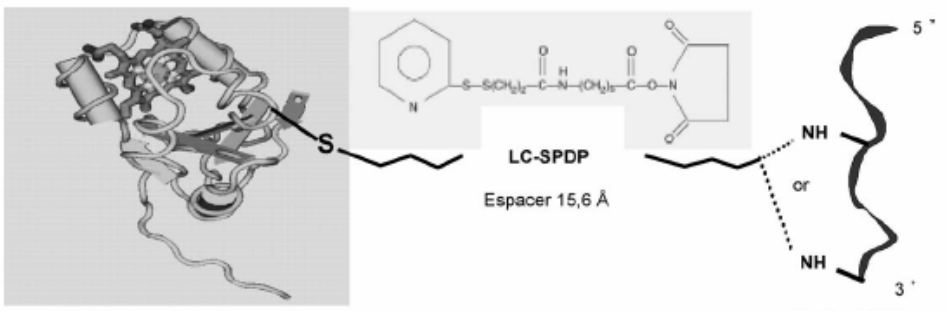

histidine tagged cytb5 modified ssDNA

Figure 9-1: Schematic structure of cytb5 coupled to single stranded DNA through a succinimidyl 6-[3´-(2-pyridylthio)-propionamidyl] hexanoate (LC-SDPD), hetero bifunctional linker [17].

A description of how the comparatively simple, ligand-modified Pluronic coupled membrane (described in chapters 6 and 8) and a histdine tagged redox protein such as cytb5$(his)_6$ (chapter 7) can also be used in biosensor development, is illustrated in Figure 9-2. Pluronic ligands can self-assemble onto the hydrophobic membrane via its hydrophobic PPO blocks, while the hydrated PEO brush prevents the non-specific adsorption of bio-macromolecules. The tethered metal chelating ligand can then specifically immobilise the poly(histidine) tagged redox protein. These self-assembled monolayers, (Figure 9-2) can thus be tailored with a variety of ligands, peptides and proteins. The interaction of this 'biochip' with complimentary ligands can be monitored with surface plasmon resonance spectroscopy [17].

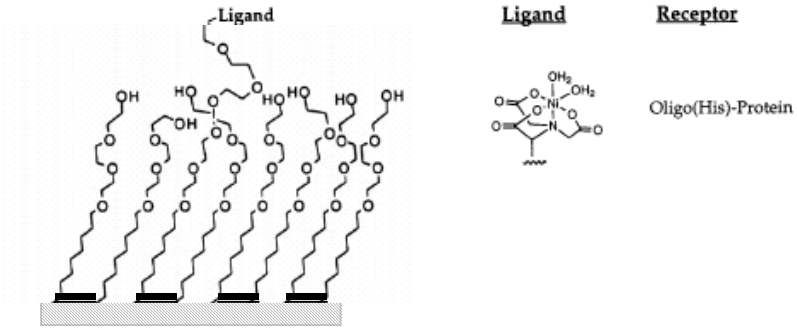

Figure 9-2: Monolayers self-assembled onto hydrophobic PVDF membranes for the bio-specific immobilisation of proteins. (Left) General structure of a monolayer presenting a ligand and PEO groups. (Right) The ligand-receptor combination discussed for this system is the binding of a his-tagged protein to a complex of Ni^{2+} chelated Pluronic.

9.3. REFERENCES

1. E. Lightfoot, J.S. Moscariello, Biotechnol. Bioeng. **87**(3) (2004) 259.
2. S. Soltys, J. Mem. Sci. **20** (2000) 145.
3. S. Stolnik, B. Daudali, B. Arien, J. Whetsone, C.R. Heald, M.C. Garnett, S.S. Davis, L. Illum, Biochimica Biophysica Acta **1514** (2001) 261.
4. M. Bohner, T.A. Ring, K.D. Caldwell, Macromolecules **35**, 6724 (2002).
5. S. Govender, E.P. Jacobs, M.W. Bredenkamp, P. Swart, J. Colloid Int. Sci. **282** (2005) 306.
6. P. Kingshott, H.J. Grissier, Curr. Opinion Solid State Mat. Sci. **4** (1999) 403.
7. I.Y. Galaev, B. Mattiasson, Bio/Technology **12** (1994) 1086.
8. A. Nilsson, C. Fant, M. Nyden, K. Holmberg, Colloids Surfaces B. **40** (2005) 99.
9. T. Segura, P.H. Chung, L.D. Shea, Biomaterials **26**(13) (2005) 1575.
10. K. Nakashini, T. Sakiyama, K. Imamura, J. Biosci. Bioeng. **91**(3) (2001) 233.
11. J.J. Ramsden, Chem. Society Rev. **24** (1995) 73.
12. S-Y. Suen, Y-C. Liu, C-S. Chang, J. Chromatogr. B. **797** (2003) 305.
13. G.S. Chaga, J. Biochem. Biophys. Methods. **49** (2001) 313.
14. A.M. Brites, J. Mem. Sci. **78**(3) (1993) 265.
15. J.C. Chen, J. Mem. Sci. **255**(1-2) (2005) 291.
16. S. Dong, X. Chen, Rev. Mol. Biotechnol. **82** (2002) 303.
17. W. Boireau, J.C. Zeeh, P.E. Puig, Biosensors Bioelectronics **20** (2005) 1631.